NASA Technical Memorandum 100 465

Flowmeter Evaluation for On-Orbit Operations

R. S. Baird
Lyndon B. Johnson Space Center
Houston, Texas

CONTENTS

TABLES

FIGURES

1.0 INTRODUCTION

On-orbit fluid management and resupply of a wide variety of fluids to a wide spectrum of on-orbit vehicles, satellites, propulsion stages, platforms, and free-flyers will require the use of flowmeters. In this context, flow testing of a wide variety of flowmetering concepts was performed to characterize their relative capabilities, limitations, and applicabilities for on-orbit fluid-transfer operations.

This test program was initiated by the Propulsion Branch and all testing was conducted by the Thermochemical Test Branch of the NASA Lyndon B. Johnson Space Center (JSC) Propulsion and Power Division using JSC thermochemical test area and KC-135 reduced-gravity aircraft test facilities. Steady-state flow, pulse flow, and two-phase flow performance of each flowmetering concept considered was determined through waterflow testing simulating potential zero-g fluid-transfer-operation flow conditions. General ground flow testing was performed on all of the flowmetering concepts. Vibration testing was performed on two of the flowmetering concepts. Zero-g testing was performed on four of the flowmetering concepts. All testing was performed using English weights and measures; however, both Système International d'Unités (SI) units and English units are presented throughout this document. English units are generally enclosed in parentheses but are listed in separate columns in some tables.

General performance trends noted in this program suggest that the older flowmetering technologies such as turbine and differential-pressure (delta p) flowmeters do relatively well over a broader range of operating conditions than do some of the newer technologies, although some of these newer technologies such as the bearingless turbine, coriolis, and vortex shedding flowmeters show significant promise under more specialized operating conditions (low-rate and two-phase flows, steady-state flow, and two-phase flow, respectively). Limitations ranged from general limitations encountered when using most flowmetering concepts, such as the sensitivity to low-flow conditions, to more flowmeter-specific limitations, such as the vibration sensitivity of the coriolis flowmeter and the cryogenic temperature sensitivity of the ultrasonic flowmeters. No one flowmetering concept demonstrated the capability of handling the entire range of potential fluid system operating requirements well. Each flowmetering concept has unique capabilities and limitations within this broad range of potential fluid system operating requirements; therefore, selection of the best flowmeter(s) for a particular application is very dependent upon the particular fluid system design and operating environment constraints of that application. The capabilities and the limitations of each flowmetering concept tested are summarized and compared in this document. A glossary of terms and calculations is given as appendix A, and a list of reference documents is contained in appendix B.

2.0 TEST FACILITIES DESCRIPTION

GROUND FLOW FACILITY

Ground flow testing was performed in the fluid systems test facility of the Thermochemical Test Area at JSC. The basic test facility configuration remained essentially the same for all test series, although minor variations (line size changes, valve changes, etc.) were made to the facility depending on the requirements of each flowmeter concept being tested. The basic flow facility (fig. 2-1) consisted of a 5.7-cubic-meter (1500 gallon) deionized water supply (pressurized with gaseous nitrogen (GN_2)), a bladder accumulator, a gas bubble and gas slug injection system, the flowmeter test article, a control valve downstream of the test article, a throttling valve, a vent valve, and a catch tank at the end of the waterflow path. The catch and weigh tank was suspended from one of two load cells having capacities of 445 newtons and 2224 newtons (100 pounds force and 500 pounds force), respectively. These load cell measurements were recorded continuously and were used as the performance evaluation standard. Load cell measurement noise caused by waterflow turbulence into the catch and weigh tank was minimized by use of a flow distributor. System flow rates were controlled through supply tank pressure and throttle valve modulation. The control valve was used to start, stop, and cycle (at various frequencies) flow through the flowmeter test article. The gas injection system injected various nitrogen gas bubble volumes at adjustable rates into the flow stream upstream of the flowmeter test article for two-phase flow testing. The bladder accumulator was installed to facilitate high-frequency pulse flow system testing. The overall flow facility error was calculated to be ± 0.1 percent based on the root sum of the squares of the individual data acquisition elements.

PORTABLE FLOW TEST STAND

The portable flow test stand (PFTS) was designed and fabricated in house to support the zero-g (KC-135) and vibration environment portions of this test program. The PFTS (fig. 2-2) consisted of an air supply, a water-piston-calibrated cylinder, connections for the flowmeter test article, metering valves, a fast-acting flow control valve, an air injection system, a receiving tank, a vacuum pump, and a control system. The flowmeter test article was hardmounted in the PFTS for zero-g testing and flexlined from the PFTS over to a shaker table for the vibration environment testing (fig. 2-3). The water piston was driven by pressurized gas (air) and incorporated a high-accuracy (± 0.02 percent uncertainty) displacement measuring system. The cylinder held approximately 0.04 cubic meter (10 gallons) of water with the piston fully extended. The air injection system consisted of an air supply, a flowmeter, a metering valve, a backpressure regulator, and an isolation valve. Because of KC-135 test time limitations, the air injection system outlet was intentionally positioned near the entrance of the flowmeter test article to minimize the time between gas injection initiation and actual test article gas ingestion. The receiving water tank had a 0.19-cubic-meter (48.9 gallon) capacity. The tank was operated at the water vapor pressure to allow a relatively constant flow rate throughout each test flow, although some pressure rise observed during two-phase

flow testing did have a minor effect on flow rates. The PFTS control panel incorporated controls to activate and deactivate waterflow, controls for the vacuum system, and a synchronization (sync) trigger. The sync trigger was manually activated and deactivated by the PFTS operator and produced a single step signal that was initiated and terminated to bracket (mark) any phenomenon of interest. One of two methods was used to record zero-g testing data. In the first method, data were recorded in real time using a Sabre 80 tape recording system and were later transferred to a four-channel Nicolet digital oscilloscope (model 4094) information storage format for evaluation. In the second method, data were recorded using a Fluke 1752A data acquisition system, which allowed immediate data evaluation during the test. The vibration test data were recorded directly on the Nicolet or the Fluke system. The overall test system flow measurement uncertainty was ±0.15 percent using the root sum of the squares of the individual data acquisition components.

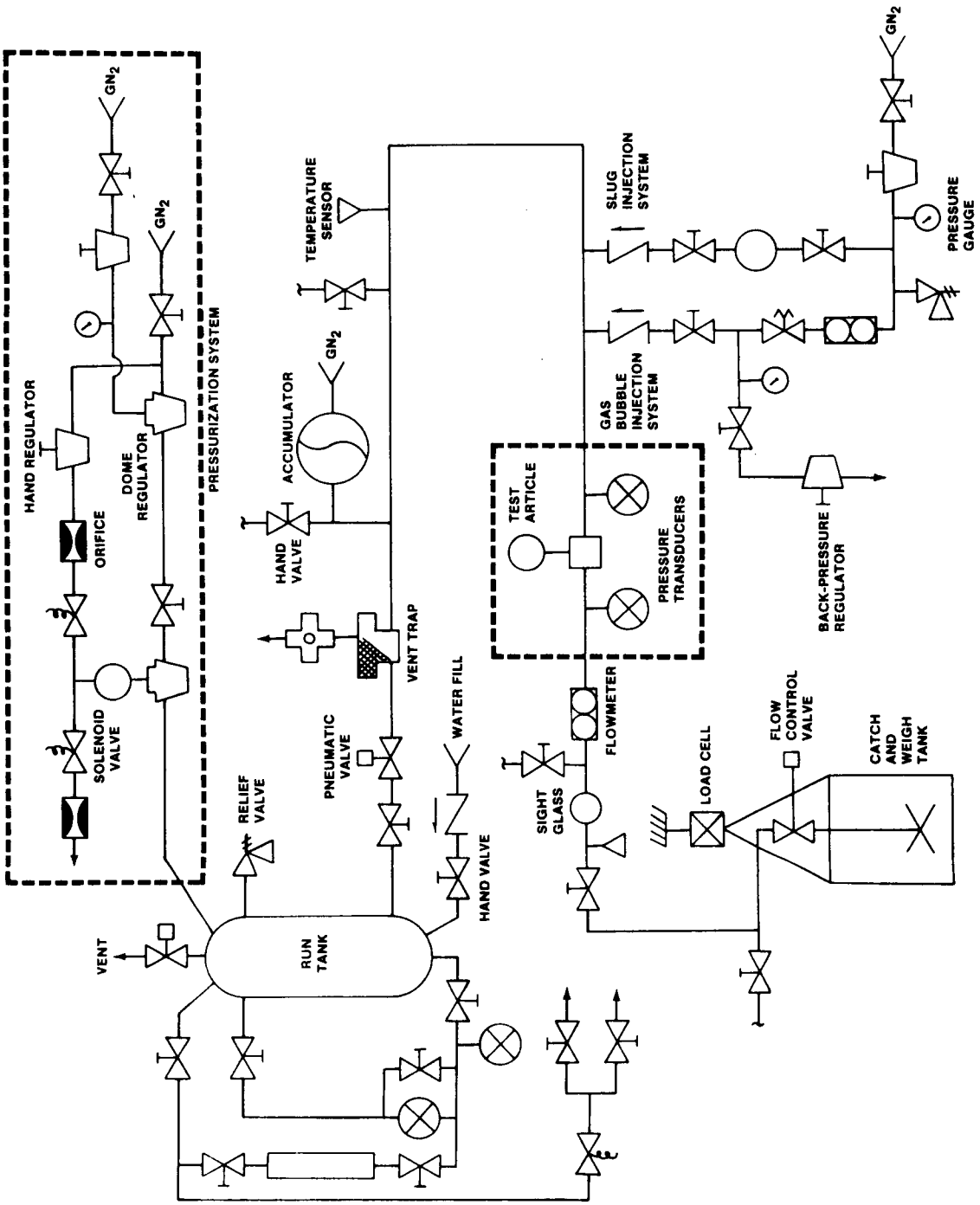

Figure 2-1.- Ground flow test facility schematic.

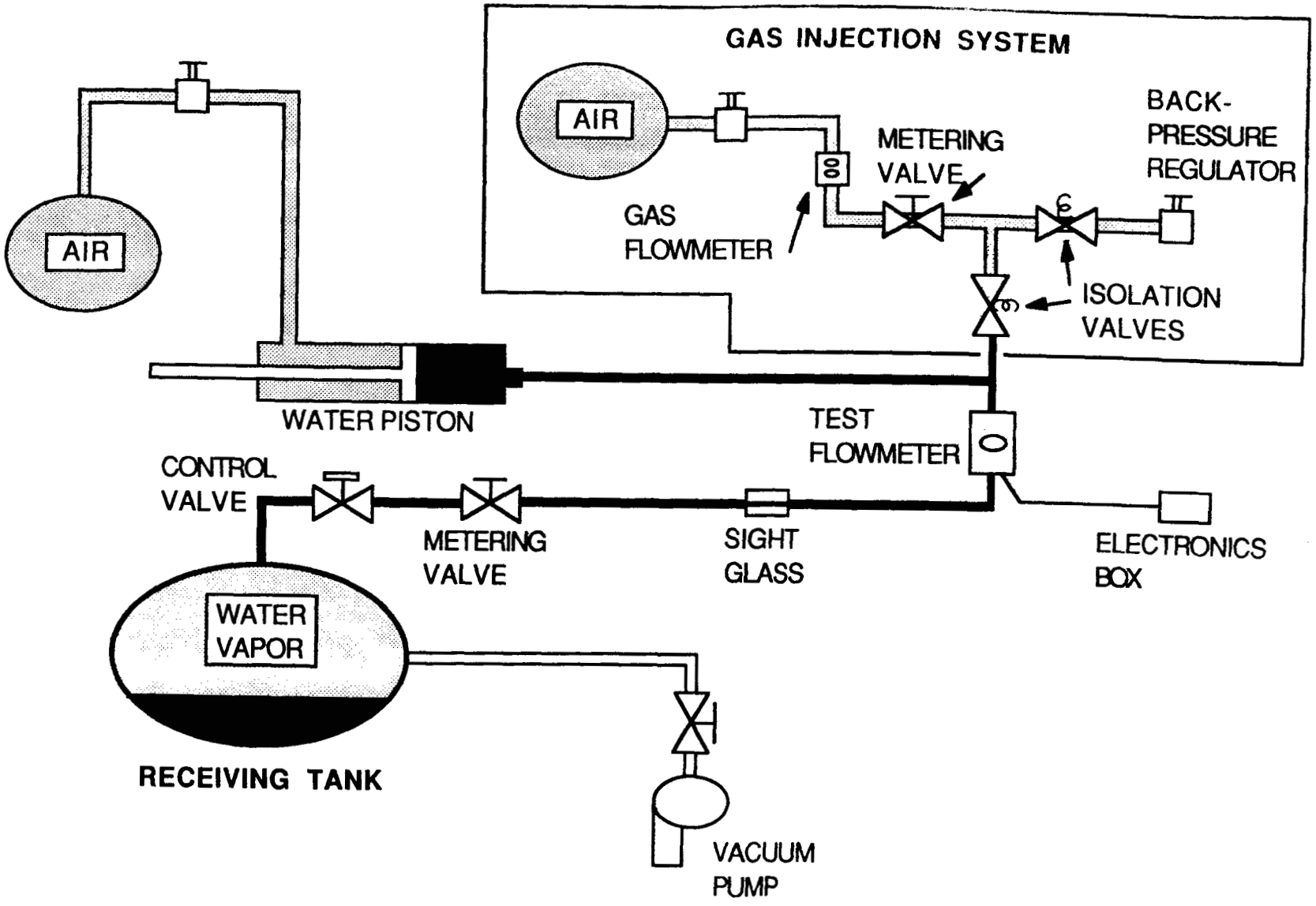

Figure 2-2.- Portable flow test stand schematic.

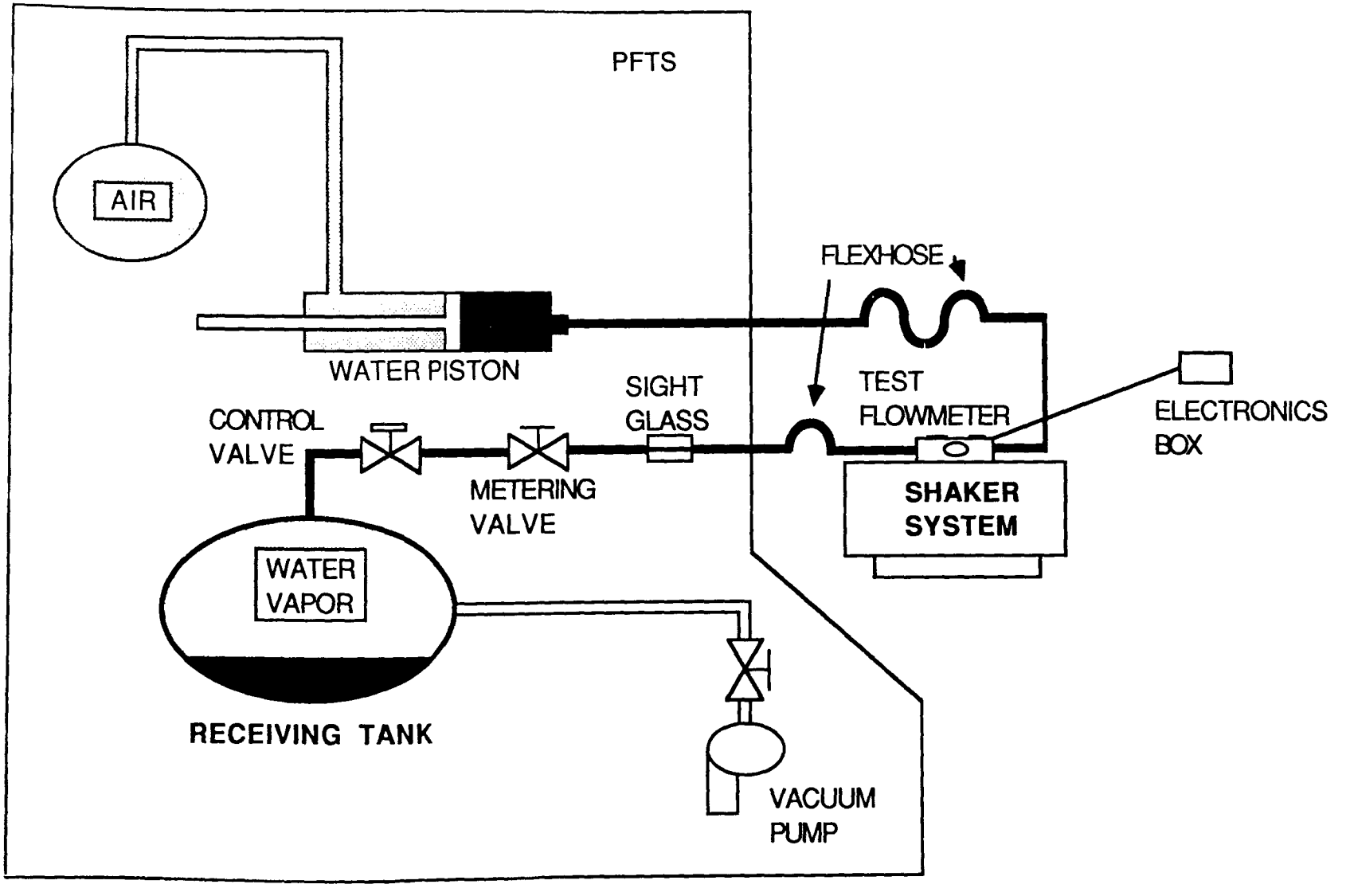

Figure 2-3.- Portable flow test stand in vibration test configuration.

3.0 TEST PROGRAM DISCUSSIONS

GROUND FLOW TESTING

Ground flow testing for most of the flowmetering concepts was performed in four phases. Phase I consisted of operating the test article under prolonged steady-state flow conditions at various flow rates. Phase II testing was identical to the steady-state testing except that the control valve was repeatedly cycled open and closed at equal intervals throughout the test run to effectively expose the test article to pulse flow conditions. Flowmeter performance for a wide range of cycle frequencies for one or more flow rates was tested. In phase III, test article performance was evaluated under general steady-state flow conditions with gas bubble ingestion. Various steady flow rates of GN_2 bubbles were injected into the flow just upstream of the test article. Phase IV testing consisted of injecting various sized GN_2 slugs (total liquid displacement) into the flow stream while operating the test article under steady-state flow conditions. Multiple tests were performed at each flow condition (flow rate, gas injection rates, etc.) for flowmeter nonrepeatability evaluation during all four phases.

ZERO-g FLOW TESTING

Zero-g testing was performed in two stages. The first stage consisted of ground steady-state and gas ingestion flow testing of the test article in the PFTS. This testing was done to establish baseline flowmeter performance for comparison with results from the zero-g testing and from previous non-PFTS ground flow testing. The second stage was the actual zero-g steady-state and gas ingestion flow testing in the KC-135.

Zero-g flow testing was constrained to within the null-gravity portion of the KC-135 maneuver. As shown in figure 3-1, the KC-135 abruptly pitches over when the aircraft approaches the apex of the maneuver at an altitude of approximately 10.4 kilometers (34 000 feet) and all aircraft cargo enter into near zero-g (free fall) conditions. This free-fall condition could repeatedly be maintained down to acceleration levels of 0.02g for periods of approximately 17 to 20 seconds.

VIBRATION TESTING

The vibration test program consisted of three phases. In phase I, the test article was exposed to low- to high-frequency sine vibration sweeps at several acceleration amplitude levels. In phase II, the test article was subjected to sine frequencies which had been found in phase I to interrupt flowmeter test article outputs or to produce large responses in the surface-mounted accelerometers. In both phases I and II, the test flowmeter was exposed to waterflow during testing via the PFTS. In phase III, random vibration testing was conducted to simulate Space Shuttle launch environments (fig. 3-2).

The general procedures for phases I and II were similar. Waterflow was initiated through the flowmeter test article. After steady-state flow

was established, the sync trigger was manually activated. A few seconds after trigger activation, the test article was subjected to the appropriate vibration environment. After vibration termination, the sync trigger was deactivated, waterflow terminated, and data recording stopped. Several test runs were performed at each flow/vibration condition.

Phase III Space Shuttle launch vibration environment testing was performed under no-flow conditions. After vibration exposure, the test article flow performance was tested. This vibration test sequence was performed for each of the flowmeter axes tested. The data recorded during phase III were the same as those recorded for phases I and II.

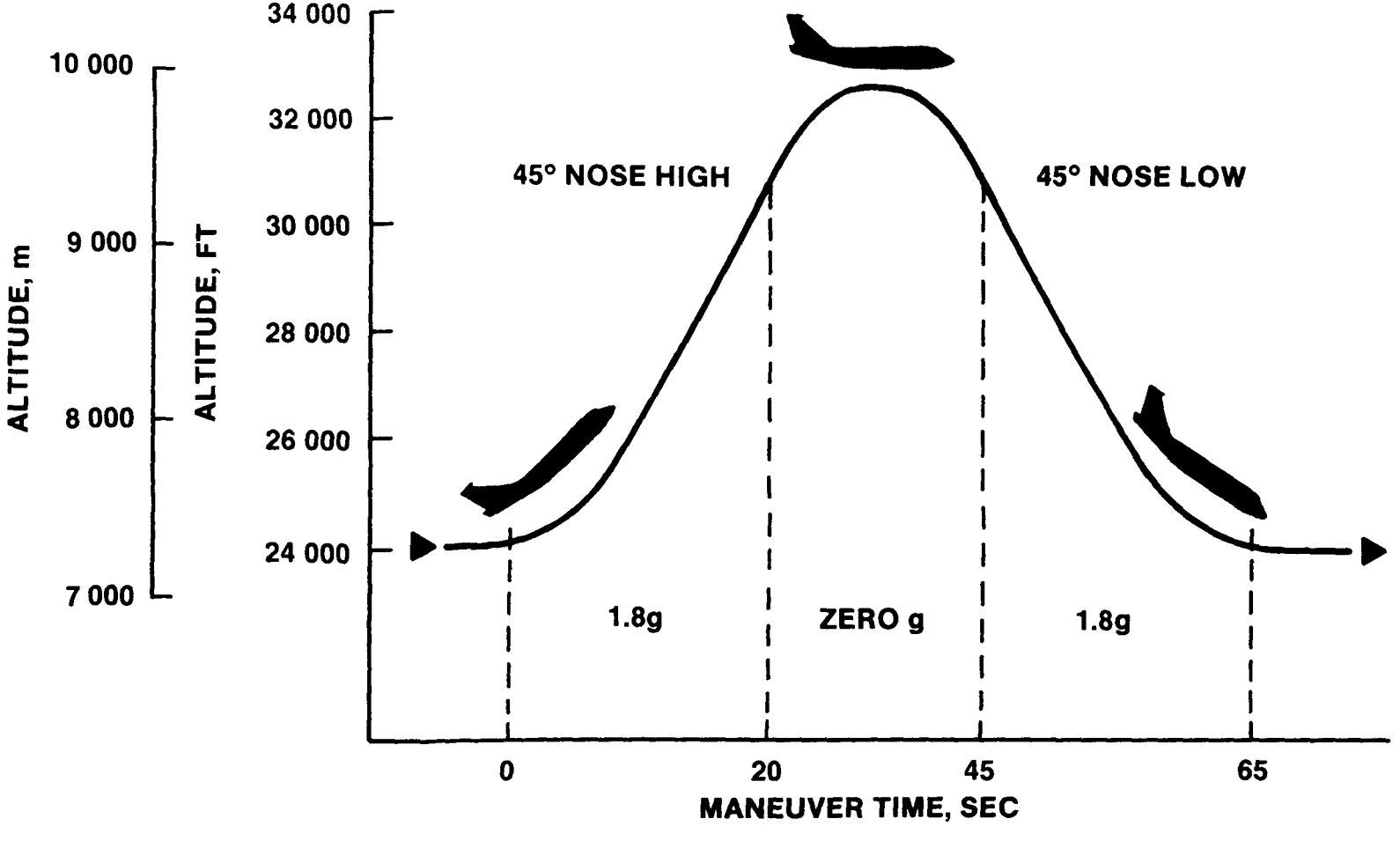

Figure 3-1.- KC-135 aircraft trajectory to establish zero-g environment.

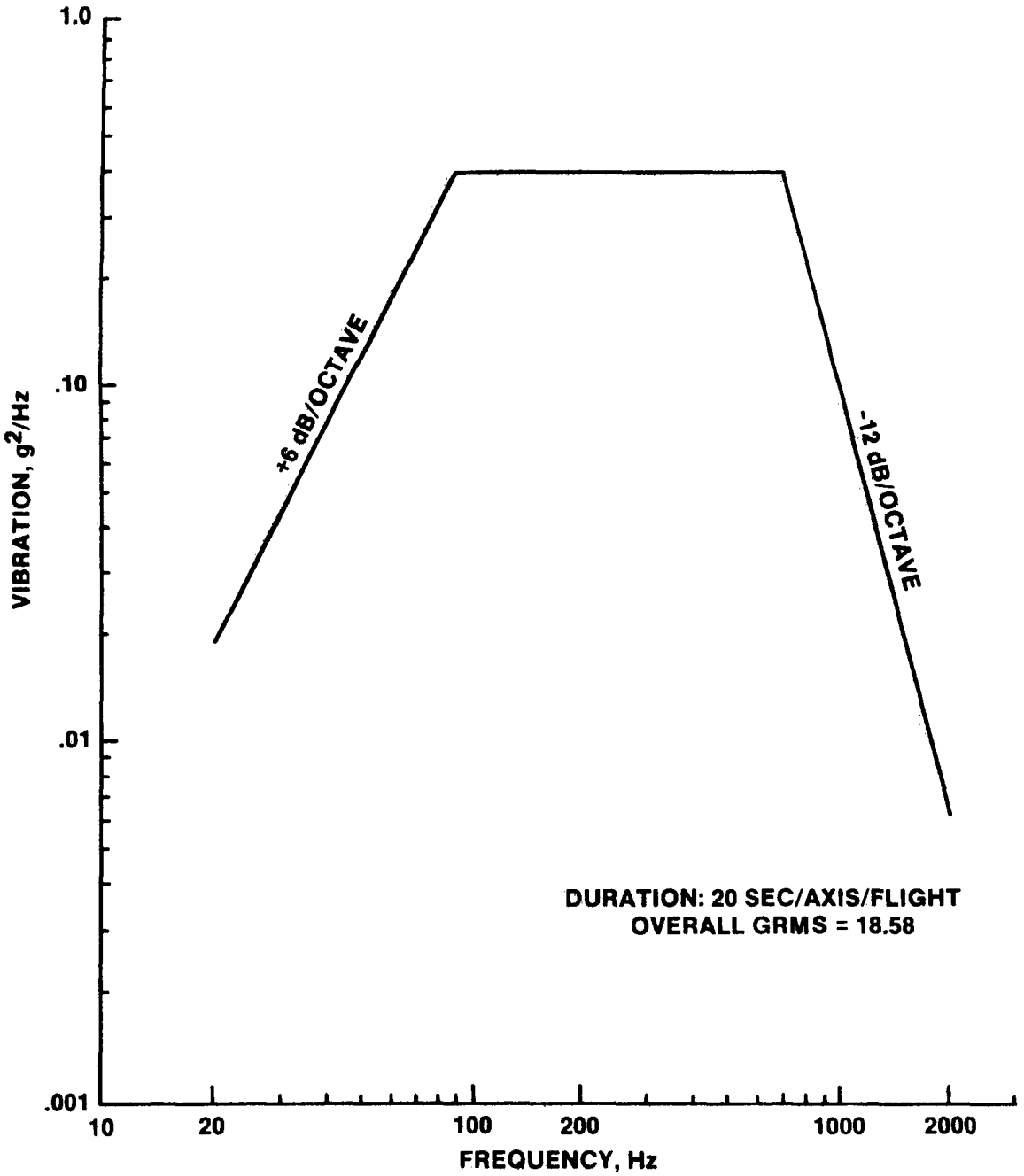

Figure 3-2.- Space Shuttle launch environment criteria (random vibration).

4.0 FLOWMETER PERFORMANCE EVALUATION DISCUSSIONS

All of the flowmetering techniques investigated in this test program were tested to common (steady-state, pulse, and gas ingestion) flow conditions. Selected performance results from these tests, as well as flowmeter theory and manufacturer's specifications, are presented in this section to outline the major capabilities and limitations uncovered for each flowmetering technique investigated. Approximate SI unit equivalents have been included in the data (text and graphics) presented in this section in addition to the original English units.

4.1 CLAMP-ON ULTRASONIC FLOWMETER

FLOWMETER DESCRIPTION

Clamp-on ultrasonic flowmetering is accomplished by using opposed, axially displaced transducers clamped to the exterior of the flow pipe. These transducers alternately send and receive ultrasonic pulses to and from one another. The pulses sent in the direction of flow have a shorter transit time across the flow than have pulses sent against the flow. The difference in transit times can be measured and correlated to flow velocity (figs. 4.1-1(a) and 4.1-1(b)). In the clamp-on configuration, the ultrasonic pulses pass through the entire flow profile. Theoretically, identification of the Reynolds number of the fluid flow should permit accurate flow profile compensation. Also, this configuration should not be affected by mount-induced low profile aberrations and echo chamber sonic beam interference because of its nonwetted transducer configuration.

The flowmeter tested was the 0.04-meter (1.5 inch) Controlotron 48-MP clamp-on ultrasonic flowmeter. It consisted of an electronics package and two nonintrusive (nonwetted) 481 transducers. The transducers (P/N 481 PF-SS3.61-EP2D116-B25962B) were clamped to a 0.04-meter (1.5 inch), schedule 40 stainless steel pipe by means of incremented mounting tracks (P/N 482 MT P-1.500SS40-1P2D116-B). This tracked clamping mechanism ensured proper alignment and spacing of the transducers. A 484-MP flow display computer (P/N 484 MP F1AF-8 25959B) was used to compute the liquid flow velocity based on differential transit time of signals and ensured proper data scaling under control of the plug-in 483 scale module. This plug-in module was programmed by the manufacturer before testing in accordance with the pipe dimensions and sonic properties. The flow velocity data were converted to analog and digital formats within the 484-MP flow display computer to service the digital, analog, and totalizer displays.

The manufacturer's stated specifications for the system are as shown in table 4.1-1.

FLOWMETER PERFORMANCE

Flowmeter performance produced the following results and recommendations.

1. The steady-state flow error ranged as high as 3 percent for an uncalibrated meter out to a turndown ratio of 16. The averaged errors of each set of three runs were all positive (i.e., the meter was reading higher than actual). Adjusting the K-factor downward by 2 percent would bring the calibrated meter error to within ±1 percent rate error over the same turndown ratio range (fig. 4.1-2).

2. The steady-state nonrepeatability of the test article was within ±1.1 percent for turndown ratios of 16 and less (fig. 4.1-3).

3. The steady-state nonlinearity ranged between ±0.3 percent and ±1.2 percent out to turndown ratios of 36 (fig. 4.1-4).

4. Pulse flow dramatically reduced flow measurement accuracy as the pulse width (1/pulse frequency) decreased (fig. 4.1-5). The flow display computer digital display did not indicate pulse flow at any time during pulse flow testing.

5. Although two-phase flow (i.e., gas bubble and slug injection) did produce an increase in flow measurement error and analog output signal noise, the meter still continued to function with a gas content as high as 6.3 percent by volume of total flow. Gas slugs momentarily interrupted the analog output of the meter but were not indicated on the flow display computer digital display. The gas slugs produced measurable analog output reductions that did not closely approximate the actual slug volumes.

6. Two-phase flow measurement errors would not improve if the meter K-factor were decreased by 2 percent. (See item 1.) Two-phase flow errors were more evenly distributed about the zero-percent value than were the steady-state errors, and reducing the K-factor would increase this error in most cases.

7. It is recommended that some type of entrained gas or intermittent flow indicator be incorporated into the real-time display of this flowmeter. The analog output and the totalizer give good indications of these conditions, but the digital display does not. Unfortunately, the digital display was the only readily available indication of the ongoing flowmeter operations.

TABLE 4.1-1.- CLAMP-ON ULTRASONIC FLOWMETER MANUFACTURER'S SPECIFICATIONS[a]

Manufacturer	Controlotron
Calibration inaccuracy (5-min integration), percent	
Intrinsic	1 to 3
Flow calibrated	0.25 to 1
Flow parameters, m/sec (ft/sec)	
Flow sensitivity (10-sec integration, at any flow rate)	3.05×10^{-4} (0.001)
Linearity (5-min integration)	3.05×10^{-3} (0.01)
Repeatability (5-min integration)	3.05×10^{-3} (0.01)
Zero drift (5-min integration)	3.05×10^{-3} (0.01)
Minimum flow range	±12.19 (±40)

[a]Not investigated in this test program.

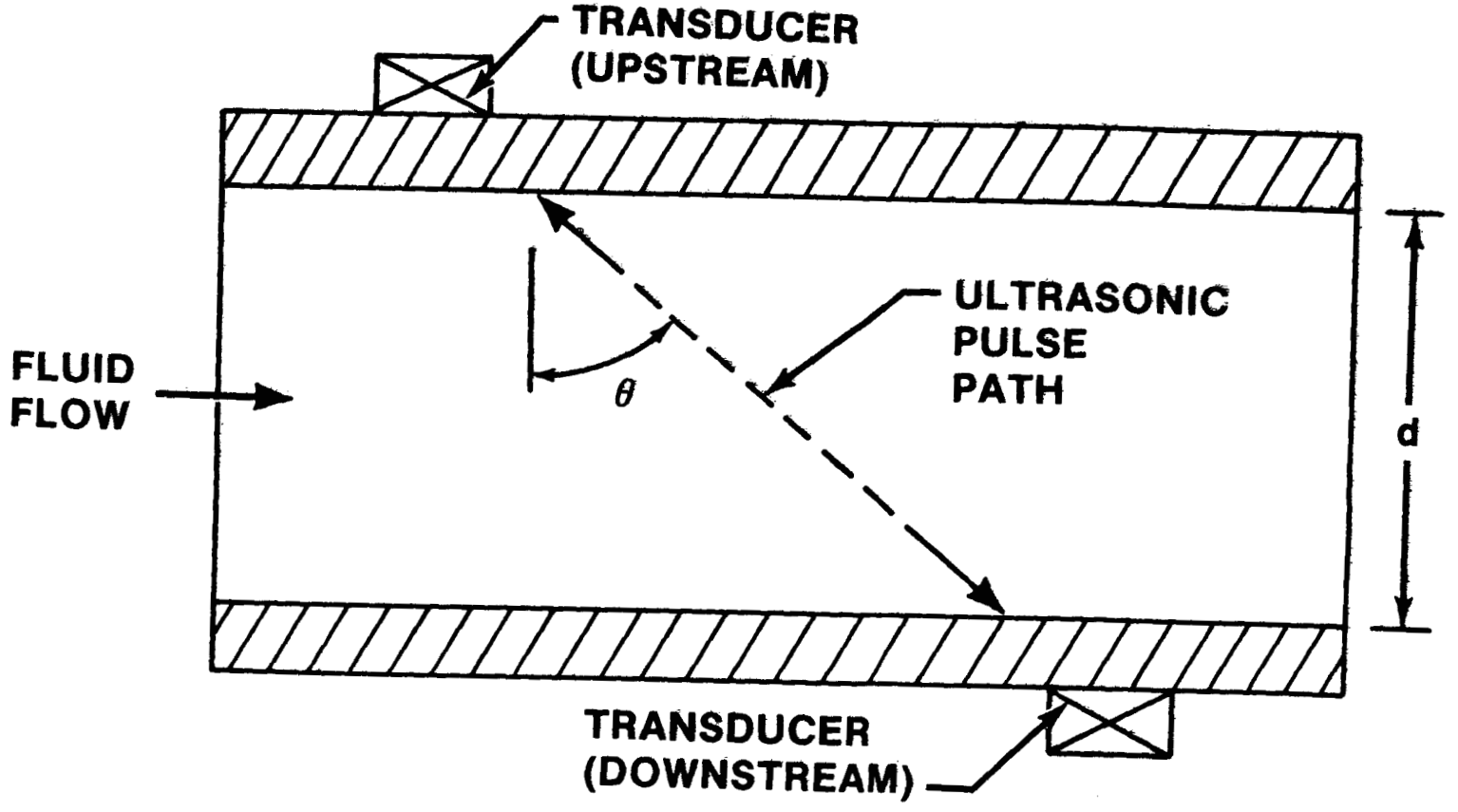

(a) Schematic diagram.

Figure 4.1-1.- Clamp-on ultrasonic flowmeter.

$$V = ((T_u - T_d)V_s/\sin\theta)\ (V_s \cos\theta/d)$$

$$\Delta T = T_u - T_d$$

$$T_L = d/V_s \cos\theta$$

$$V = ((\Delta T)V_s/\sin\theta)\ (1/T_L)$$

$$K = V_s/\sin\theta$$

$$V = K(\Delta T)/T_L$$

$$Q = AV$$

$$Q = AK(\Delta T)/T_L$$

Where:

V	Flow velocity
V_s	Fluid sonic velocity
T_u	Pulse transit time upstream
T_d	Pulse transit time downstream
ΔT	Upstream vs. downstream pulse transit time difference
T_L	Minimum pulse transit time across pipe diameter d
d	Flow diameter
A	Flow area
θ	Angle between transducers
Q	Volumetric flow rate

(b) Equations and symbol definitions.

Figure 4.1-1.- Concluded.

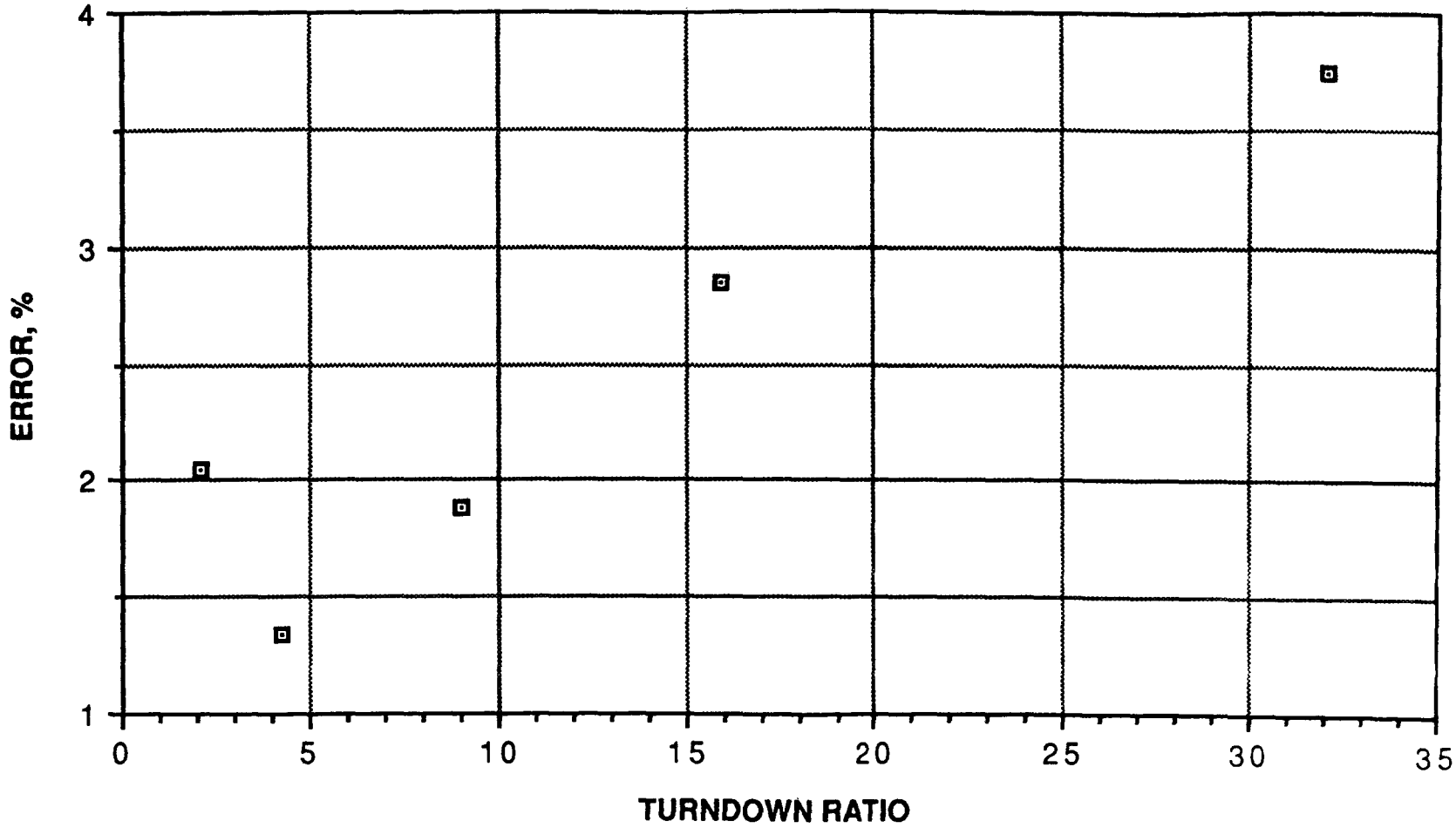

Figure 4.1-2.- Clamp-on ultrasonic flowmeter steady-state error versus turndown ratio.

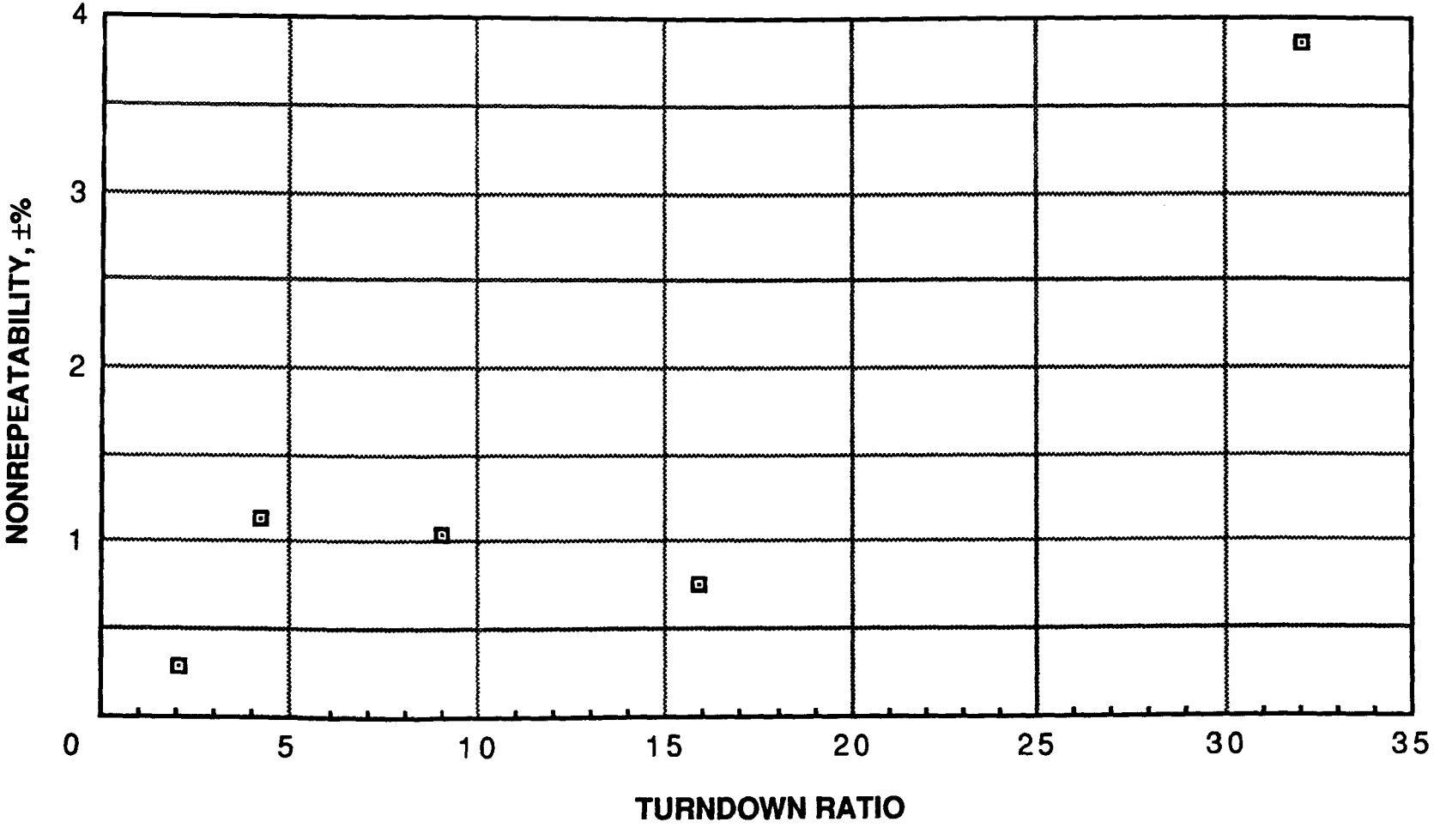

Figure 4.1-3.- Clamp-on ultrasonic flowmeter steady-state nonrepeatability versus turndown ratio.

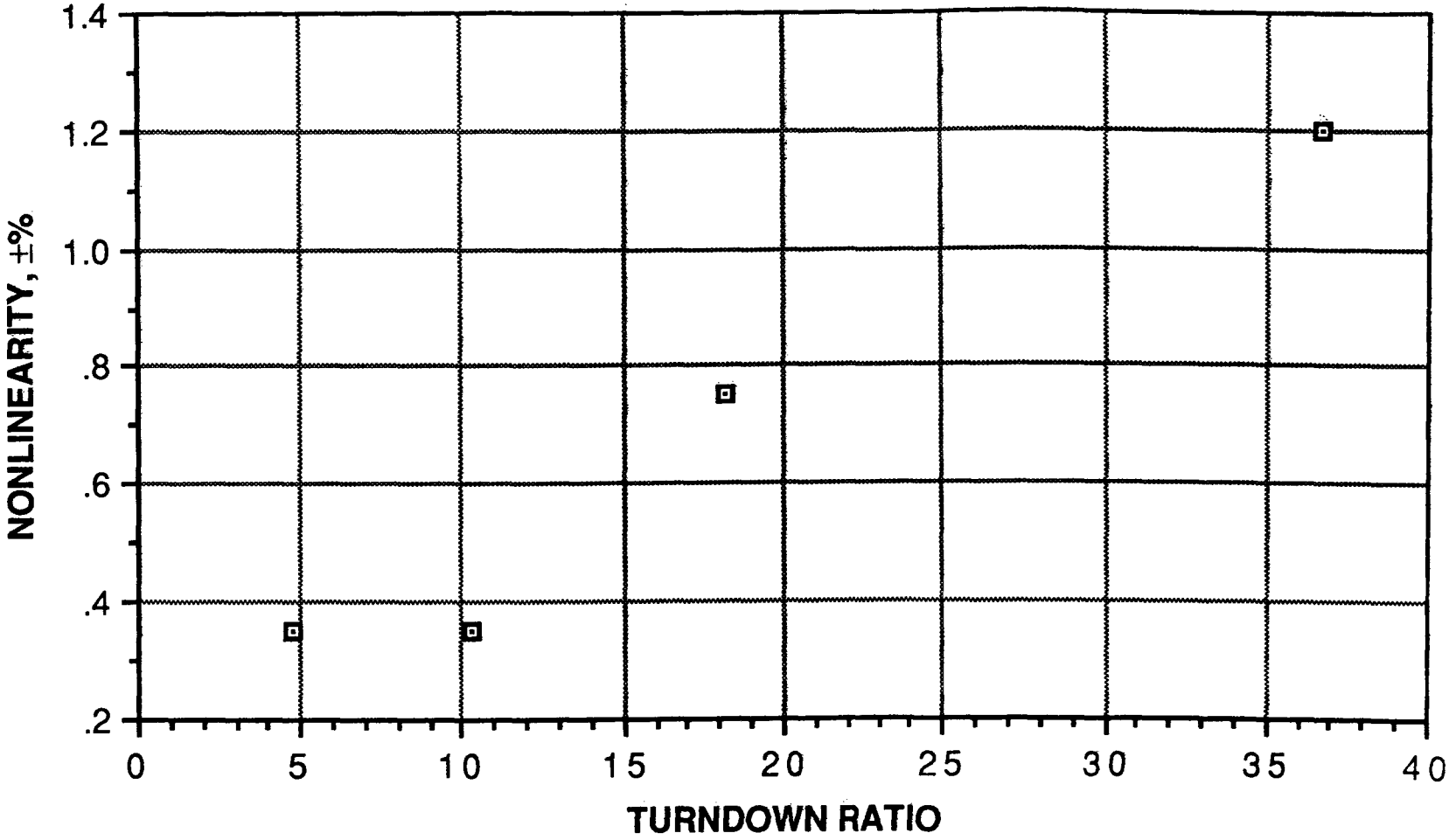

Figure 4.1-4.- Clamp-on ultrasonic flowmeter steady-state nonlinearity versus turndown ratio.

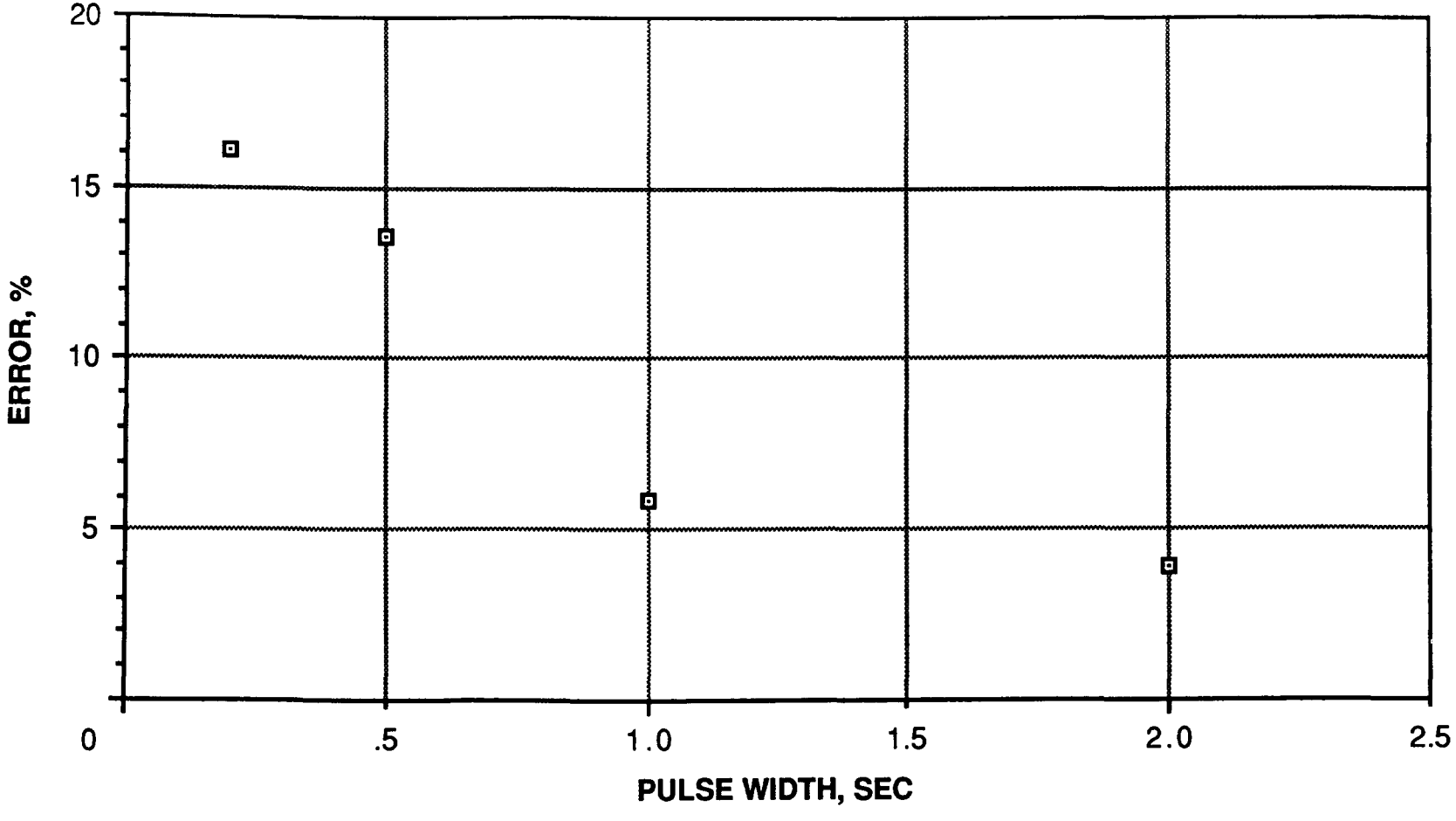

Figure 4.1-5.- Clamp-on ultrasonic flowmeter pulse flow overall error versus pulse width.

4.2 AREA AVERAGING ULTRASONIC FLOWMETER

FLOWMETER DESCRIPTION

The technique used in the area averaging ultrasonic flowmetering concept is the standard ultrasonic flowmetering technique of sending ultrasonic pulses upstream and downstream of the flow stream being metered and of comparing differences in pulse traveltime to calculate flow rate (fig. 4.2-1(b)). This standard technique has been modified in two significant ways for use in the area averaging flowmeter. First, the interior (fig. 4.2-1(a)) cross-sectional flow area of the metering pipe is square, theoretically making the flow field more uniform and flow rate calculations more accurate. The second difference is that the ultrasonic pulse is reflected off of the metering pipe walls one or more times before being received by the second transducer. The use of multiple passes through the fluid increases the traveltime differences between the upstream and downstream pulses and thereby makes flow-rate calculations more accurate.

The test article examined was the 0.04-meter (1.5 inch) Panametrics area averaging flowmeter. The flowmeter system consisted of the 0.04-meter (1.5 inch) square cross-section flow cell body, two ultrasonic transducers, and the flowmeter microprocessor (model 6001). The manufacturer's specifications for the test article are given in table 4.2-1. However, this particular flow cell is a factory prototype; therefore, these performance specifications may not necessarily be accurate for the final configuration of this flowmeter.

FLOWMETER PERFORMANCE

Flowmeter performance results were as follows.

1. Steady-state K-factor nonlinearity ranged from ±3.7 percent to ±16.1 percent over the flow range tested (fig. 4.2-2).

2. Steady-state nonrepeatability ranged from ±0.15 percent to ±22.2 percent. The best performance of the test article was in the middle portion of the flow range tested (fig. 4.2-3).

3. The test article performed erratically at turndown ratios below 1.2 at steady-state flow conditions.

4. The gas injection error from steady state ranged from -2.5 percent to -28.2 percent (fig. 4.2-4) over the gas flow range tested. The nonrepeatability was erratic over the same flow range.

5. No pulse flow or gas slug ingestion flow testing was performed on this test article because of the transient response limitations of the test article electronics.

TABLE 4.2-1.- AREA AVERAGING ULTRASONIC FLOWMETER MANUFACTURER'S SPECIFICATIONS[a]

Manufacturer	Panametrics
Range, m/sec (ft/sec)	0.03 to 9.1 (0.1 to 30)
Turndown ratio	300:1
Accuracy, percent of full scale	1
Repeatability, percent of full scale	0.2
Operating temperature, K (°C)	263 to 328 (-10 to 55)
Output, V	0 to 1

[a]Not investigated in this test program.

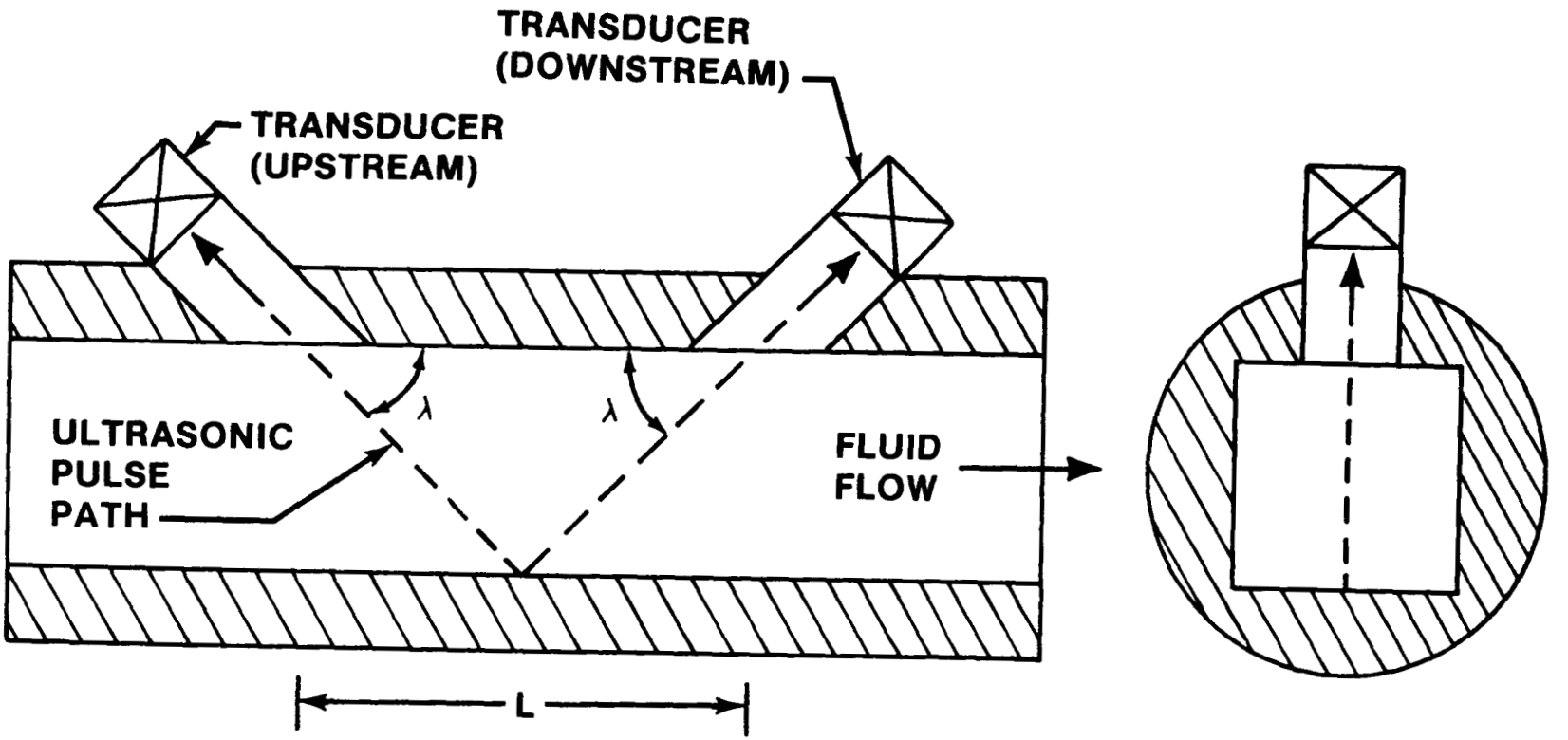

(a) Schematic diagram.

Figure 4.2-1.- Area averaging ultrasonic flowmeter.

$$T_u = L/(V_s \cos \lambda - V)$$

$$T_d = L/(V_s \cos \lambda + V)$$

$$\Delta T = T_u - T_d = T_u Z_u - T_d Z_d$$

$$Z_u = (V_s \cos \lambda + V)/(V_s \cos \lambda + V)$$

$$Z_d = (V_s \cos \lambda - V)/(V_s \cos \lambda - V)$$

$$\Delta T = 2LV/(V_s^2 \cos^2 \lambda - V^2)$$

$$\Delta T \approx 2LV/ZV_s^2$$

For: $V \ll V_s$

$$Z = \cos^2 \lambda$$

$$V \approx ZV_s^2(\Delta T)/2L$$

$$Q = AV$$

$$Q = ACZV_s^2(\Delta T)/2L$$

Where:

V	Flow velocity
V_s	Fluid sonic velocity
L	Axial projection of ultrasonic wave in fluid
P	Pulse path length in fluid
A	Flow area
T_d	Pulse transit time downstream
T_u	Pulse transit time upstream
C	Calibration constant
Q	Volumetric flow rate

(b) Equations and symbol definitions.

Figure 4.2-1.- Concluded.

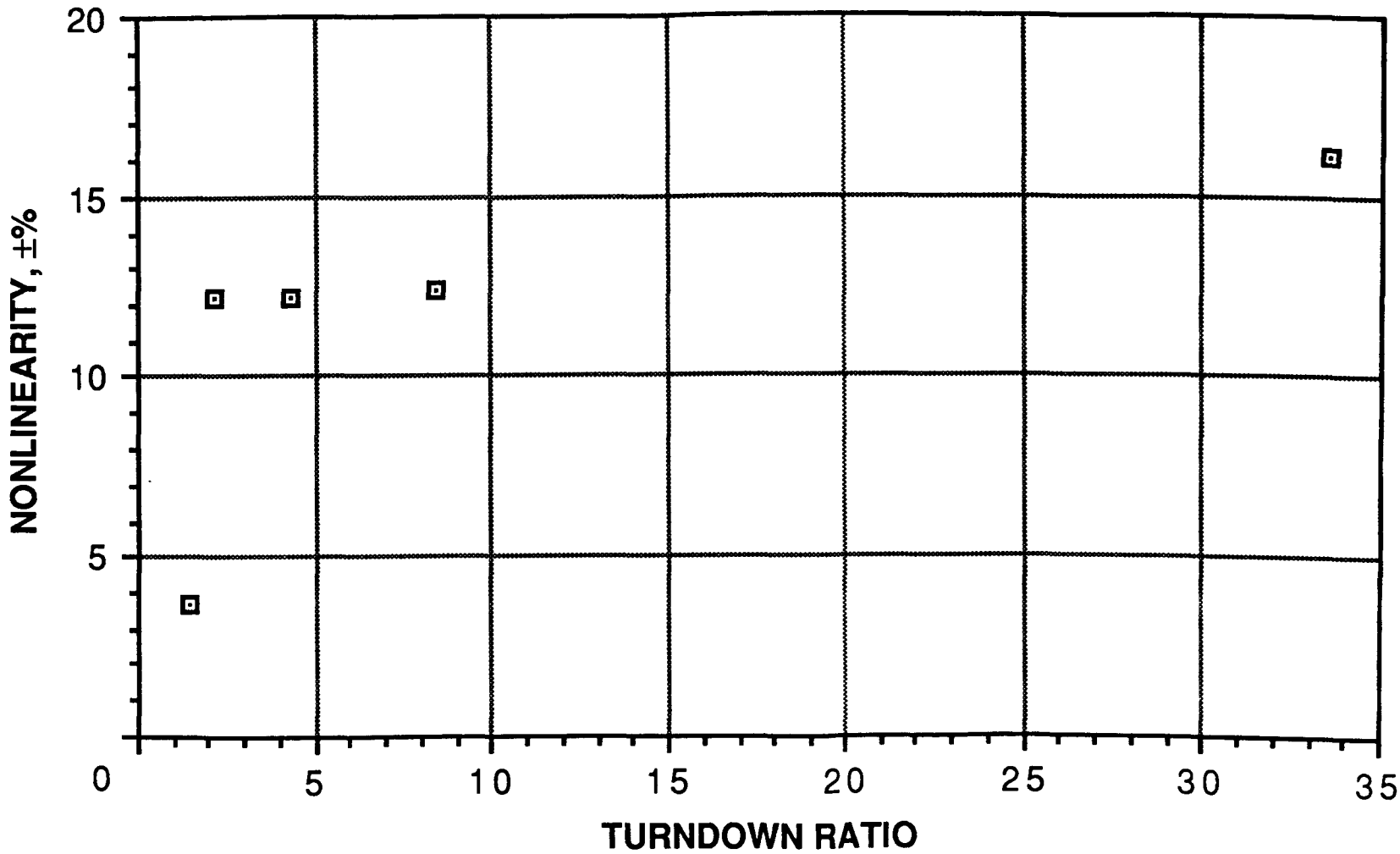

Figure 4.2-2.- Area averaging ultrasonic flowmeter steady-state nonlinearity versus turndown ratio.

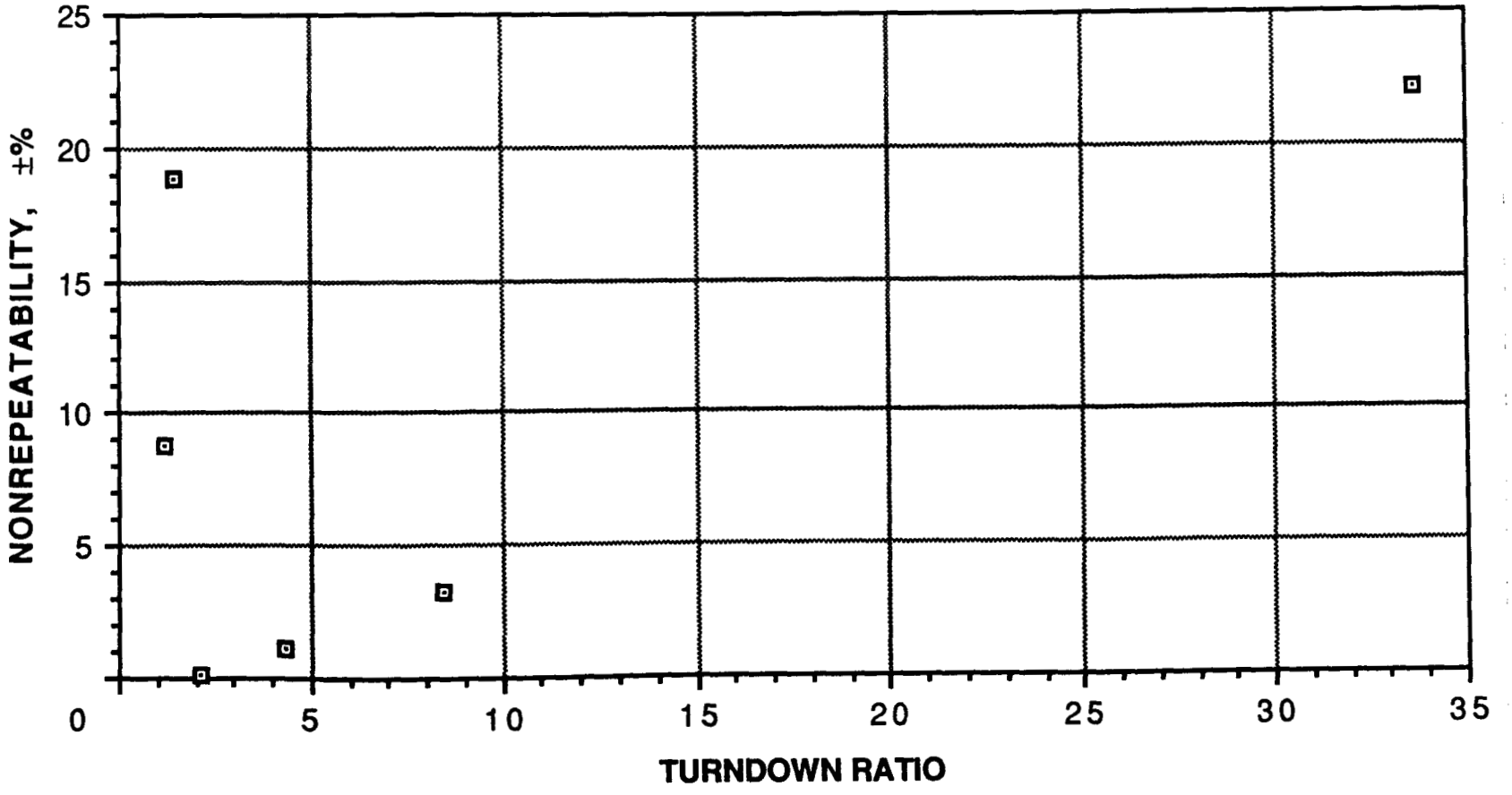

Figure 4.2-3.- Area averaging ultrasonic flowmeter steady-state nonrepeatability versus turndown ratio.

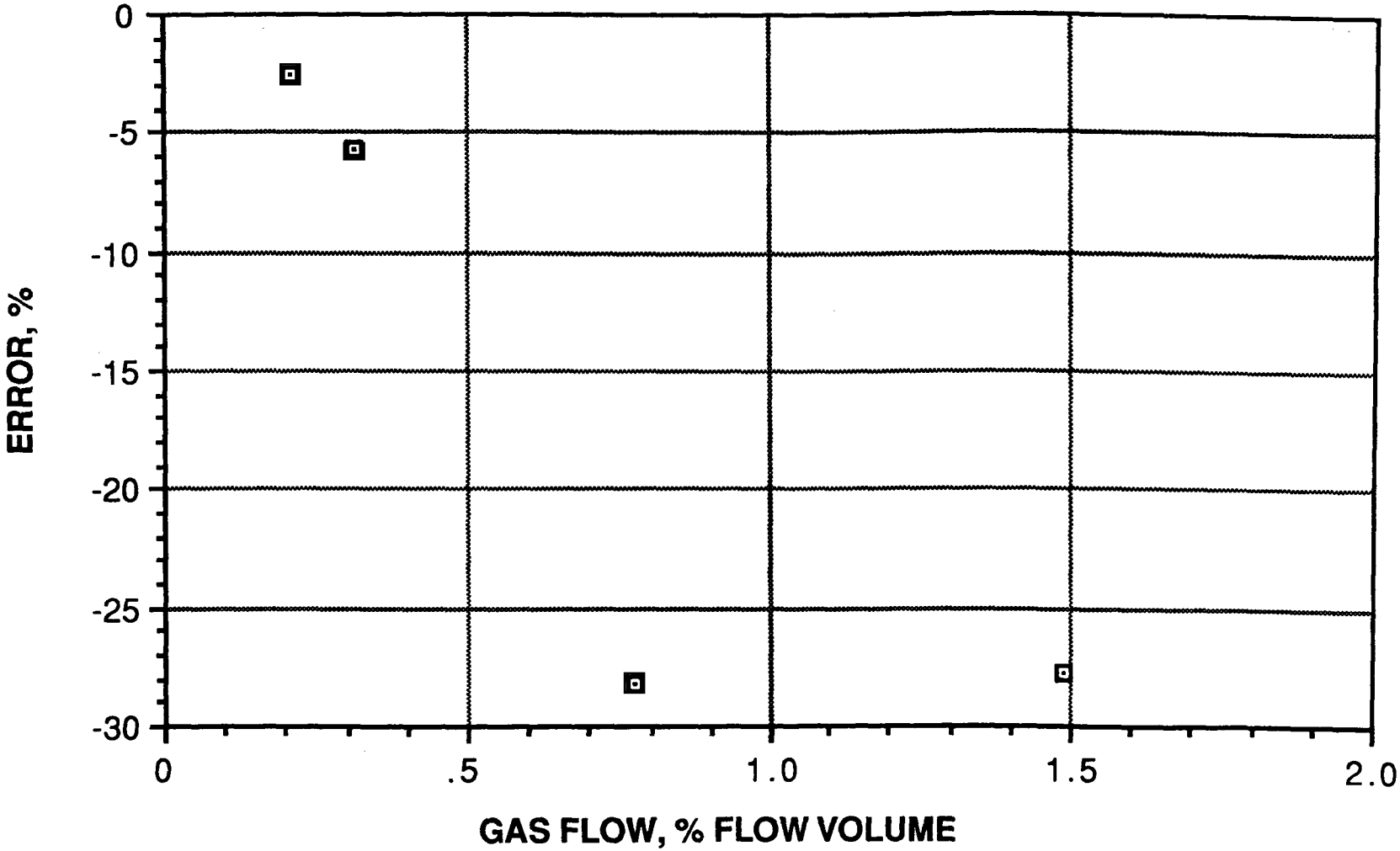

Figure 4.2-4.- Area averaging ultrasonic flowmeter two-phase flow error versus gas flow.

4.3 OFFSET ULTRASONIC FLOWMETER

FLOWMETER DESCRIPTION

The offset ultrasonic flowmetering concept uses the standard ultrasonic flowmetering technique of sending ultrasonic pulses upstream and downstream of the flow stream being metered, and comparing differences in pulse traveltime to calculate flow rate (fig. 4.3-1(b)). The offset flowmeter (fig. 4.3-1(a)) is different from other ultrasonic flowmeters in that the pulse path is straight along the flow between the transducers and the fluid flow path is diverted 45° at both the entrance and the exit of the flow cell. The single, long pulse path increases the traveltime differences between the upstream and downstream pulses and, thereby, theoretically makes flow rate calculation more accurate.

The test article examined consisted of the 0.013-meter (0.5 inch), 45° inlet/outlet offset flowmeter flow cell, two ultrasonic transducers, and the Panametrics model 6001 flowmeter microprocessor. The manufacturer's specifications are the same as for the area averaging flowmeter (table 4.2-1).

FLOWMETER PERFORMANCE

Performance results are as follows.

1. The steady-state K-factor nonlinearity ranged from ±2.4 percent to ±8.5 percent over the turndown ratio range tested (fig. 4.3-2).

2. Steady-state nonrepeatability ranged from ±1.06 to ±12.15 percent over the turndown ratio range tested (fig. 4.3-3).

3. Gas ingestion flow error from steady state ranged from -42.33 percent to 61.37 percent (fig. 4.3-4) over the gas flow range tested.

4. No pulse flow or gas slug ingestion flow testing was performed on this test article because of the transient response limitations of the test article electronics.

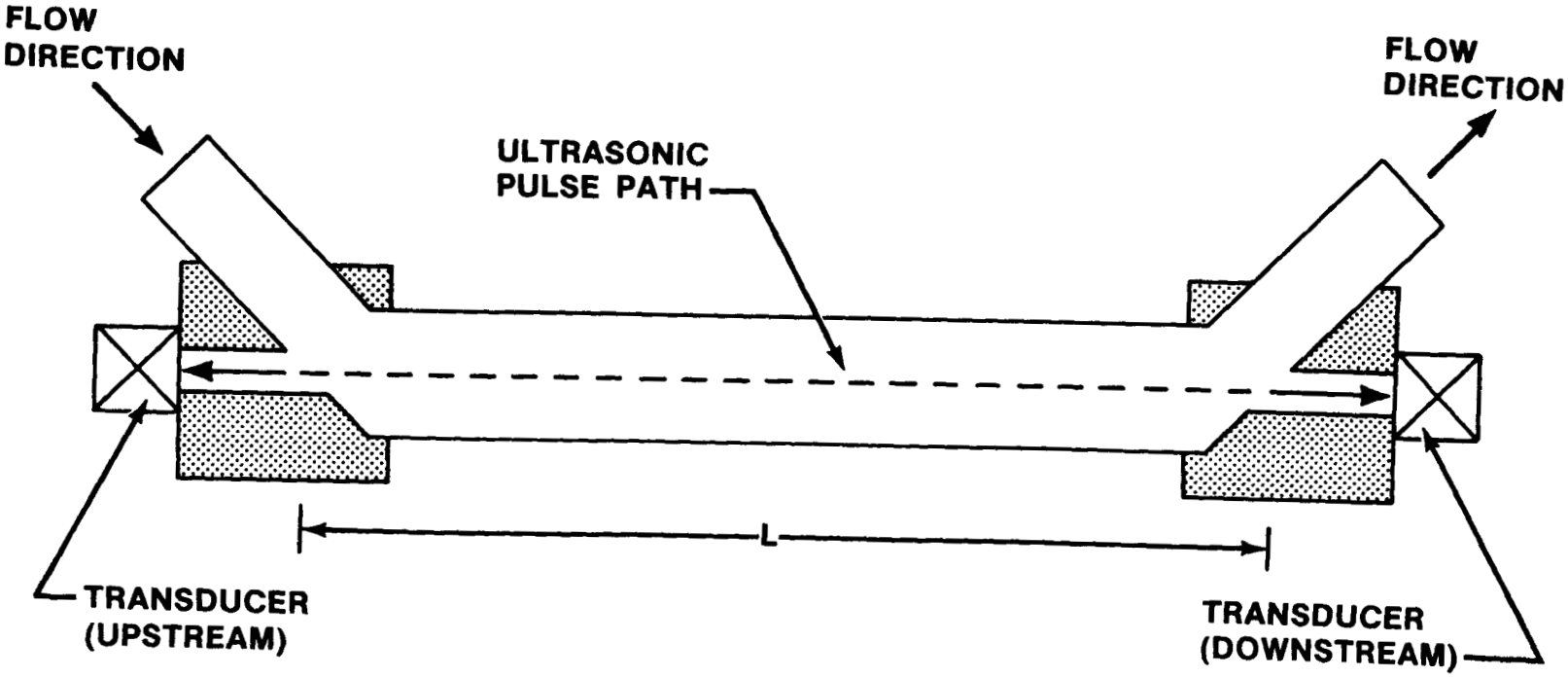

(a) Schematic diagram.

Figure 4.3-1.- Offset ultrasonic flowmeter.

$$T_u = L/(V_s - V)$$

$$T_d = L/(V_s + V)$$

$$\Delta T = T_u - T_d = T_u Z_u - T_d Z_d$$

$$Z_u = (V_s + V)/(V_s + V)$$

$$Z_d = (V_s - V)/(V_s - V)$$

$$\Delta T = 2LV/(V_s^2 - V^2)$$

$$\Delta T \approx 2LV/V_s^2$$

For: $V \ll V_s$

$$V \approx V_s^2(\Delta T)/2L$$

$$Q = AV$$

$$Q = ACV_s^2(\Delta T)/2L$$

Where:

V	Flow velocity
V_s	Fluid sonic velocity
L	Axial projection of ultrasonic wave in fluid
P	Pulse path length in fluid
A	Flow area
T_d	Pulse transit time downstream
T_u	Pulse transit time upstream
C	Calibration constant
Q	Volumetric flow rate

(b) Equations and symbol definitions.

Figure 4.3-1.- Concluded.

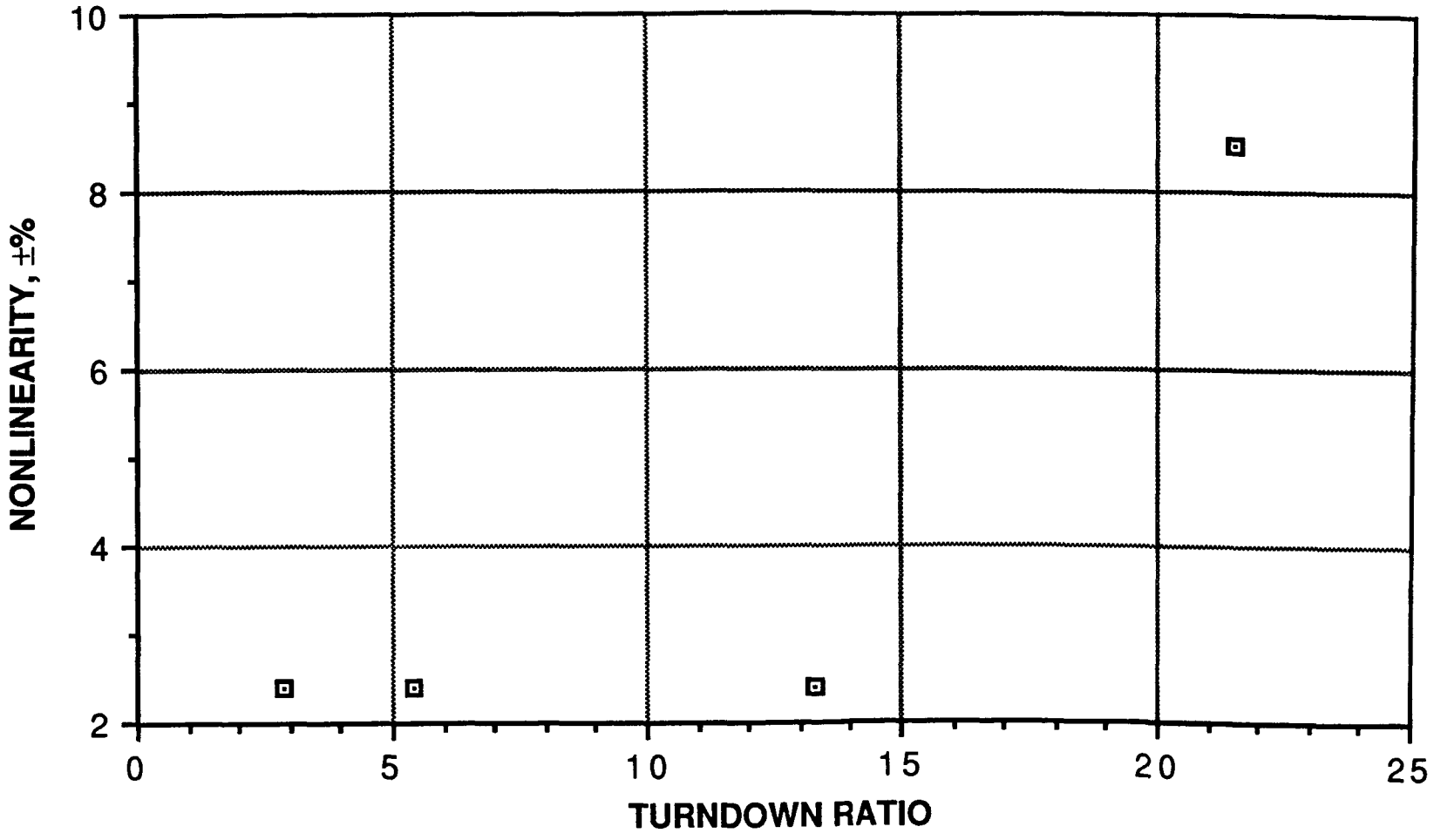

Figure 4.3-2.- Offset ultrasonic flowmeter steady-state nonlinearity versus turndown ratio.

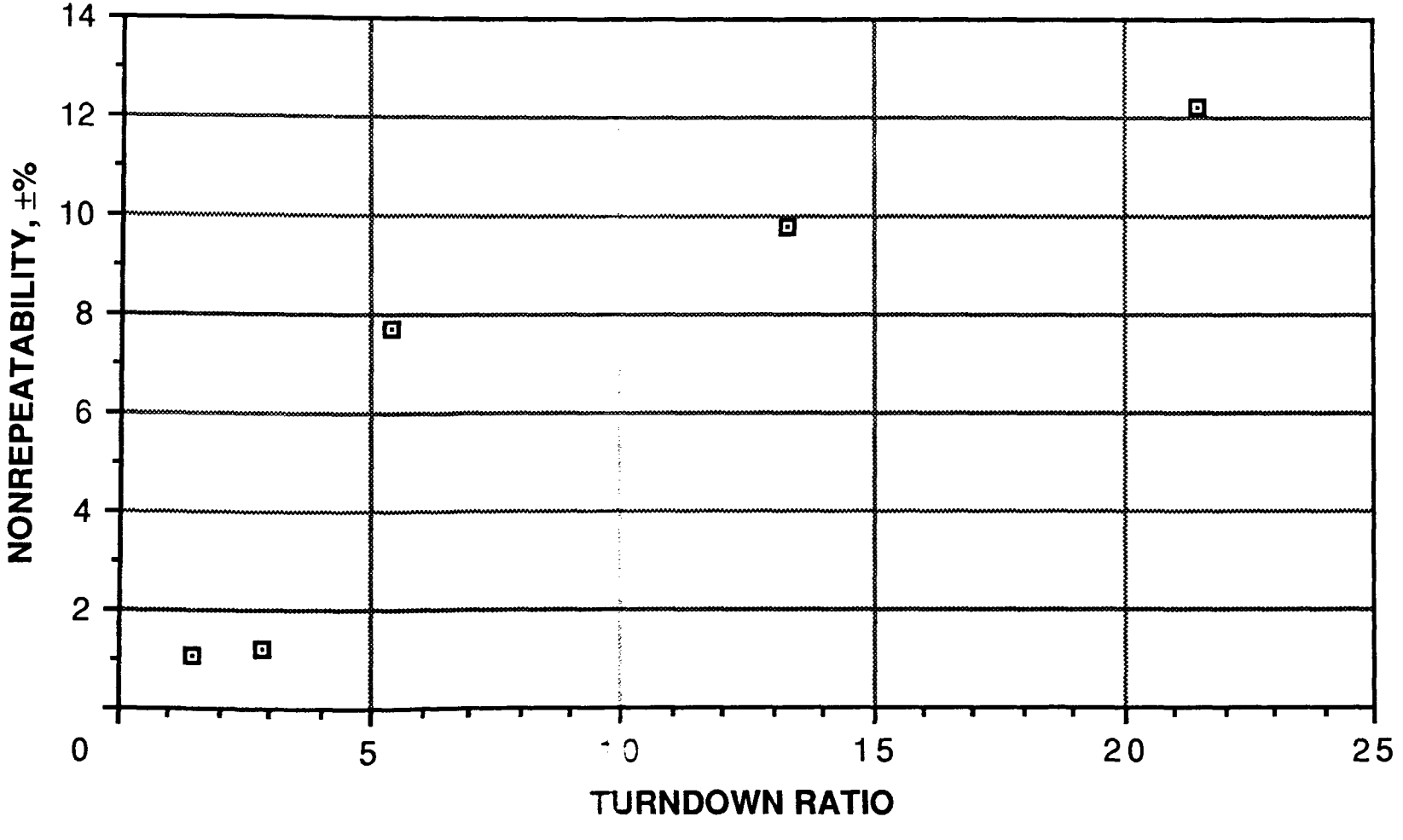

Figure 4.3-3.- Offset ultrasonic flowmeter steady-state nonrepeatability versus turndown ratio.

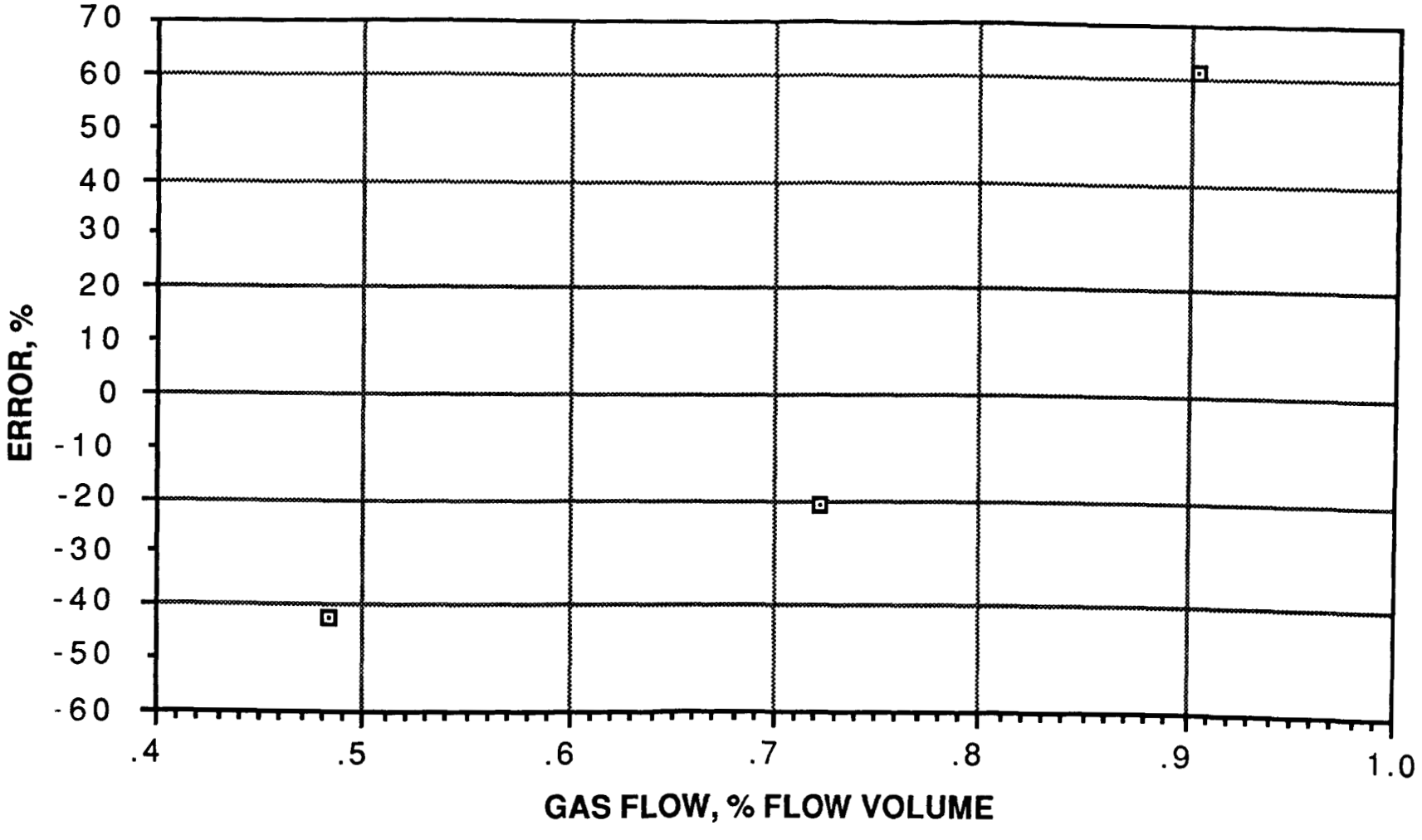

Figure 4.3-4.- Offset ultrasonic flowmeter two-phase flow error versus gas flow.

4.4 CORIOLIS MASS FLOWMETER

FLOWMETER DESCRIPTION

Coriolis flowmetering operates on the gyroscopic or coriolis principle to produce a mass flow measurement (figs. 4.4-1(a) and 4.4-1(b)). This process is achieved by vibrating a sensor tube at its natural frequency perpendicular to the direction of flow. A twist is induced in the sensor tube by the coriolis force (angular acceleration and deceleration of the fluid particles in the tube) generated by this process. The magnitude and the direction of this twist are used to calculate the mass flow rate of the flow. A temperature measurement is used to compensate for the thermal effects on the modulus of rigidity of the flow tube.

The flowmeter used for ground testing was the 0.04-meter (1.5 inch) Micro Motion D1505-SS flowmeter. The 0.013-meter (0.5 inch) Micro Motion D40AF-US flowmeter (Burge, S., 1988, JSC-22780, to be published) was used exclusively for PFTS ground and zero-g testing because of PFTS flow capacity and packaging volume limitations. These Micro Motion flowmeters contain a sensor unit (fig. 4.4-2), a remote electronics package, and a digital flow display. The sensor unit consists of two parallel, rigid, U-shaped sensor tubes; a drive coil; two position detectors; and a temperature sensor, which are enclosed in a stainless steel housing.

A summarization of the manufacturer's stated specifications is provided in table 4.4-1.

FLOWMETER PERFORMANCE

A summary of performance results and recommendations follows.

1. The coriolis flowmeter tested performs best under one-phase, steady-state flow conditions of run durations greater than 2 seconds, with adjustment to the output signal.

2. Flowmeter orientation did affect the steady-state performance of the test article in ground testing. As demonstrated in figures 4.4-3 and 4.4-4, the nonlinearity and the nonrepeatability varied with the flow rate nonlinearly for both ground test orientations (vertical and horizontal) but with significantly different characteristics for each.

3. Zero-g flow did affect flowmeter steady-state performance relative to ground testing performance. The nonrepeatability was shifted uniformly higher over the entire turndown ratio range tested (fig. 4.4-4). The nonlinearity was similarly shifted higher but only over the 5 to 19 turndown ratio ranges tested (fig. 4.4-3).

4. Pulse flow nonrepeatability degrades significantly for pulse widths of less than 2 seconds (0.5 hertz frequency), as shown in figure 4.4-5. This degradation is attributed to flow startup and termination transients. Therefore, use of this flowmeter should be constrained to pulse flows of 2 seconds or higher pulse widths.

5. This flowmeter is not recommended for two-phase flow measurement. The errors demonstrated by this flowmeter under two-phase flow conditions are relatively large with increasing gas flow for both flowmeters tested (fig. 4.4-6). The two-phase flow zero-g and ground nonrepeatabilities are similar in trend (fig. 4.4-7), although there is an apparent increased sensitivity to the zero-g environment.

6. The performance characteristics of the two (large and small) flowmeters tested were distinctly different. Further testing with multiple flowmeters of the same size would be required to determine whether these performance differences were due to differences in size classifications or merely to variations from one flowmeter to another. Either way, this performance difference could affect operational calibration and maintenance requirements of this flowmeter significantly.

7. This flowmeter is not recommended for vibration environment flow operations. Flow performance degraded significantly at relatively low acceleration ($\leq$6g) resonant-frequency vibration inputs during ground vibration testing. There were multiple performance degrading frequencies for each axis tested, and these resonant frequencies differed for each axis. Use of this flowmetering technique would require a significant understanding of the local and/or system level multiaxial vibration environment during all flow operations.

8. This flowmeter is structurally sensitive to vibration environments. The test article was permanently damaged during exposure to relatively low acceleration ($\leq$3g) vibration inputs along the axis perpendicular to the U-tube radius of curvature. This result suggests that this flowmeter may be restricted to low-vibration launch, operations, and non-operations applications and/or will require special vibration-compensating hardware for protection.

9. The zero-adjustment setting indication shifted erratically during KC-135 testing. Subsequent vibration testing duplicated this erratic zero-adjustment behavior.

10. A change to the zero-adjustment technique is recommended. The potentiometer/flashing light-emitting diode (LED) technique used in the flowmeter tested was affected by a deadband (i.e., the potentiometer can be turned slightly without causing the LED indicator to start flashing), which made adjustment repeatability difficult.

TABLE 4.4-1-.- CORIOLIS MASS FLOWMETER MANUFACTURER'S SPECIFICATIONS[a]

Manufacturer	Micro Motion
Flow range, kg/sec (lbm/sec)	
Model D1505-SS	1.21 to 24.18 (2.67 to 53.3)
Model D40AF-US	0.05 to 0.91 (0.1 to 2)
Rated operating pressure, MPa (psi)	
Model D1505-SS	10.3 (1500)
Model D40AF-US	8.6 (1250)
Zero stability, kg/sec (lbm/sec)	2.27×10^{-3} (5.0×10^{-3})
Accuracy, percent of rate plus or minus zero stability	±0.4
Sensor operating temperature, K (°F)	33 to 478 (-400 to 400)
Electronics operating temperature, K (°F)	420 to 339 (-40 to 150)
Response time, sec	Adjustable from 0.1 to 1.1

[a]Not investigated in this test program.

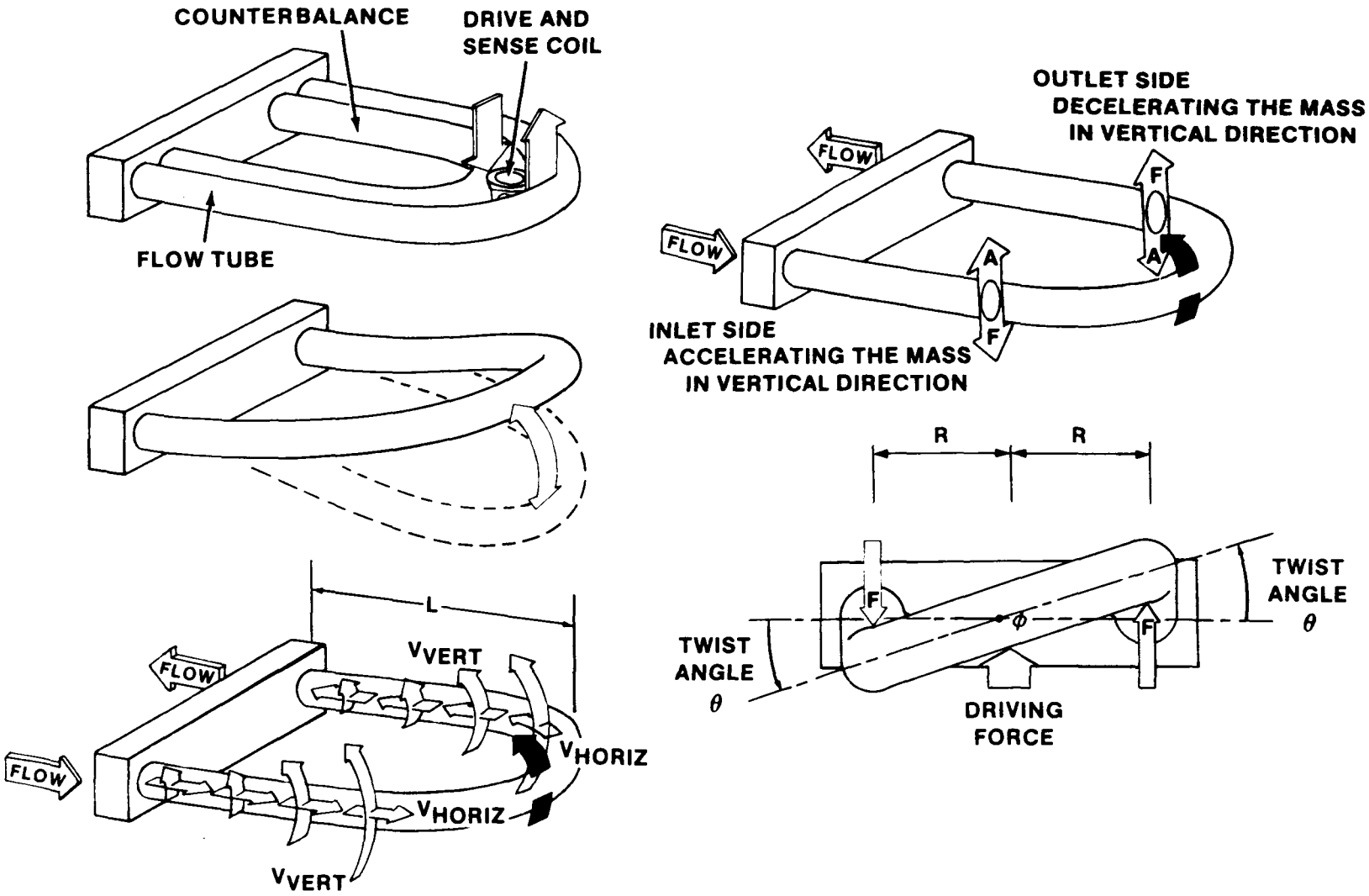

(a) Schematic diagram.

Figure 4.4-1.- Coriolis mass flowmeter.

$$\vec{F} = 2m\vec{\omega} \times \vec{V}$$

$$\Delta\underline{M} = F_1R_1 + F_2R_2$$

$$F_1 = F_2 = F$$
$$R_1 = R_2 = R$$

$$\Delta\underline{M} = 2FR = 4m\omega VR = 4\omega R(\Delta M)$$

$$\underline{M} = \int \Delta\underline{M} = 4\omega RM$$

$$\underline{M} = T = K_S\theta$$

$$K_S\theta = 4\omega RM$$

$$M = K_S\theta/4\omega R$$

$$\tan\theta = V_T(\Delta T)/2R$$

$$\theta \approx \tan\theta \text{ (if } \theta \text{ small)}$$

$$V_T \approx L\omega$$

$$\theta = CL\omega(\Delta T)/2R$$

$$M = CK_SL\omega(\Delta T)/8R^2\omega$$

$$M = CK_SL(\Delta T)/8R^2$$

Where:

F	Coriolis force on tube
m	Fluid mass flowing in tube
M	Fluid mass flow rate
$\underline{M}$	Moment about ϕ axis
V	Fluid flow velocity
V_T	Velocity at midpoint of tube travel
ω	Angular velocity about reference base
L	Tube length from reference base to bend
R	Tube loop radius
θ	Tube twist angle
T	Torque
K_S	Tube spring stiffness
ΔT	Time interval between inlet and outlet tube motions
C	Calibration constant
X	Vector cross product operator

(b) Equations and symbol definitions.

Figure 4.4-1.- Concluded.

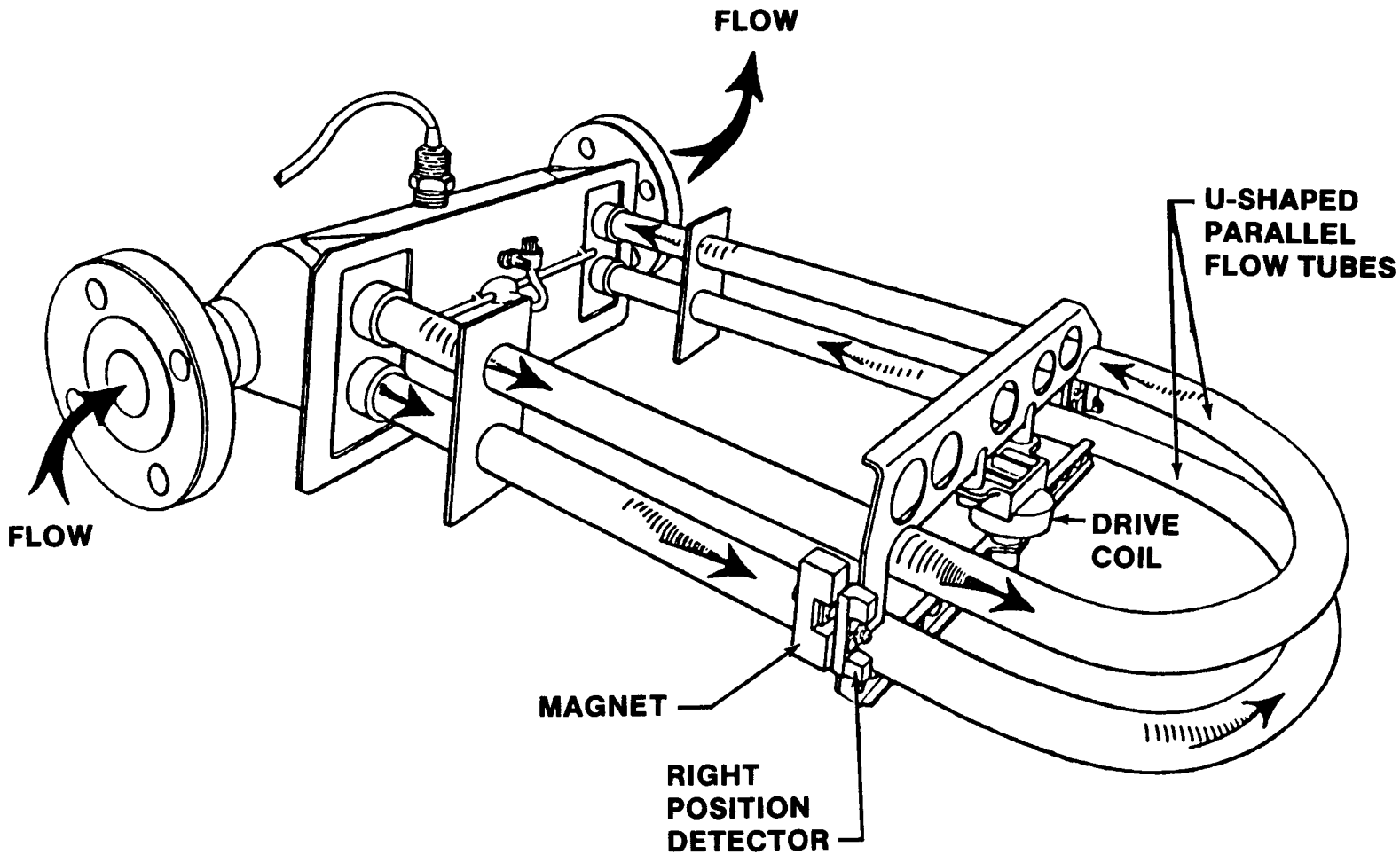

Figure 4.4-2.- Coriolis mass flowmeter flow tube assembly.

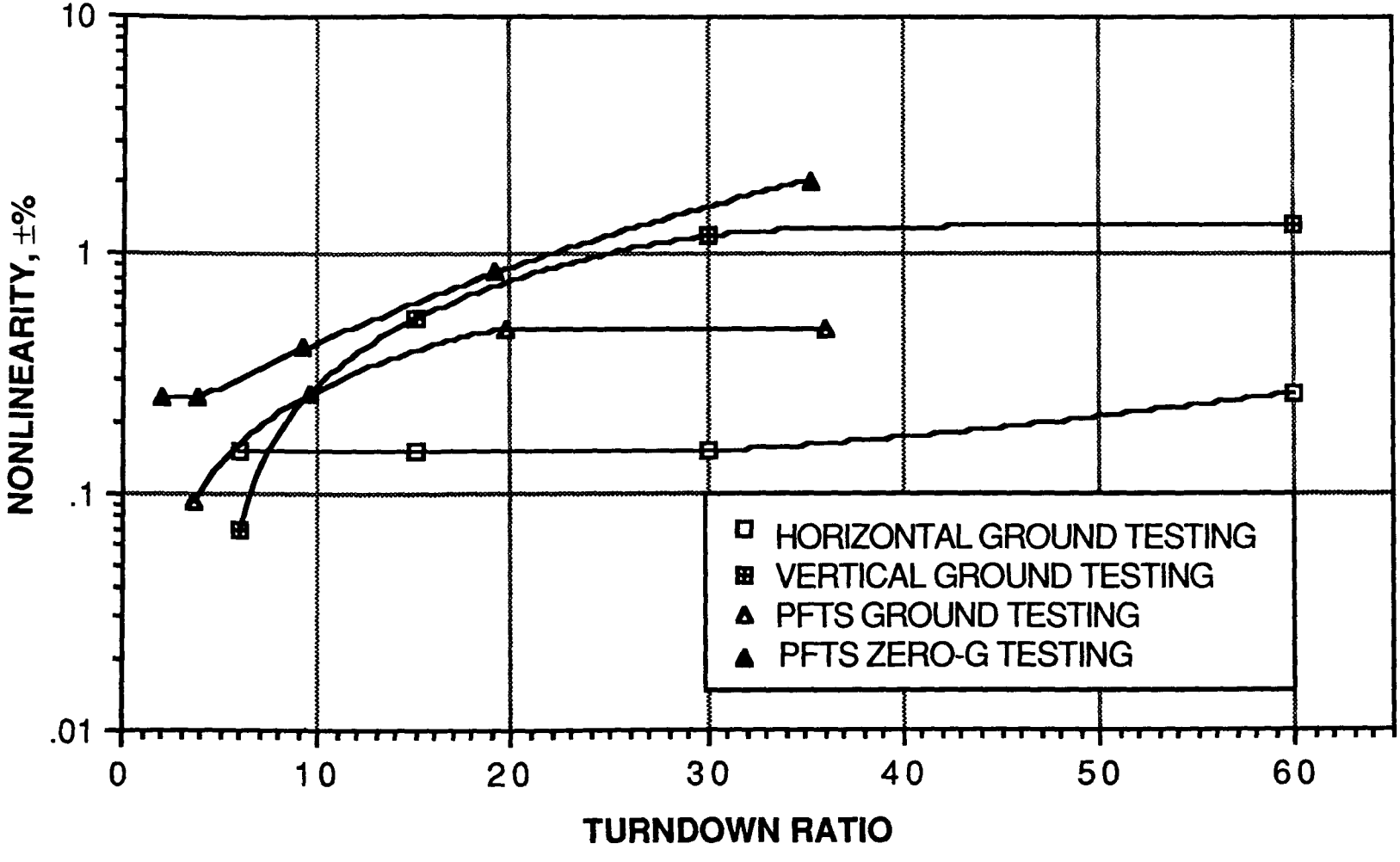

Figure 4.4-3.- Coriolis mass flowmeter steady-state nonlinearity versus turndown ratio.

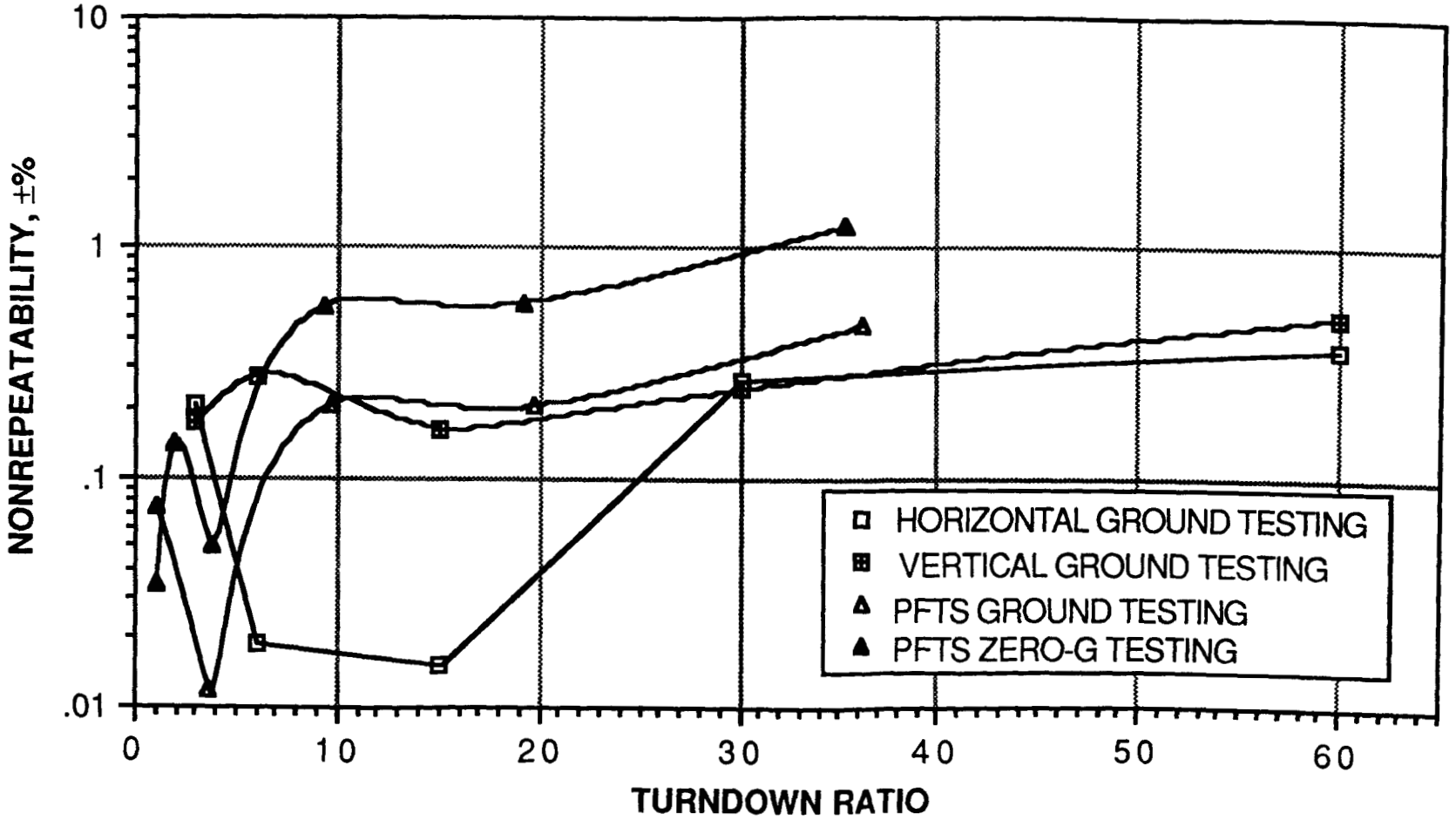

Figure 4.4-4.- Coriolis mass flowmeter steady-state nonrepeatability versus turndown ratio.

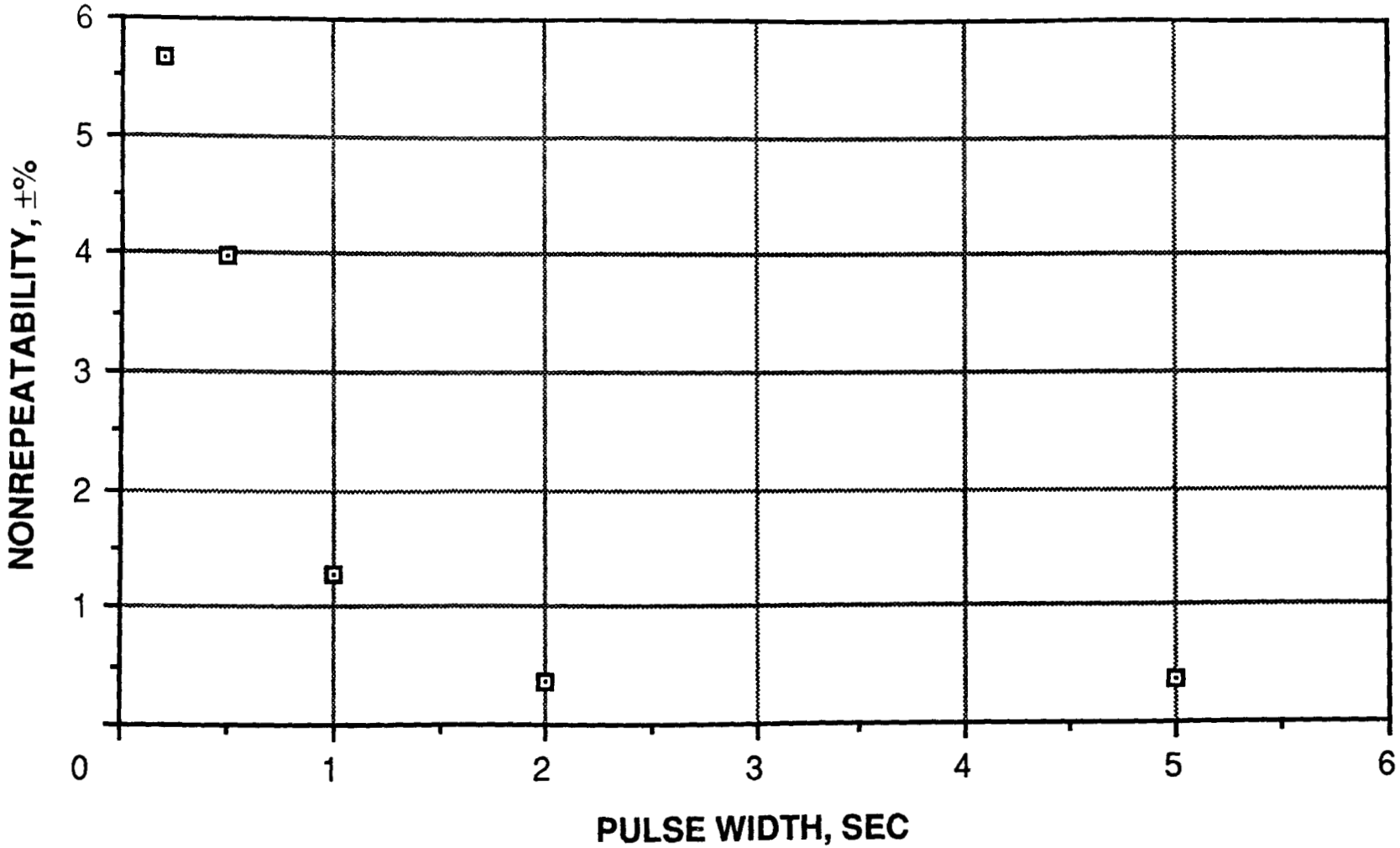

Figure 4.4-5.- Coriolis mass flowmeter pulse flow totalizer nonrepeatability versus pulse width.

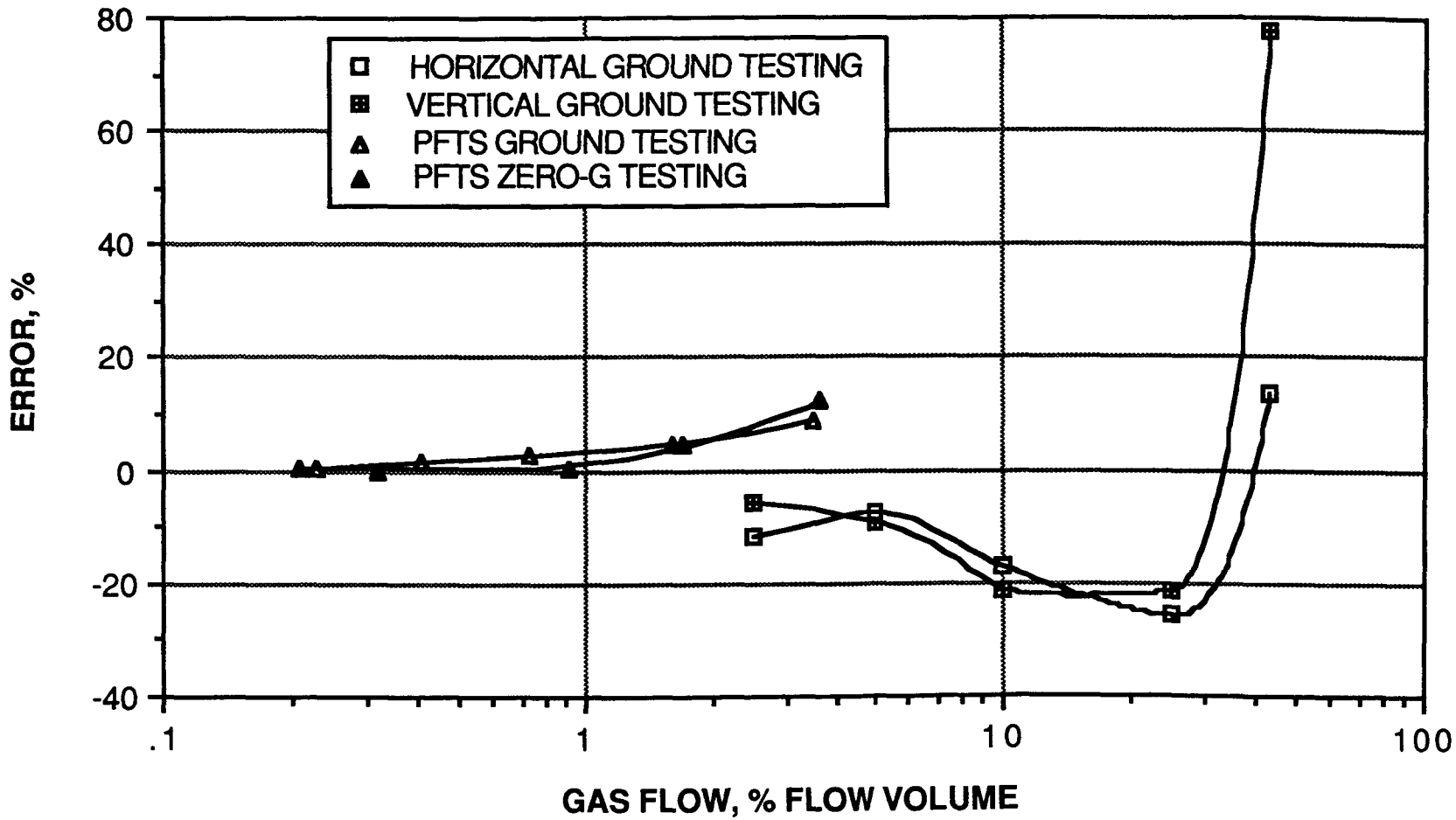

Figure 4.4-6.- Coriolis mass flowmeter two-phase flow error versus gas flow.

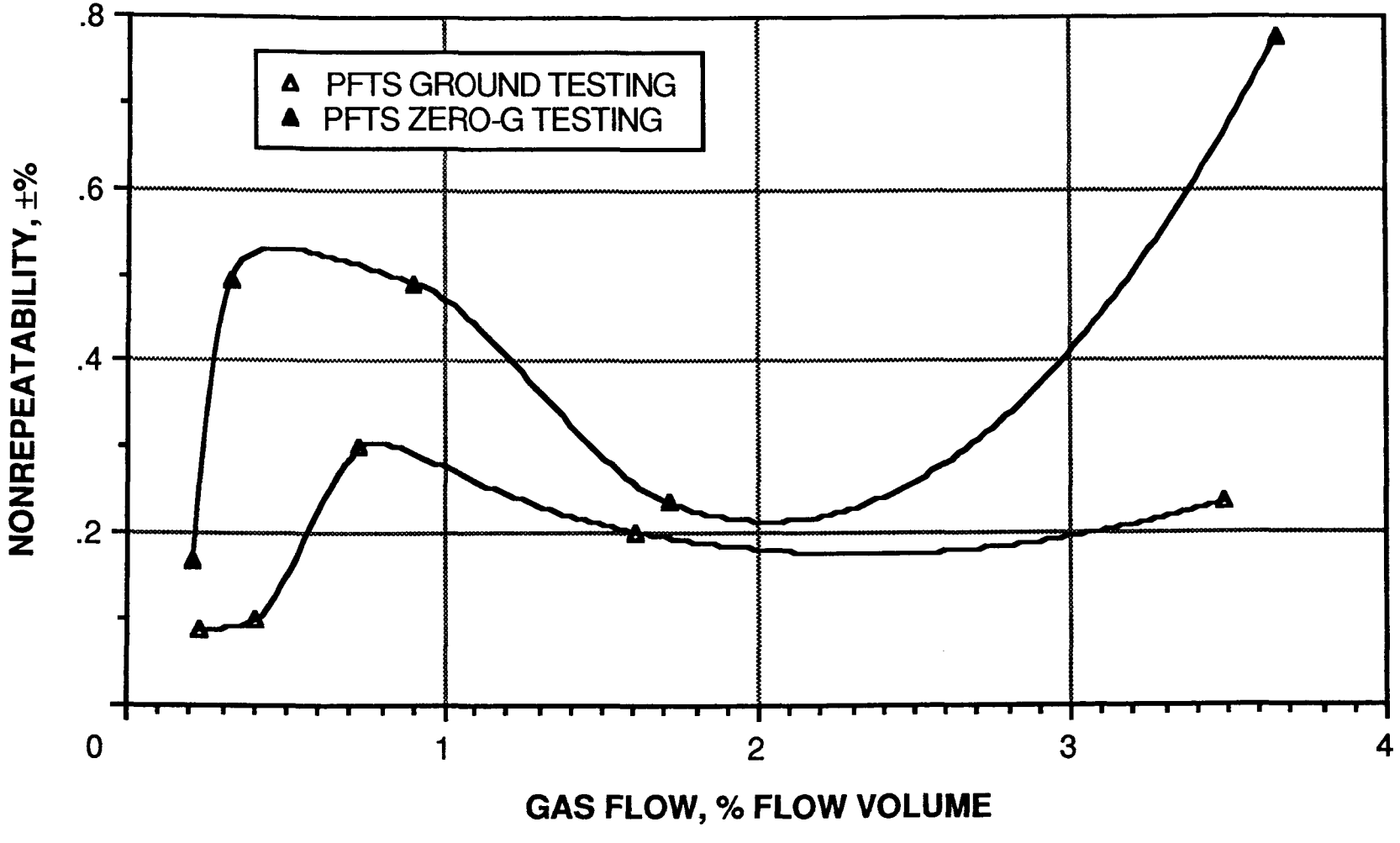

Figure 4.4-7.- Coriolis mass flowmeter two-phase flow nonrepeatability versus gas flow.

4.5 VORTEX SHEDDING FLOWMETER

FLOWMETER DESCRIPTION

Vortex shedding flowmetering uses the advantage inherent in the phenomenon of eddy or vortex generation within fluids flowing past a blunt body in that flow field. Within certain flow constraints (figs. 4.5-1(a) and 4.5-1(b)), these vortices are generated in direct proportion to the flow rate. Techniques for detecting vortices include optical, ultrasonic, mechanical, and thermal methods operable over a wide range of environmental conditions. In the flowmeter tested, vortices are sensed by the cyclic cooling (changes in resistivity) of a thermistor caused by the passing of the vortices. The sensor output is a nearly sinusoidal alternating voltage with a frequency that is directly proportional to vortex shedding. The signal processor receives the thermistor sensor output, processes it, and provides flow rate as output.

The test article used in this test program was the 0.05-meter (2 inch) Eastech vortex shedding flowmeter, model 2150. The flowmeter consisted of a meter body and flow element, a thermistor assembly, and a signal processor (model 4650). The manufacturer's specifications for this flowmeter are listed in table 4.5-1.

FLOWMETER PERFORMANCE

A summary of flowmeter performance results follows.

1. The maximum steady-state nonrepeatability ranged from ±0.127 percent to ±3.46 percent over the flow range tested (fig. 4.5-2).

2. Test article steady-state nonlinearity ranged from ±0.08 percent to ±0.77 percent for the flow range tested (fig. 4.5-3).

3. Measured pressure drop across the test article agreed closely with the predicted pressure drop, reaching a high of 41.4 kPa (6 psid) at full-scale flow.

4. Pulse flow error (deviation from steady-state performance) ranged from -2.18 percent to 11.9 percent, decreasing sharply with increasing pulse width (fig. 4.5-4). The sensitivity of this flowmeter to startup/shutdown transients effectively limits its practical use to pulse widths greater than 2 seconds.

5. The test article performance was consistently under 1 percent error for gas ingestion of less than 2.98 percent of total flow (fig. 4.5-5). The test article exhibited rapid return to normal flow rate when gas ingestion was terminated.

6. The test article exhibited rapid recovery from gas slug passage; however, that recovery was not rapid enough to accurately measure slug volume.

7. Random spike output by the test article caused inconsistent calibration factor determination during the original testing of this flowmeter. Test article checkout by the manufacturer revealed improper factory settings (gas flow sensitivity rather than liquid flow sensitivity) on the thermistor sensor. These settings were corrected and the flowmeter retested with no further recurrence of the problem. This variable sensitivity capability could be an asset for on-orbit operations with proper care and further research.

TABLE 4.5-1.- VORTEX SHEDDING FLOWMETER MANUFACTURER'S SPECIFICATIONS[a]

Manufacturer	Eastech
Repeatability, percent of reading	±0.1
Linearity, percent of reading	±1 at Re ≥ 10 000
Meter uncertainty factor, percent of reading	±1
Turndown ratio	32:1 (nominal for water)
Response time, msec	5 at 100 Hz signal frequency
Pressure drop at waterflow rate of 6.09 m/sec (20 ft/sec), kPa (psi)	41.4 (6)
Operating pressure at maximum temperature of 478 K (400° F), MPa (psi)	10.3 (1500)
Temperature range, K (°F)	77.6 to 477.6 (-320 to 400)
Fluid temperature span within temperature range, K (°F)	55.6 (100)

[a]Not investigated in this test program.

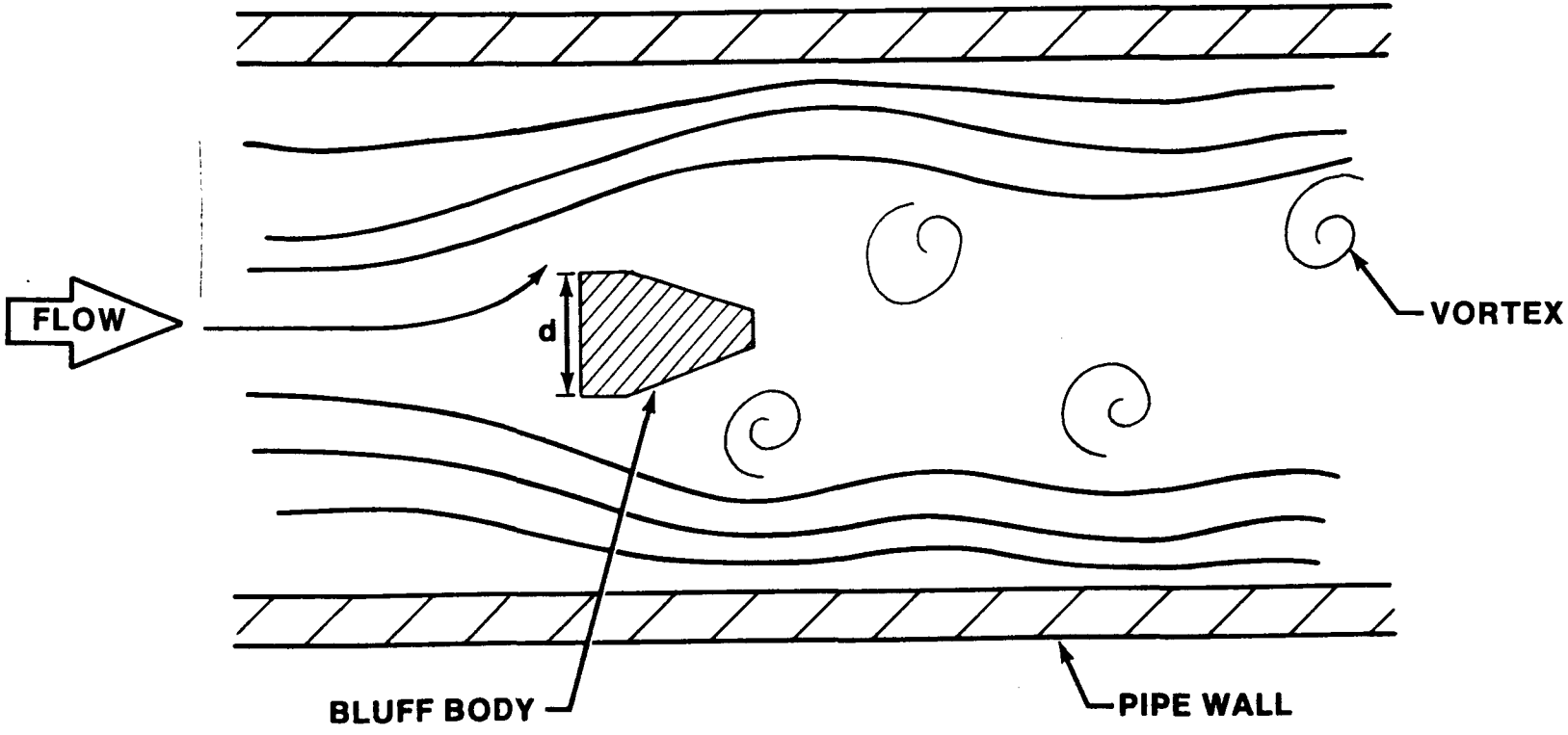

(a) Schematic diagram.

Figure 4.5-1.- Vortex shedding flowmeter.

$$F = (S_T V/d)\,(1 - (20/Re))$$

If: $10^3 \leq Re \leq 10^5$

$S_T \sim 0.2$

$1 - (20/Re) \sim 1.0$

$$V \sim Fd/S_T$$

$$Q = AV$$

$$Q = CAFd/S_T$$

Where:

F	Vortex shedding frequency
S_T	Strouhal number
V	Fluid flow velocity
d	Diameter of bluff body
A	Flow area
Re	Reynolds number
Q	Volumetric flow rate
C	Calibration constant

(b) Equations and symbol definitions.

Figure 4.5-1.- Concluded.

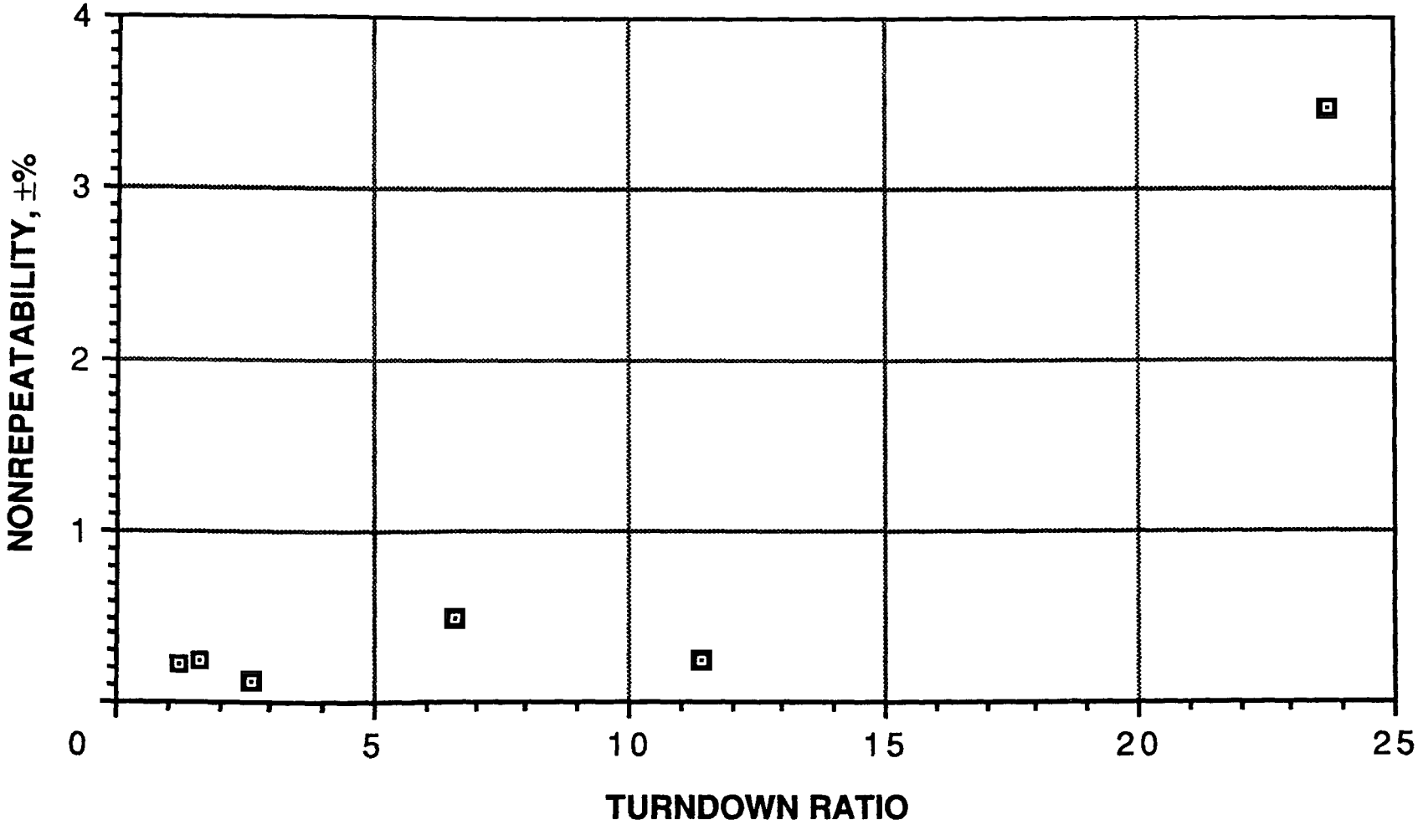

Figure 4.5-2.- Vortex shedding flowmeter steady-state nonrepeatability versus turndown ratio.

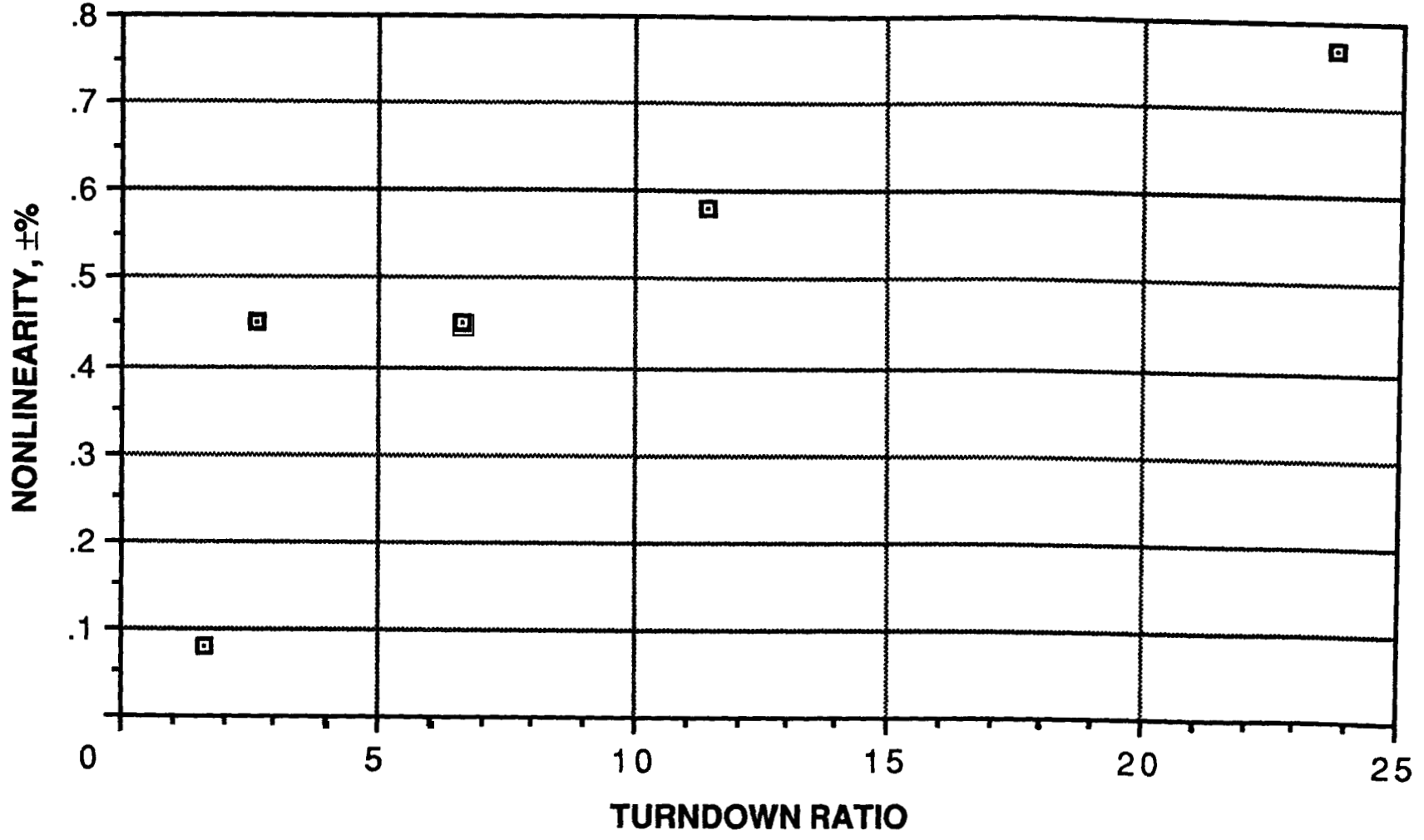

Figure 4.5-3.- Vortex shedding flowmeter steady-state nonlinearity versus turndown ratio.

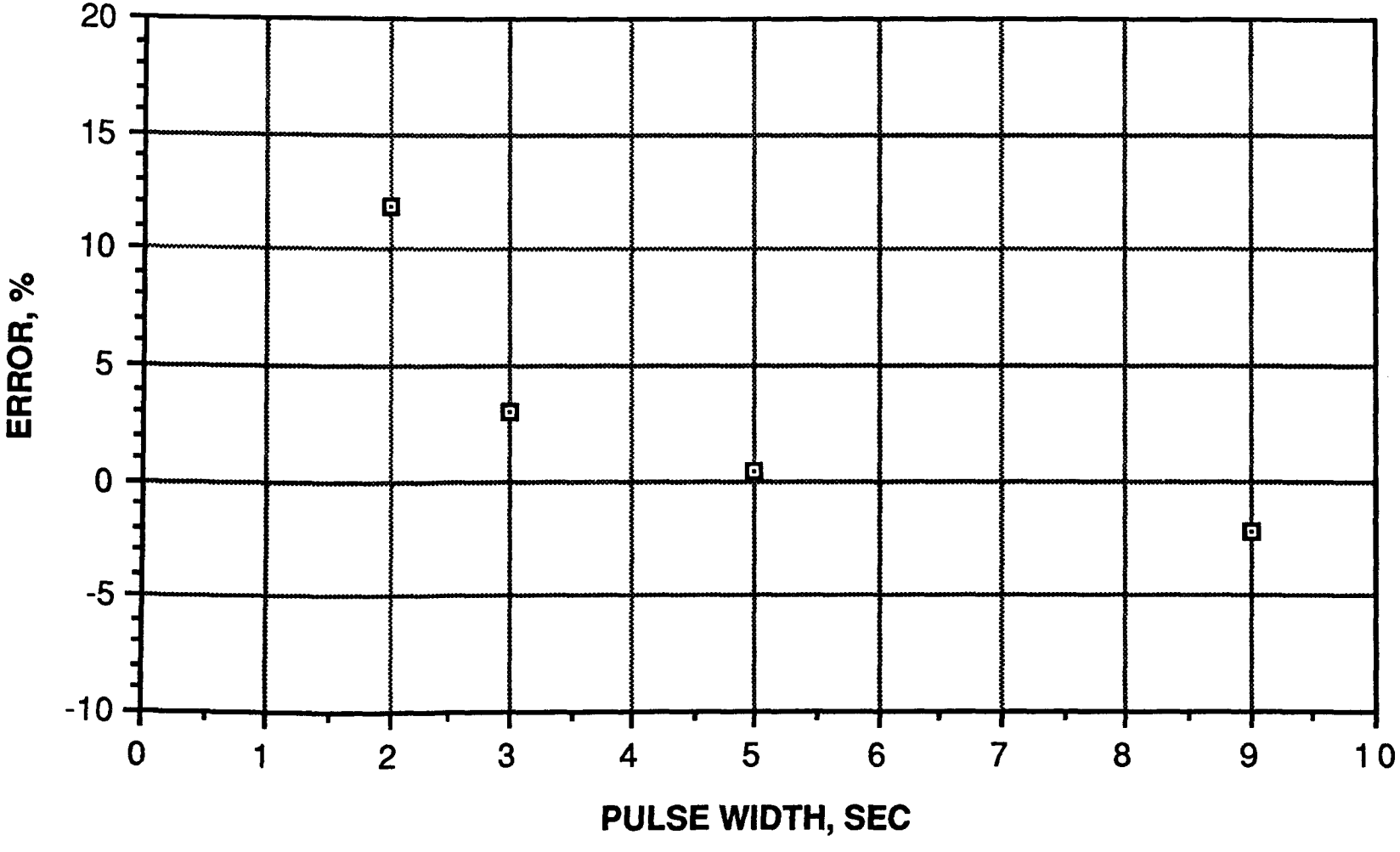

Figure 4.5-4.- Vortex shedding flowmeter pulse flow error (deviation from steady-state performance) versus pulse width.

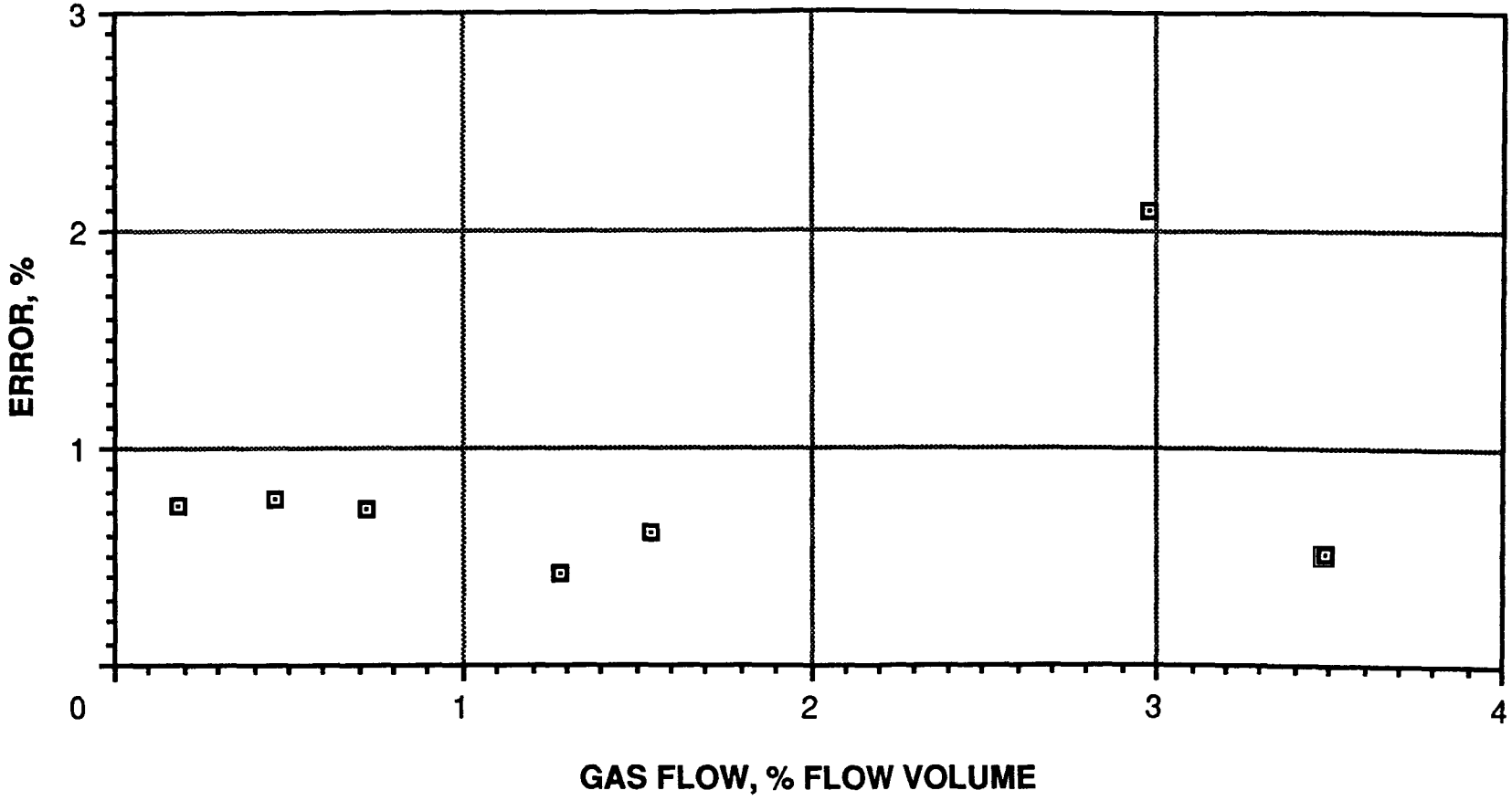

Figure 4.5-5.- Vortex shedding flowmeter two-phase flow overall error versus gas flow.

4.6 UNIVERSAL VENTURI TUBE FLOWMETER

FLOWMETER DESCRIPTION

Venturi tube flowmetering is based upon the Bernoulli relationships of pressure to velocity in flowing fluids. In this flowmetering technique, flow area is reduced from the entrance of the flowmeter to a minimum area at the throat and, thereby, the fluid is forced to trade pressure head for velocity (figs. 4.6-1(a) and 4.6-1(b)). This measurable change in pressure is directly proportional to the volumetric flow rate of the fluid being metered. Velocity is then converted back into pressure head with as small a net energy loss as possible in a gradually diverging section of pipe from the flowmeter throat to the exit. The universal venturi tube tested differs from the classical venturi tube design by having a two-stage entrance to the throat converging section and by being shorter in overall length. These design differences magnify the differential pressures observable while regulating hydraulic effects, such as boundary-layer tripping, and thus substantially increase the potential accuracy of this flowmeter.

The test article examined was the BIF universal venturi tube, model 0183-01-99, serial number 99794-1. The test article was fabricated from a single piece of 304L stainless steel for installation in a 0.025-meter (1 inch) pipe. The test article was designed to maintain a constant flow coefficient of ± 0.25 percent for the Reynolds number range of 75 000 to 225 000.

FLOWMETER PERFORMANCE

The following flowmeter performance results were obtained.

1. Different delta-pressure transducers were used for different flow ranges in order to obtain the most reliable throat pressure drop measurements. Accuracies will probably be reduced in the field from those determined in this test series because of reliance on one delta-pressure transducer optimized for the entire operational flow range instead of portions of the flow range as tested here.

2. The steady-state flow coefficient nonlinearity ranged as high as ± 1.99 percent over the flow range tested (fig. 4.6-2).

3. The steady-state nonrepeatability ranged as high as ± 0.331 percent for the full flow range tested (fig. 4.6-3). The nonrepeatabilities presented for turndown ratios of less than 3 are within the measuring capabilities of the test facility and may not reflect accurate flowmeter nonrepeatabilities.

4. The overall pressure recovery for the flowmeter tested ranged from 88.16 percent at 0.98 turndown ratio to 100 percent at 10.6 turndown ratio.

5. The pulse flow error ranged from 4.5 percent to 17.6 percent (fig. 4.6-4) but was extremely repeatable ($\leq \pm 0.16$ percent nonrepeatability).

6. The test article performed best for gas bubble ingestion rates of less than 4 percent of total volumetric flow and at higher inlet pressures (fig. 4.6-5). Two-phase flow nonrepeatabilities were consistently small, less than ±0.12 percent for both high- and low-pressure conditions.

7. The test article tended to measure liquid flow only, rather than total volumetric flow, and thereby made transition back to normal flow characteristics quite rapid when gas injection was terminated.

8. Gas slug flow test article error ranged from -0.076 percent to 0.16 percent.

9. Gas slug flow nonrepeatabilities were less than ±0.0373 percent.

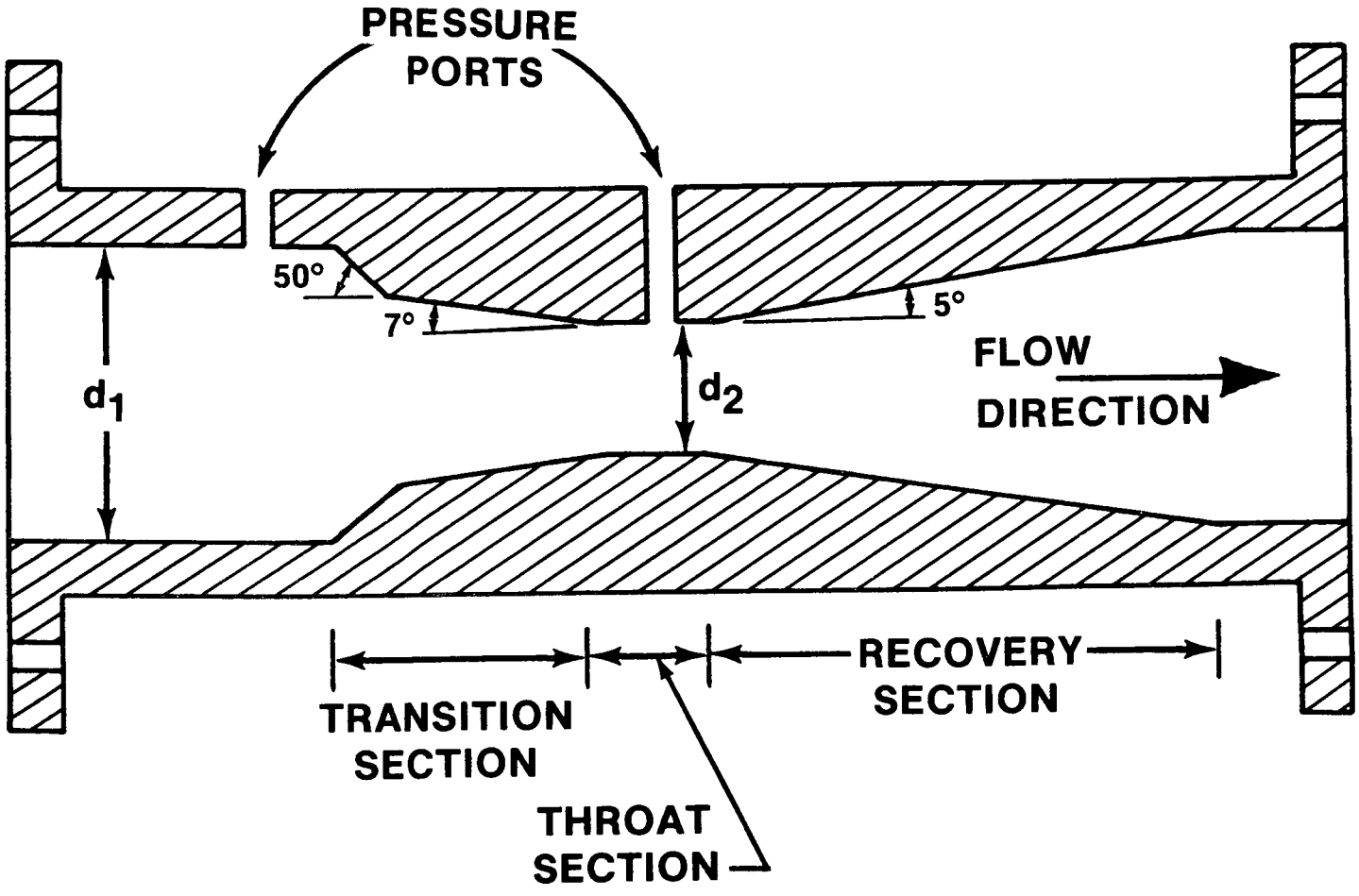

(a) Schematic diagram.

Figure 4.6-1.- Universal venturi tube flowmeter.

$$(P_1/\gamma) + Z_1 + (V_1^2/2g) = (P_2/\gamma) + Z_2 + (V_2^2/2g)$$

$$Z_1 \approx Z_2$$

$$(V_2^2 - V_1^2)/2g \approx (P_1 - P_2)/\gamma$$

$$V_1A_1 = V_2A_2$$

$$A = \pi r^2 = \pi d^2/4$$

$$\therefore V_1 = V_2(d_2^2/d_1^2)$$

$$V_2^2 - V_2^2(d_2^2/d_1^2)^2 \approx 2g(P_1 - P_2)/\gamma$$

$$V_2^2(1 - (d_2/d_1)^4) \approx 2g(P_1 - P_2)/\gamma$$

$$V_2 \approx (1/(1 - (d_2/d_1)^4))^{\frac{1}{2}}(2g(P_1 - P_2)/\gamma)^{\frac{1}{2}}$$

$$Q = A_2V_2$$

$$Q = A_2C(1/(1 - (d_2/d_1)^4))^{\frac{1}{2}}\ (2g(P_1 - P_2)/\gamma)^{\frac{1}{2}}$$

Where:

$()_1$	Inlet conditions
$()_2$	Throat conditions
P	Pressure
V	Fluid velocity
Z	Elevation
γ	Fluid specific weight
g	Gravitational constant
d	Flow diameter
A	Flow area
C	Discharge coefficient
Q	Volumetric flow rate

(b) Equations and symbol definitions.

Figure 4.6-1.- Concluded.

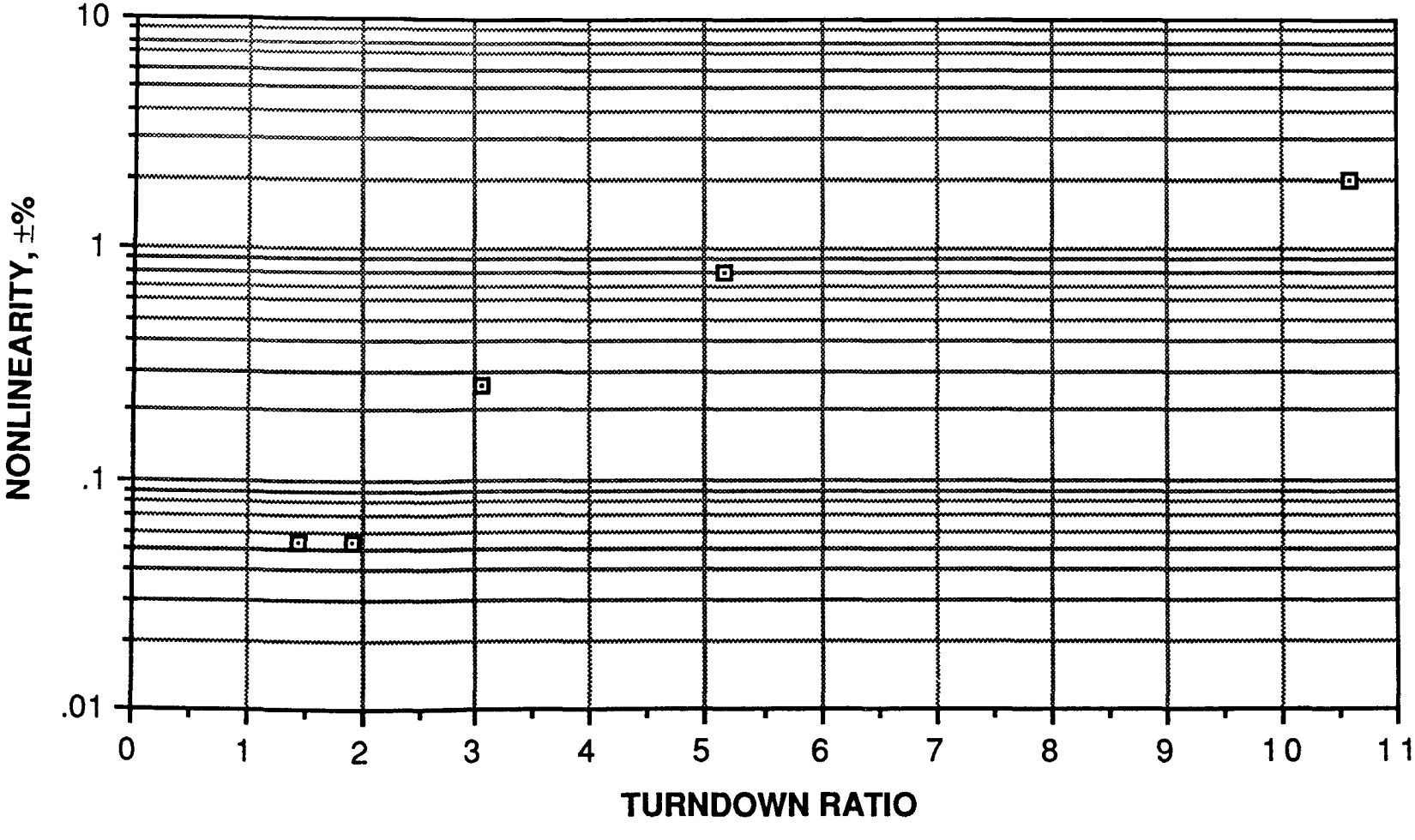

Figure 4.6-2.- Universal venturi tube steady-state nonlinearity versus turndown ratio.

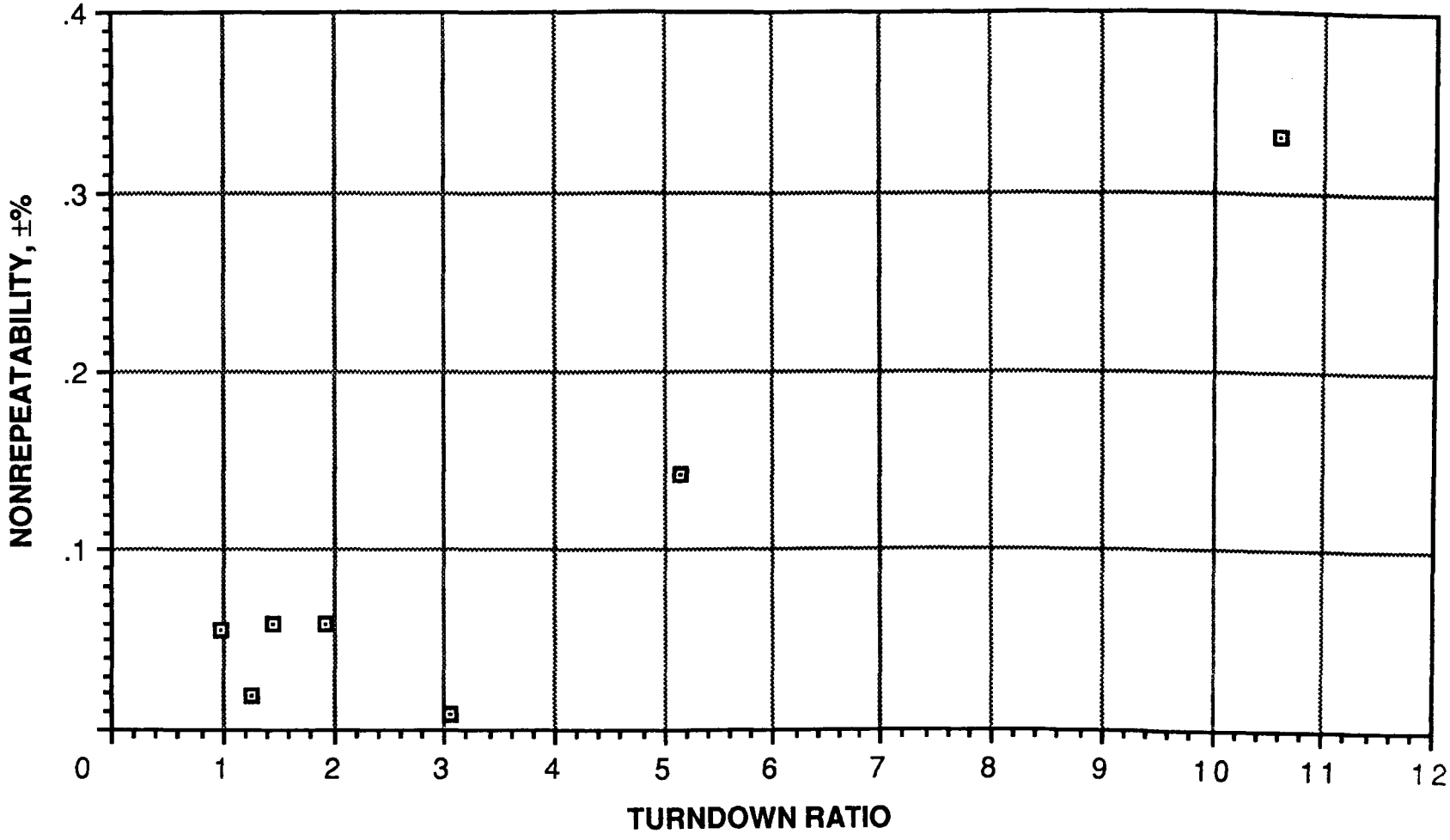

Figure 4.6-3.- Universal venturi tube steady-state nonrepeatability versus turndown ratio.

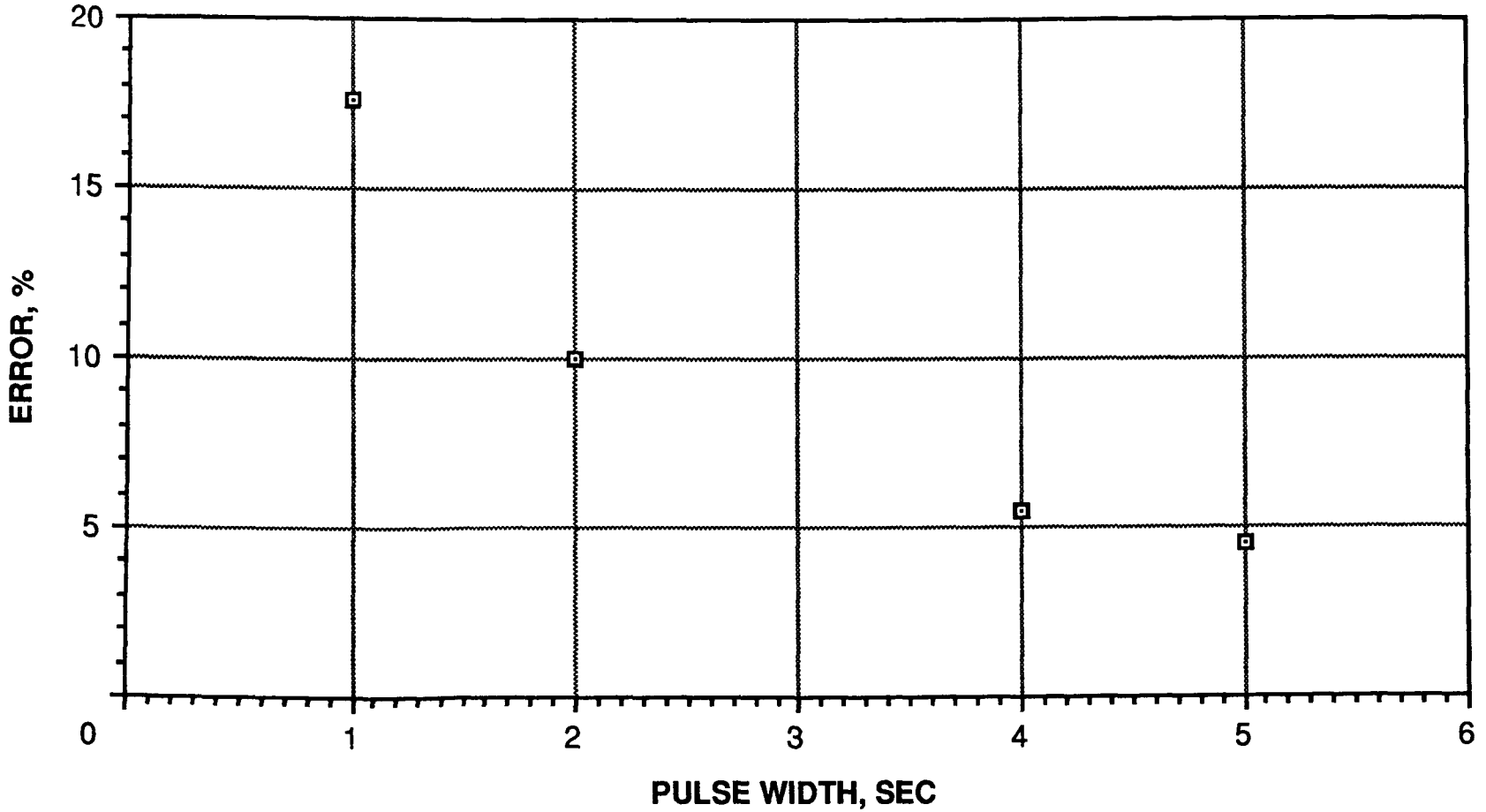

Figure 4.6-4.- Universal venturi tube pulse flow error (deviation from steady-state performance) versus pulse width.

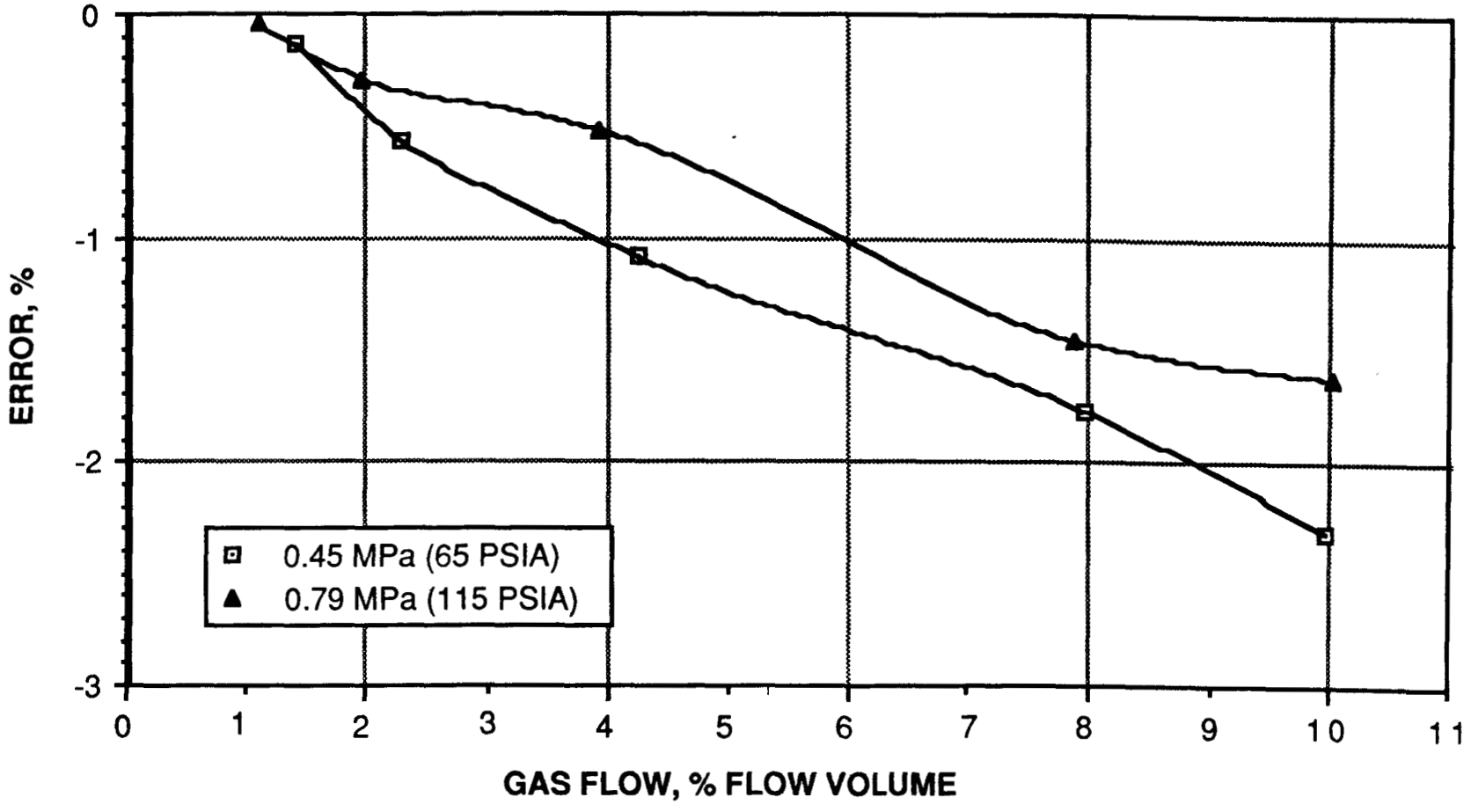

Figure 4.6.5.- Universal venturi tube two-phase flow error (deviation from steady-state performance) versus gas flow.

4.7 TURBINE FLOWMETER

FLOWMETER DESCRIPTION

Typically, turbine flowmetering measures the rotary motion of a turbine in a flow field and then relates that motion directly to the volumetric flow rate of that flow field. Turbine flowmetering is a relatively well established and commonly used form of flow measurement. Because of this widespread use, various turbine motion measurement methods and flowmeter configurations have been developed to operate over a broad range of thermal, flow-rate, and flow quality operating conditions making turbine flowmetering an attractive contender for on-orbit flow system applications.

The turbine flowmeter performance data presented in this document were gathered as part of the turbine/turbine delta p hybrid flowmeter test series. Two turbine flowmeters were examined as part of that test series. A 0.05-meter (2 inch) Flow Technology model FT-32C250-LB turbine meter was tested in the ground flow facility and a 0.02-meter (0.75 inch) Hersey/ITT Barton model 7186-0006A turbine flowmeter was ground and zero-g tested in the PFTS. The smaller flowmeter incorporated a hydrodynamic turbine bearing which should theoretically enhance flowmeter performance. For more information on these two flowmeters and on the test series, see section 4.9.

FLOWMETER PERFORMANCE

Flowmeter performance results obtained were as follows.

1. Steady-state nonlinearity was a very constant ± 0.36 percent for the larger model used for ground testing (fig. 4.7-1). The ground testing and zero-g nonlinearities for the smaller model were relatively low compared to the larger model. This improved nonlinearity may be due to the hydrodynamic bearing used in the smaller turbine flowmeter.

2. The smaller turbine flowmeter demonstrated a higher ground testing nonrepeatability at the lower turndown ratios than did the larger model (fig. 4.7-2).

3. Pulse flow errors are generally low for all pulse width flows tested (fig. 4.7-3).

4. Two-phase flow nonrepeatability was less than ± 1.0 percent for PFTS ground testing gas flow volumes of less than 38 percent of total flow (fig. 4.7-4). Zero-g nonrepeatabilities were significantly better.

5. Two-phase flow errors were generally high but consistent for both ground and zero-g testing (fig. 4.7-5).

It should be noted that the 0.02-meter (0.75 inch) flowmeter was used only in the PFTS testing. All data not labeled "PFTS" were generated using the 0.05-meter (2 inch) flowmeter.

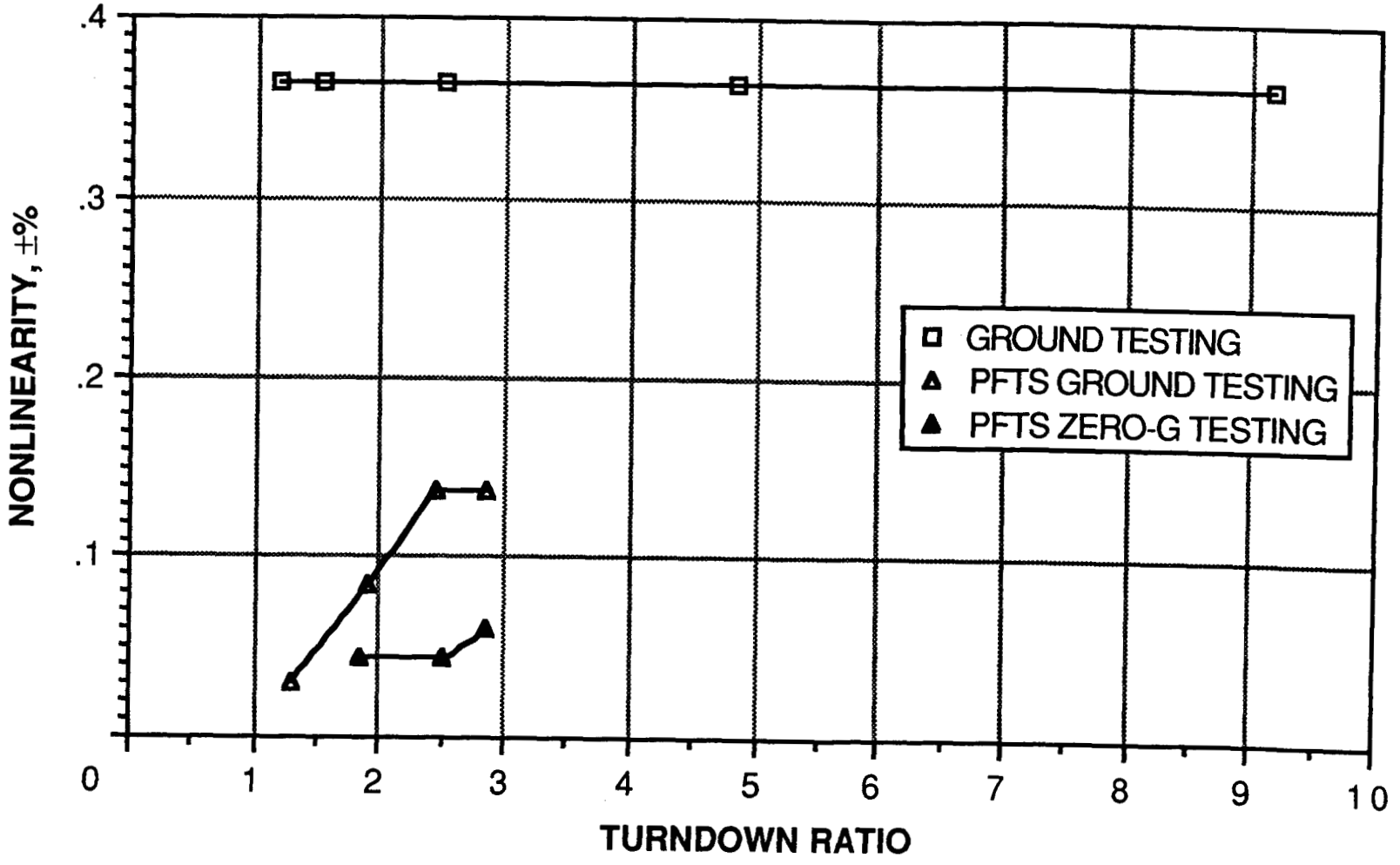

Figure 4.7-1.- Turbine flowmeter steady-state nonlinearity versus turndown ratio.

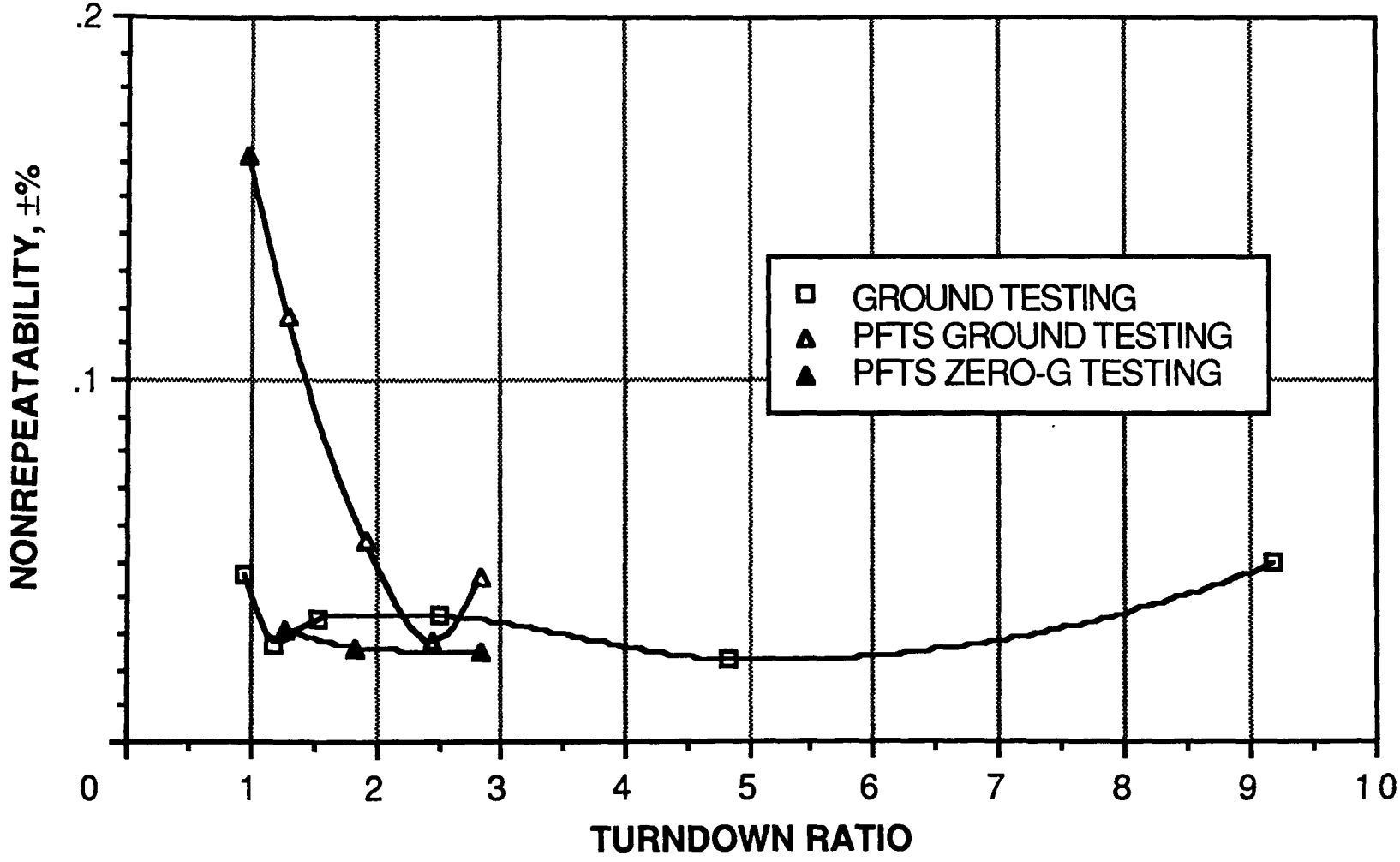

Figure 4.7-2.- Turbine flowmeter steady-state nonrepeatability versus turndown ratio.

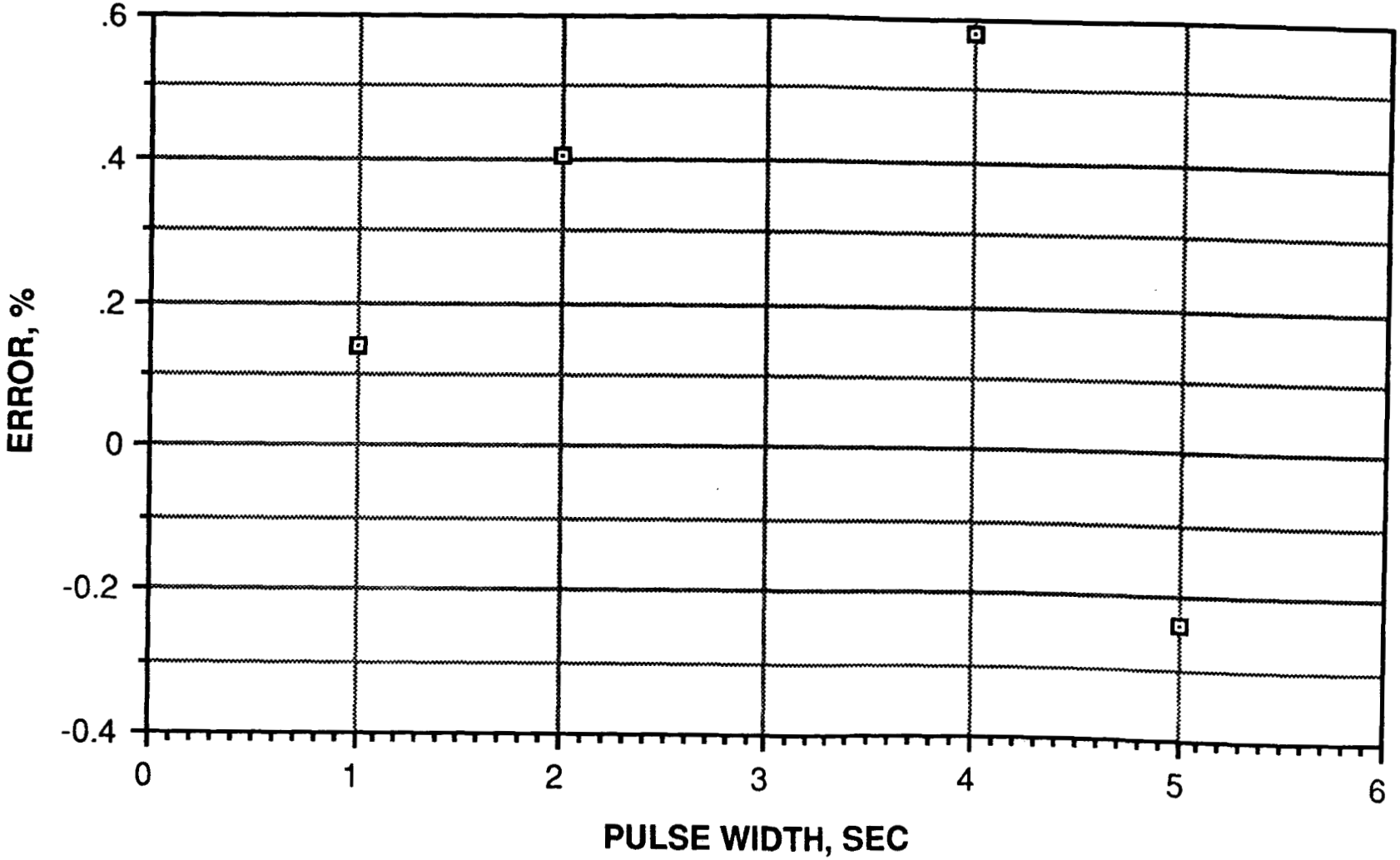

Figure 4.7-3.- Turbine flowmeter pulse flow error versus pulse width.

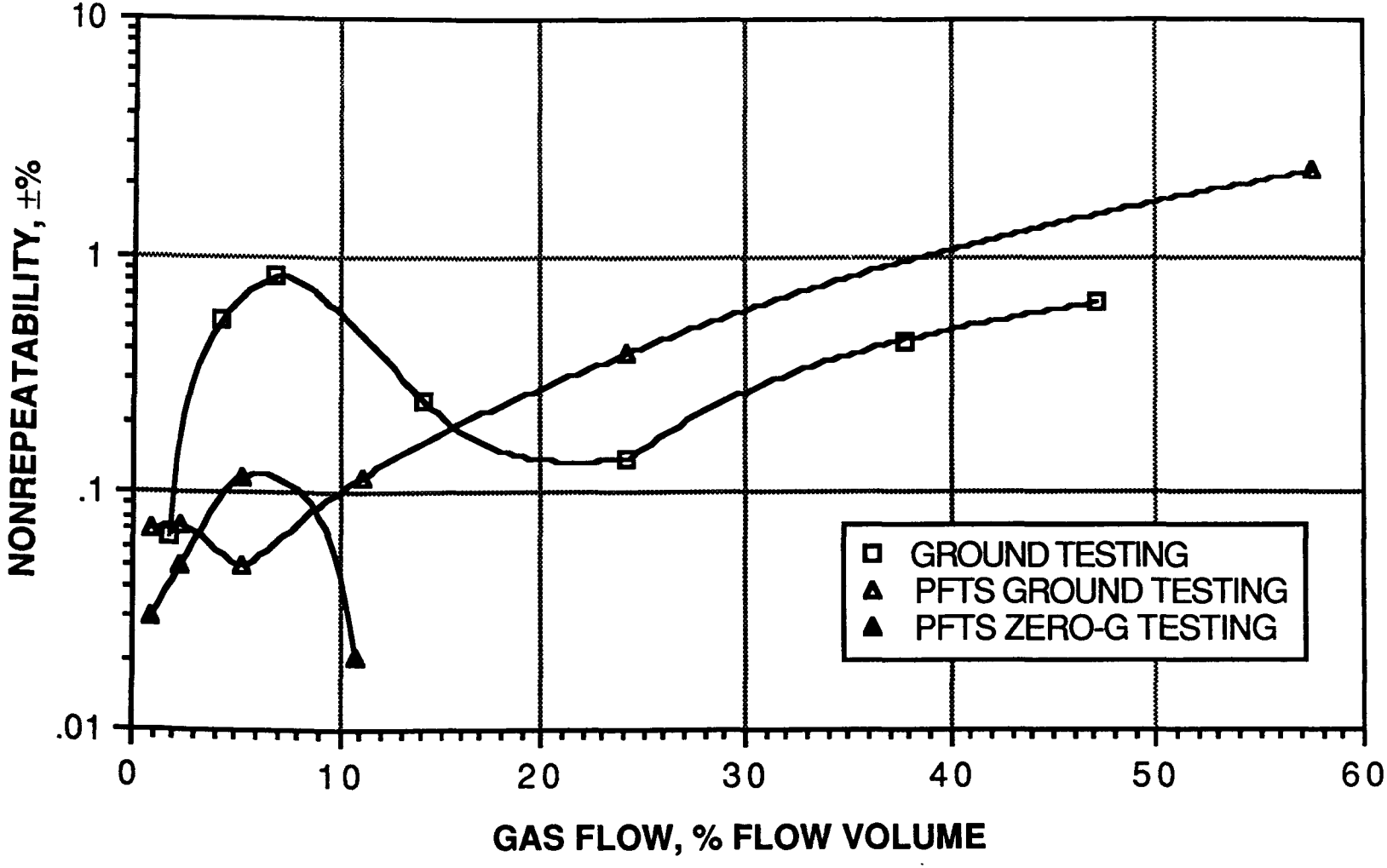

Figure 4.7-4.- Turbine flowmeter two-phase flow nonrepeatability versus gas flow.

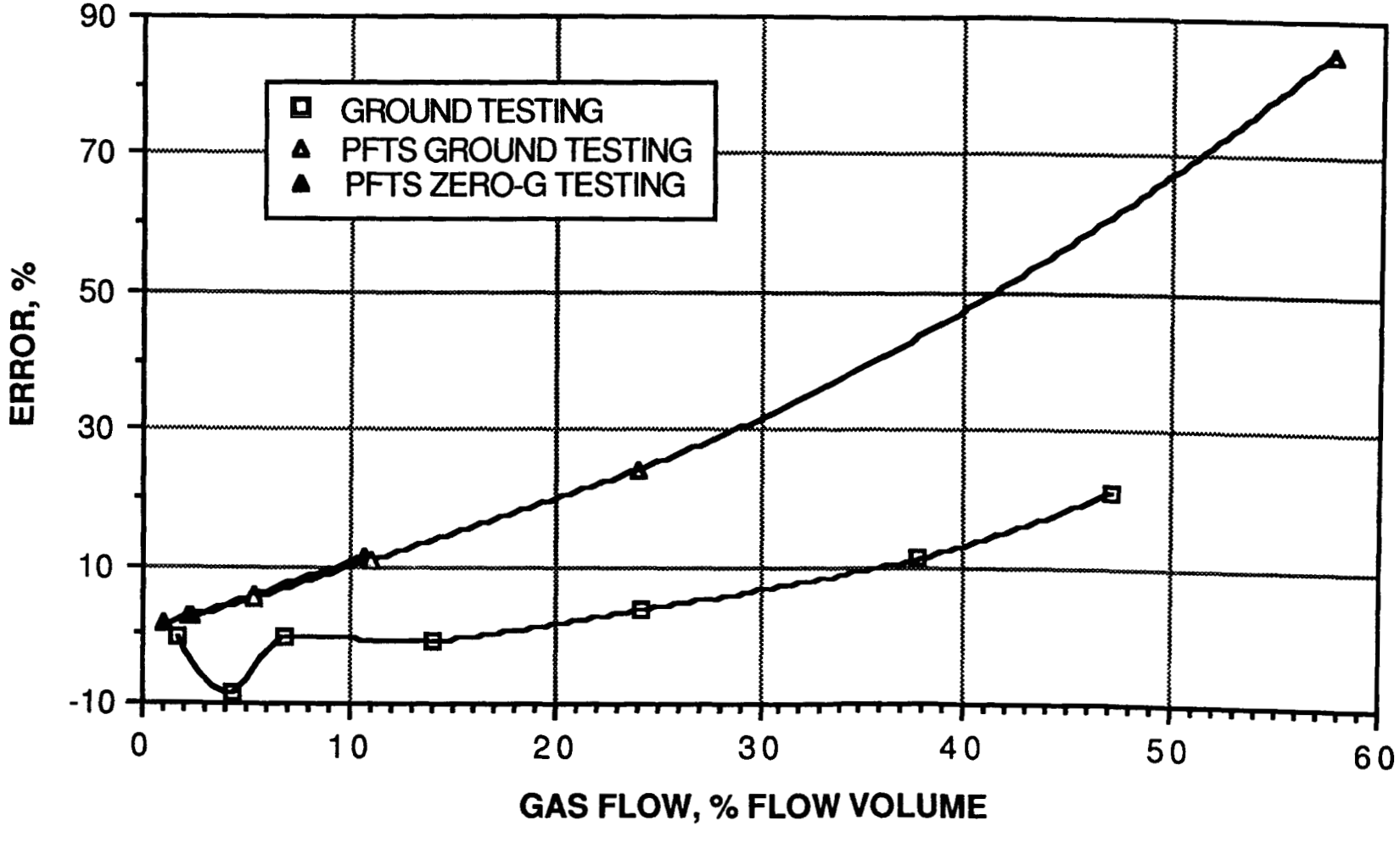

Figure 4.7-5.- Turbine flowmeter two-phase flow error versus gas flow.

4.8 BEARINGLESS TURBINE FLOWMETER

FLOWMETER DESCRIPTION

The bearingless turbine flowmeter is a variant of a typical turbine flowmeter. The turbine flowmeter measures the motion of a rotor in a flow field and relates that motion directly to the volumetric flow rate of that flow field.

The bearingless turbine flowmeter tested (fig. 4.8-1) was a 0.025-meter (1 inch), model E100, manufactured by Flow Systems Corp. The flowmeter consists of a free-floating, ring-shaped rotor inside a coin-shaped chamber. The fluid to be metered flows into the operating chamber through its periphery, by means of tangentially angled jets. Fluid motion is converted from linear flow to a spiral swirl flow from the chamber periphery, across the rotor, and out the center, where it is returned to linear flow. The spiral rotation of the fluid spins and stabilizes the rotor in the middle of the chamber, where it rotates without contacting the chamber walls. The electronics package contains an illumination source. The light from this lamp is transmitted via a fiber optics meter/box connection to the inner chamber of the meter. White marks on the rotor reflect this light back through the fiber optics cable to the electronics box in pulses, which are used to calculate flow rate.

The manufacturer's stated specifications for the model E100 are shown in table 4.8-1.

FLOWMETER PERFORMANCE

Flowmeter performance results and recommendations are as follows.

1. Test article orientation affected the output of the flowmeter at low flow rates in a one-g environment (fig. 4.8-2).

2. This test article demonstrated better performance in zero-g testing. The one-g phenomenon of severely decreasing K-factor for turndown ratios greater than 15 was not evident during zero-g testing, when the meter measured much lower flow rates than at one-g conditions (fig. 4.8-2). The meter demonstrated essentially identical steady-state K-factor performance in the two environments for turndown ratios less than 8. (Normal flowmeter operating turndown ratios tend to be less than 5 to 10.) Ground testing nonrepeatabilities and nonlinearities were generally higher than zero-g testing levels at the higher turndown ratios (figs. 4.8-3 and 4.8-4).

3. Pulse flow reduced flow measurement accuracy significantly.

4. In a one-g environment, the errors of this meter were slightly high during gas bubble ingestion flow when calculations were based on waterflow alone. In a zero-g environment, this meter demonstrated better two-phase flow error performance (fig. 4.8-5). Zero-g and ground two-phase flow nonrepeatabilities were essentially the same (fig. 4.8-6).

5. Gas slug flow interrupted the analog output of the test article, but flowmeter function returned upon passage of the slug. The slugs produced measurable analog output reductions (and/or spikes) that did not closely approximate the actual slug volumes.

6. At low flow rates, performance of this test article was seriously affected only by low-frequency sine vibration (20 to 72 hertz). At turndown ratios below 5.3, the performance of the test article was not greatly affected by sine vibration at any frequency, producing steady-state errors within ±1.0 percent.

7. Performance was not noticeably affected after exposure of the flowmeter to Space Shuttle launch vibration environments.

8. Vibration testing was performed with the test article electronics box isolated from the shaker system. This isolation was required because of problems with the fiber optics connection to the box being extremely sensitive to vibration. It is strongly recommended that a new method of connection be found.

9. It is recommended that testing be performed to determine the effects of fluid density and viscosity on meter K-factor.

10. It is recommended that other rotor/sensor technologies be investigated. Minor dulling of paint on the test article rotor surface was observed after the completion of the entire test series. Over prolonged periods of operation, this surface degradation might impact performance of the optical sensor.

TABLE 4.8-1.- BEARINGLESS TURBINE FLOWMETER MANUFACTURER'S SPECIFICATIONS[a]

Manufacturer	Flow Systems Corp.
Linearity +0.5% of reading to 34 kPa (5 psi), m^3/sec (gal/min)	0.25×10^{-4} to 3.78×10^{-4} (0.4 to 6)
Linearity +0.5% of reading to 68.9 kPa (10 psi), m^3/sec (gal/min)	0.25×10^{-4} to 5.05×10^{-4} (0.4 to 8)
Extended low-flow nonlinear range, m^3/sec (gal/min) . . .	0.13×10^{-4} to 0.25×10^{-4} (0.2 to 0.4)
Readout pulses per unit volume, pulses/m^3 (pulses/gal) . . .	8.72×10^5 (3300)
Nonrepeatability, percent . . .	+0.05

[a]Specifications apply to laboratory tests on pure water at a temperature of 295.4 K (22.2° C (72° F)): operating temperature of 422 K (148.9° C (300° F)) and static pressure of 6.89 MPa (1000 psi). These manufacturer specification claims were not investigated in this test program.

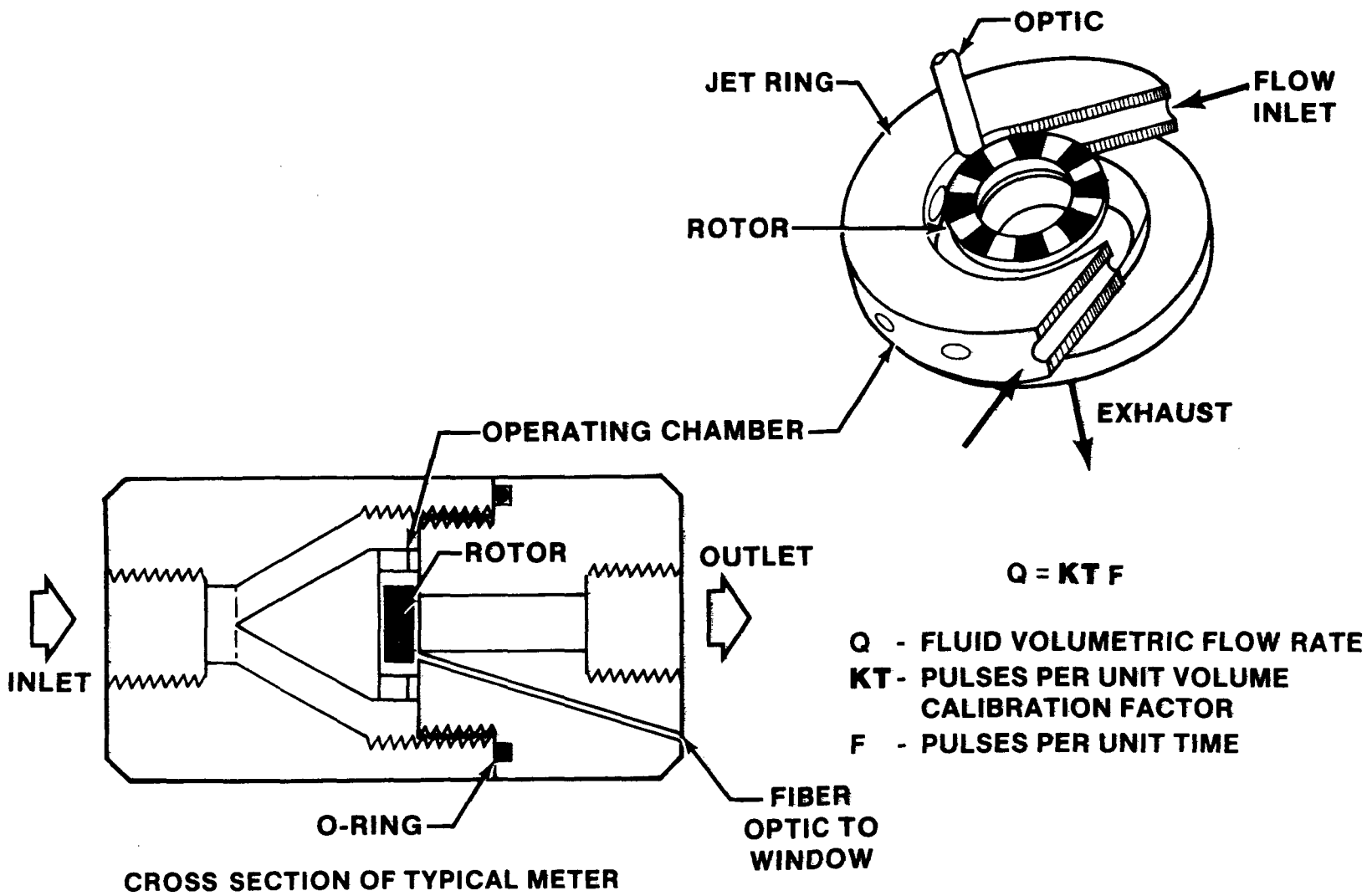

Figure 4.8-1.- Bearingless turbine flowmeter.

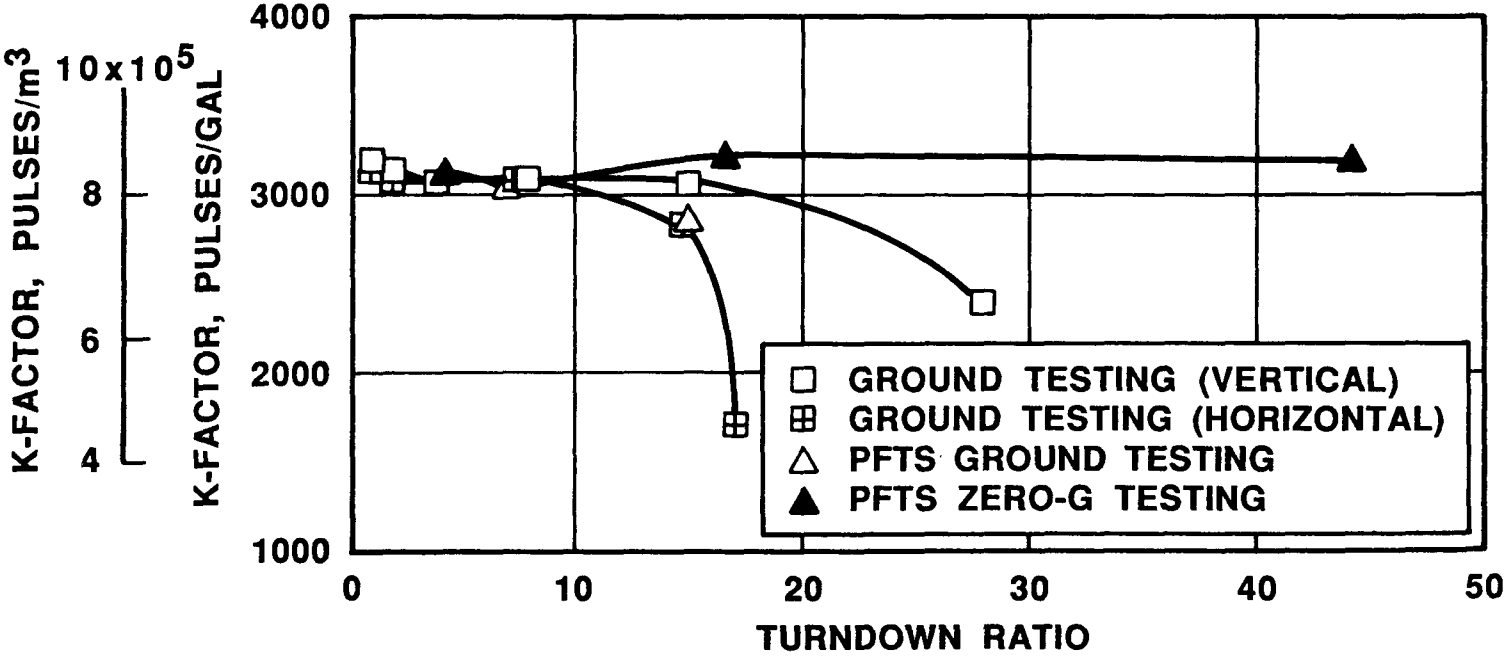

Figure 4.8-2.- Bearingless turbine flowmeter steady-state K-factor versus turndown ratio.

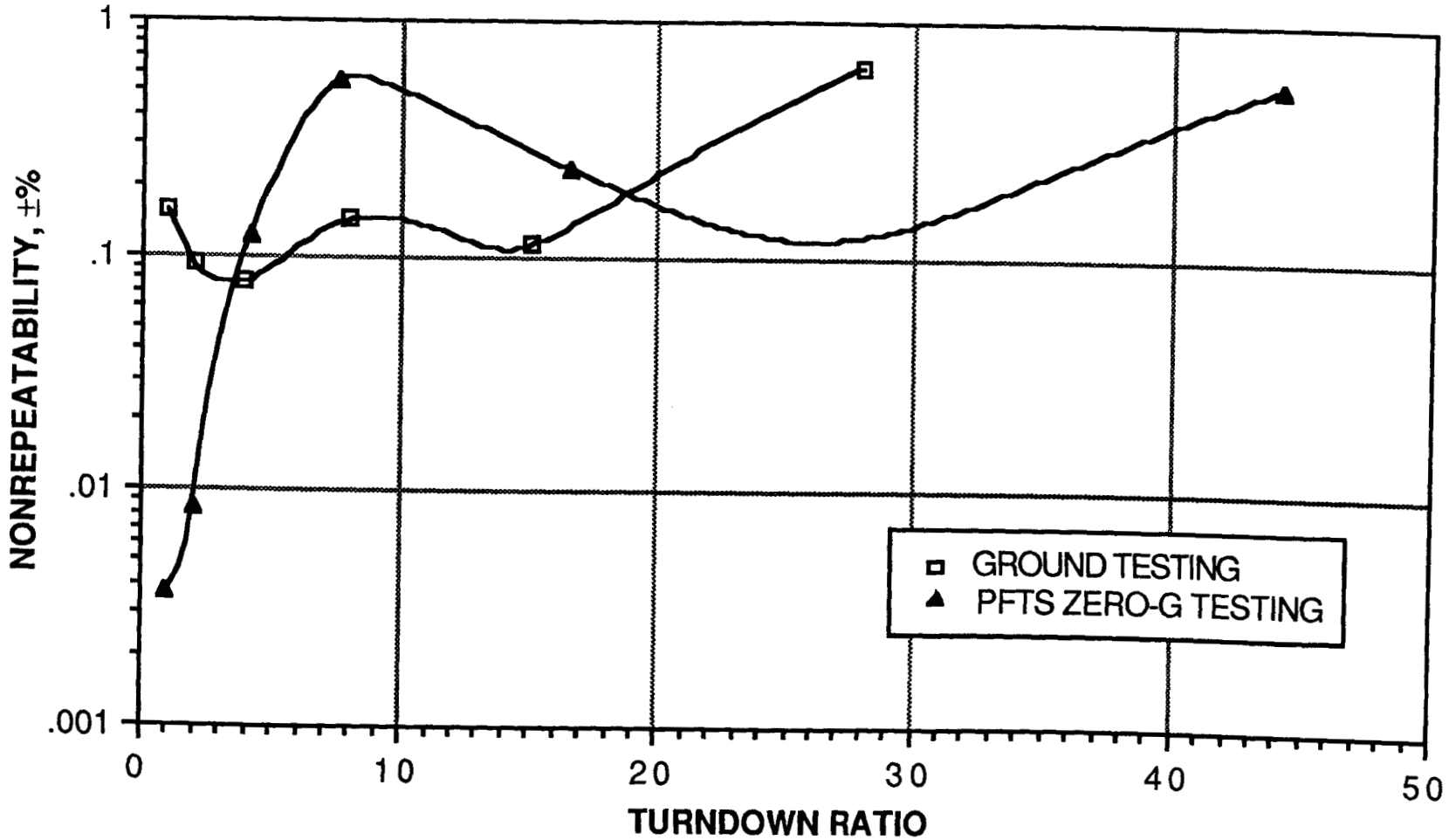

Figure 4.8-3.- Bearingless turbine flowmeter steady-state nonrepeatability versus turndown ratio.

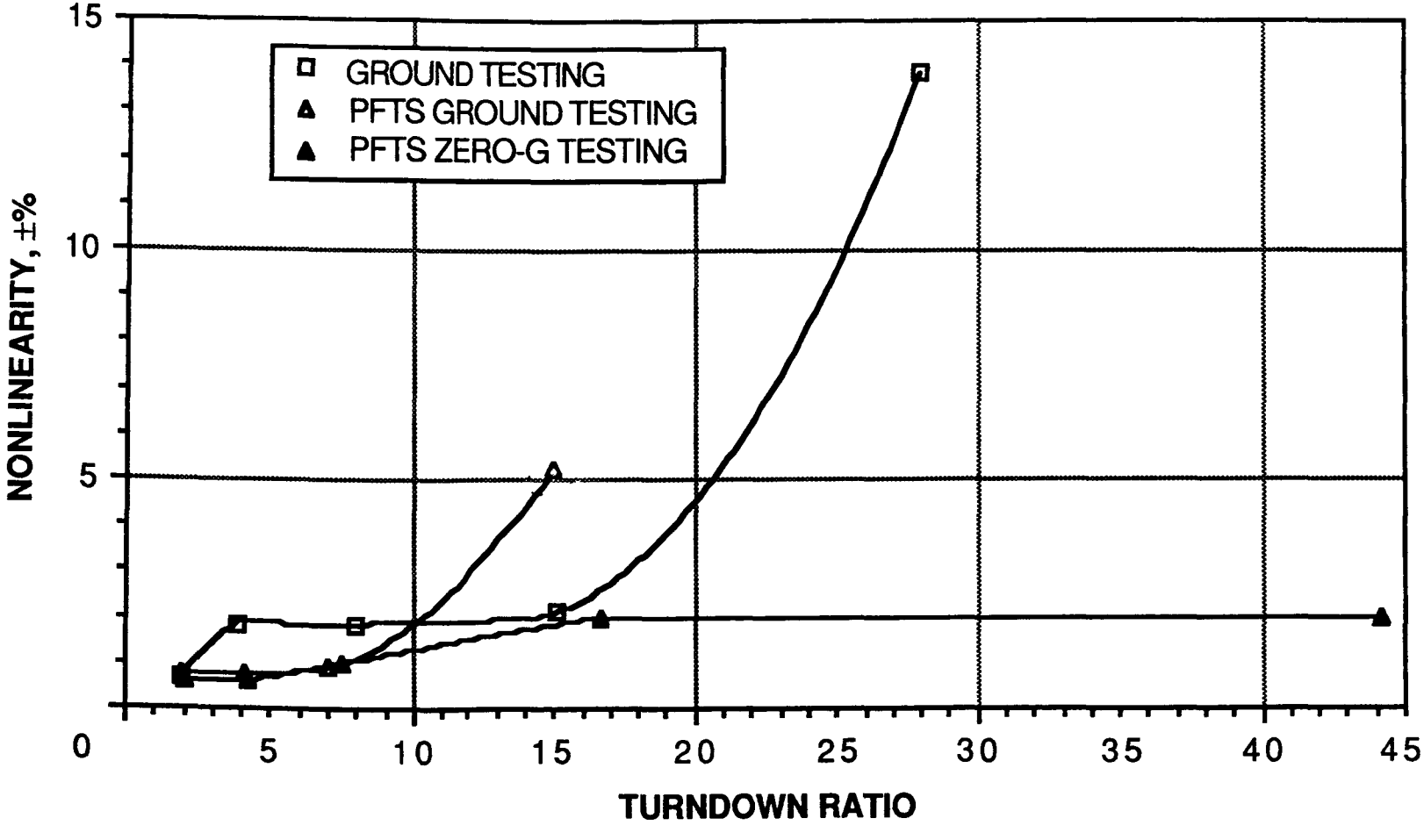

Figure 4.8-4.- Bearingless turbine flowmeter steady-state nonlinearity versus turndown ratio.

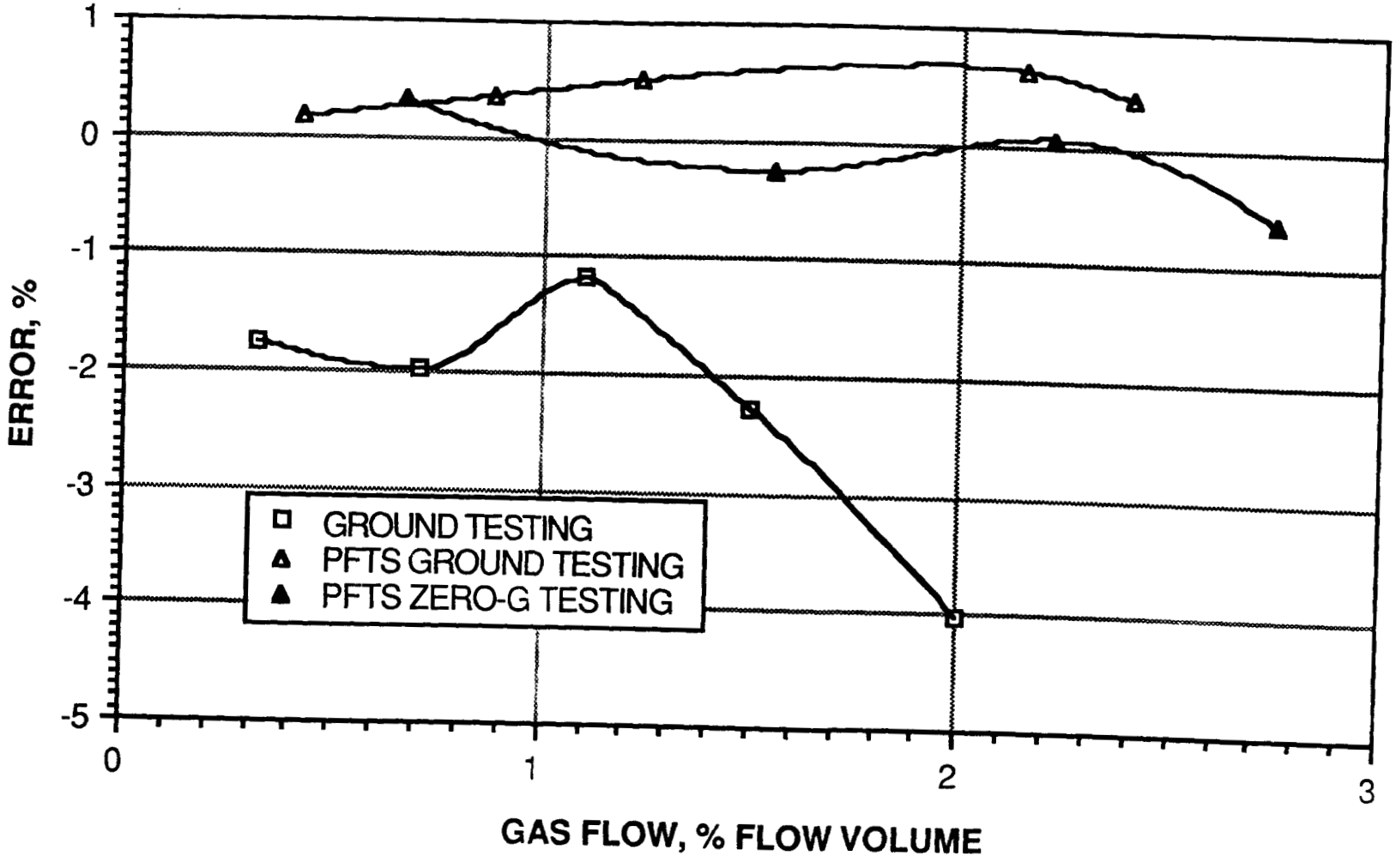

Figure 4.8-5.- Bearingless turbine flowmeter two-phase flow error versus gas flow.

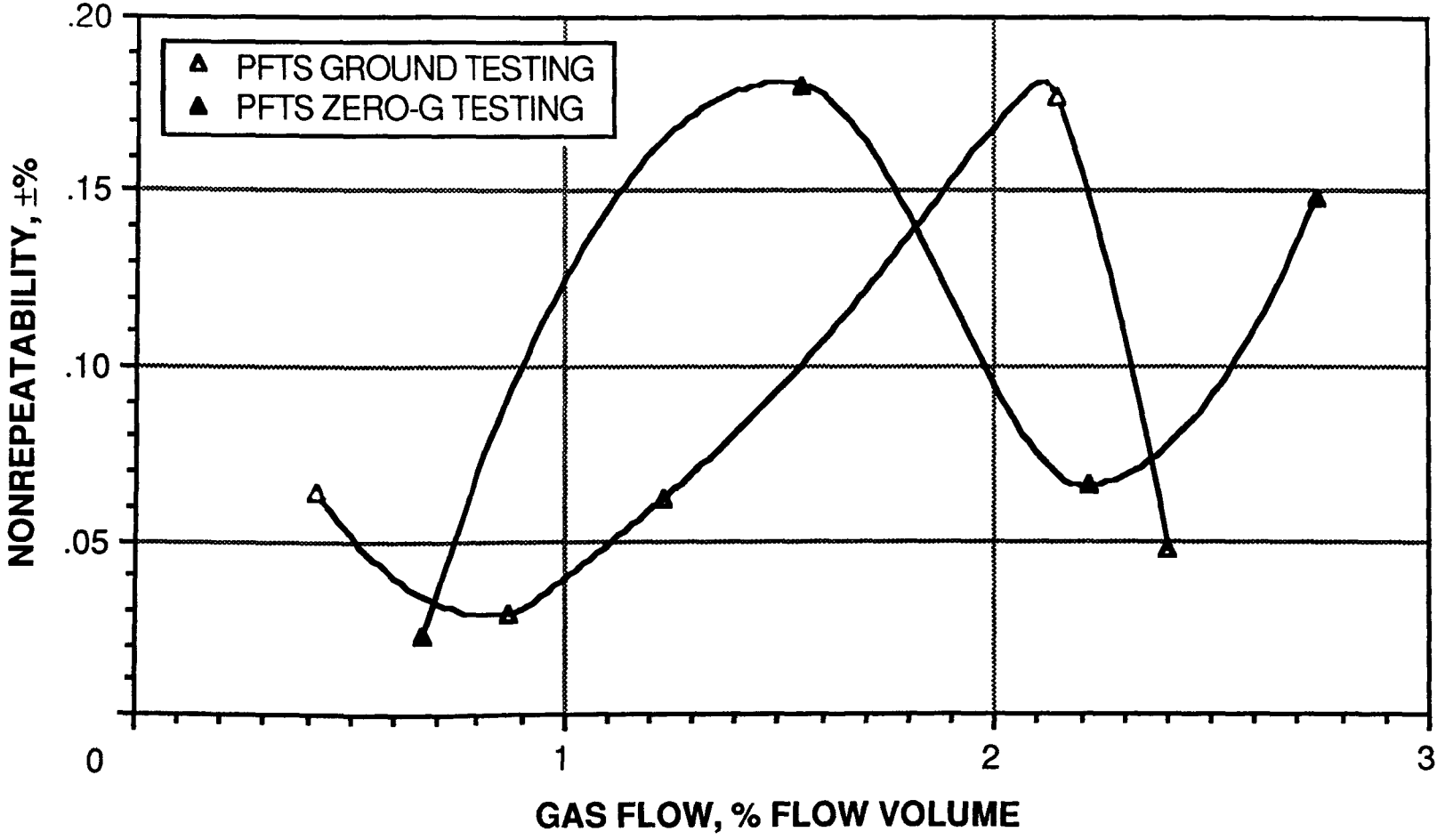

Figure 4.8-6.- Bearingless turbine flowmeter two-phase flow nonrepeatability versus gas flow.

4.9 TURBINE/TURBINE DELTA P HYBRID FLOWMETER

FLOWMETER DESCRIPTION

The turbine/turbine differential-pressure (delta p) flowmeter is a hybrid flowmeter that combines typical turbine and venturi/nozzle/orifice (delta pressure) flowmetering techniques (figs. 4.9-1(a) and 4.9-1(b)) to measure one- and two-phase fluid mass flow rates.

The turbine/turbine delta p flowmeter used for ground testing was constructed through the modification of an existing Flow Technology model FT-32C250-LB (serial number 32059) 0.05-meter (2 inch) turbine flowmeter. The turbine flowmeter was modified to accept two delta-p transducers. The two pressure drops measured were the inlet to outlet delta p and the inlet to turbine hub (effective throat/orifice) delta p.

The turbine/turbine delta p flowmeter combination used for zero-g testing consisted of a 0.02-meter (0.75 inch) Hersey/ITT Barton model 7186-0006A turbine flowmeter and typical facility delta-pressure transducers measuring only the overall inlet to outlet pressure drop. The turbine flowmeter used in this combination incorporated a hydrodynamic turbine bearing which should increase its performance.

The turbine/turbine delta p combination flowmeter, along with a fluid temperature measurement, can theoretically provide totally redundant two-phase mass-flow-rate measurement or can, without the temperature measurement, switch over to volumetric flow measurement if one of the two subcomponent flowmeters fails and thereby can provide functional flowmetering redundancy.

FLOWMETER PERFORMANCE

A summary of flowmeter performance results and recommendations follows.

1. Steady-state nonlinearities are more significantly affected by flowmeter hardware configuration than by acceleration environments (ground versus zero-g) as shown in figure 4.9-2.

2. Ground testing flowmeter nonrepeatabilities were significantly affected by the selection of delta-pressure measuring techniques (throat versus inlet to outlet) as shown in figures 4.9-3 and 4.9-4. Zero-g nonrepeatability was significantly improved relative to ground testing. This improvement may be partly due to use in the zero-g testing of the turbine flowmeter hydrodynamic rotor bearing, which decreases rotor friction.

3. Pulse flow error decreased with increasing pulse width but was never particularly low (fig. 4.9-5).

4. Two-phase flow nonrepeatabilities improved with increasing line operating pressures (figs. 4.9-6 and 4.9-7). Zero-g two-phase flow

nonrepeatability was slightly better than that of ground level (fig. 4.9-8).

5. Two-phase flow errors are more affected by flowmeter configuration than by gas flow rate (fig. 4.9-9).

6. Special two-phase flow calibrations will be required to characterize the K-factor of this flowmetering concept as a function of gas percentage and line pressure. It is recommended that the overall delta-p measurement be used for two-phase flow operations because the correction factors for the overall delta-p measurement are linear and pressure independent (fig. 4.9-10).

The following constraints should be noted.

1. The 0.02-meter (0.75 inch) flowmeter was used only in the PFTS testing. All data not labeled "PFTS" were generated using the 0.05-meter (2 inch) flowmeter.

2. Unless specified otherwise, all of the data presented were generated using the overall (inlet to outlet) delta-pressure and turbine measurements.

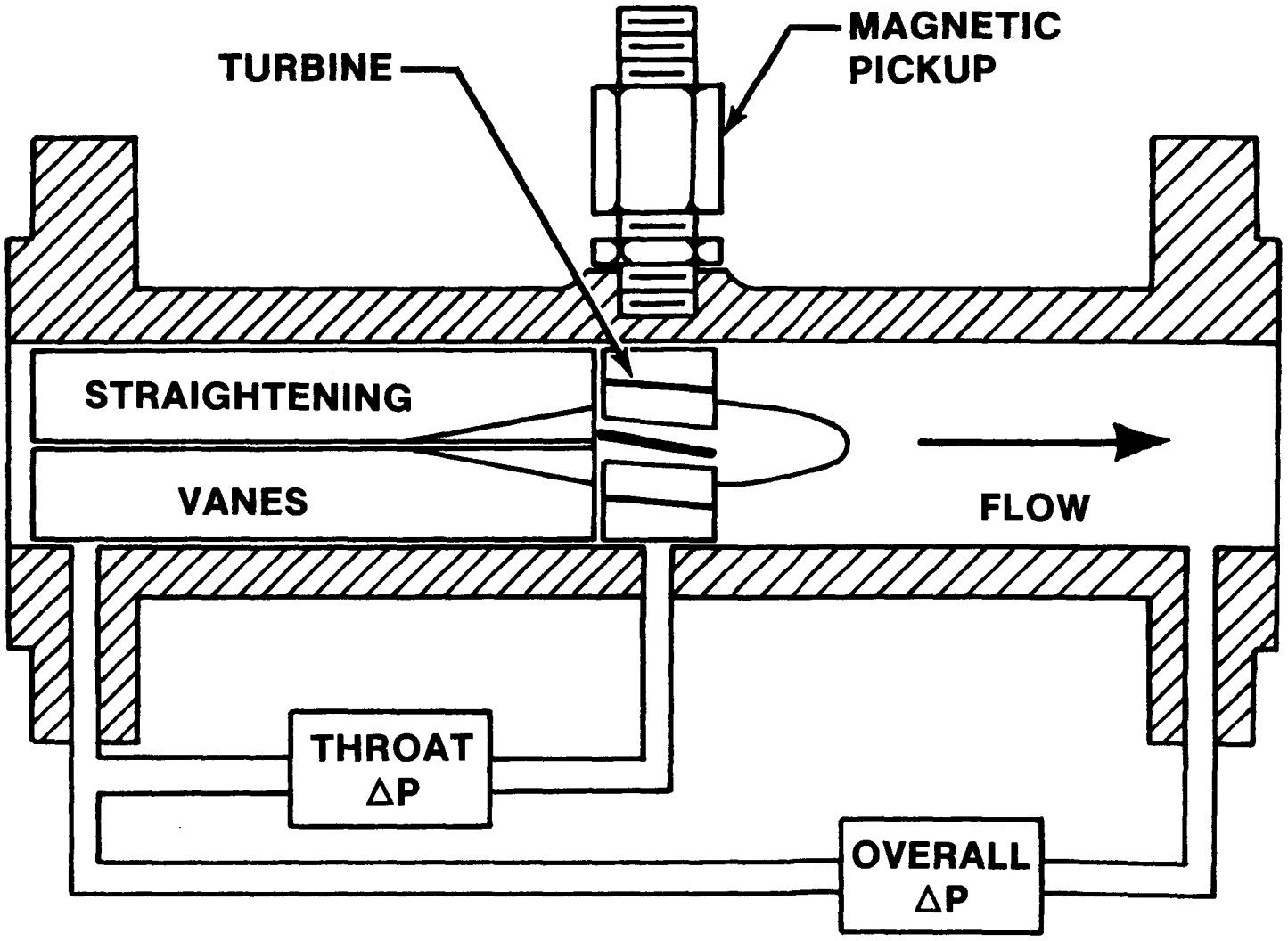

(a) Schematic diagram.

Figure 4.9-1.- Turbine/turbine delta p hybrid flowmeter.

Turbine flowmeter:

$$Q_T = \mathbf{KTF}$$

Delta pressure flow rate:

$$Q_{\Delta P} = \mathbf{K_{\Delta P}}\ (\Delta P/\rho)^{\frac{1}{2}}$$

Combined:

$$Q_T = Q_{\Delta P}$$

$$\mathbf{KTF} = \mathbf{K_{\Delta P}}\ (\Delta P/\rho)^{\frac{1}{2}}$$

$$\rho = \Delta P(\mathbf{K_{\Delta P}})^2/(\mathbf{KTF})^2$$

$$\mathbf{M} = Q_T\rho$$

$$\mathbf{M} = \Delta P(\mathbf{K_{\Delta P}})2/\mathbf{KTF}$$

Where:

Q_T	Turbine volumetric flow rate
$Q_{\Delta P}$	ΔP volumetric flow rate
KT	Turbine calibration constant
$\mathbf{K_{\Delta P}}$	ΔP calibration constant
ΔP	Change in pressure across turbine
F	Measured turbine frequency
ρ	Fluid density
M	Mass flow rate

(b) Equations and symbol definitions.

Figure 4.9-1.- Concluded.

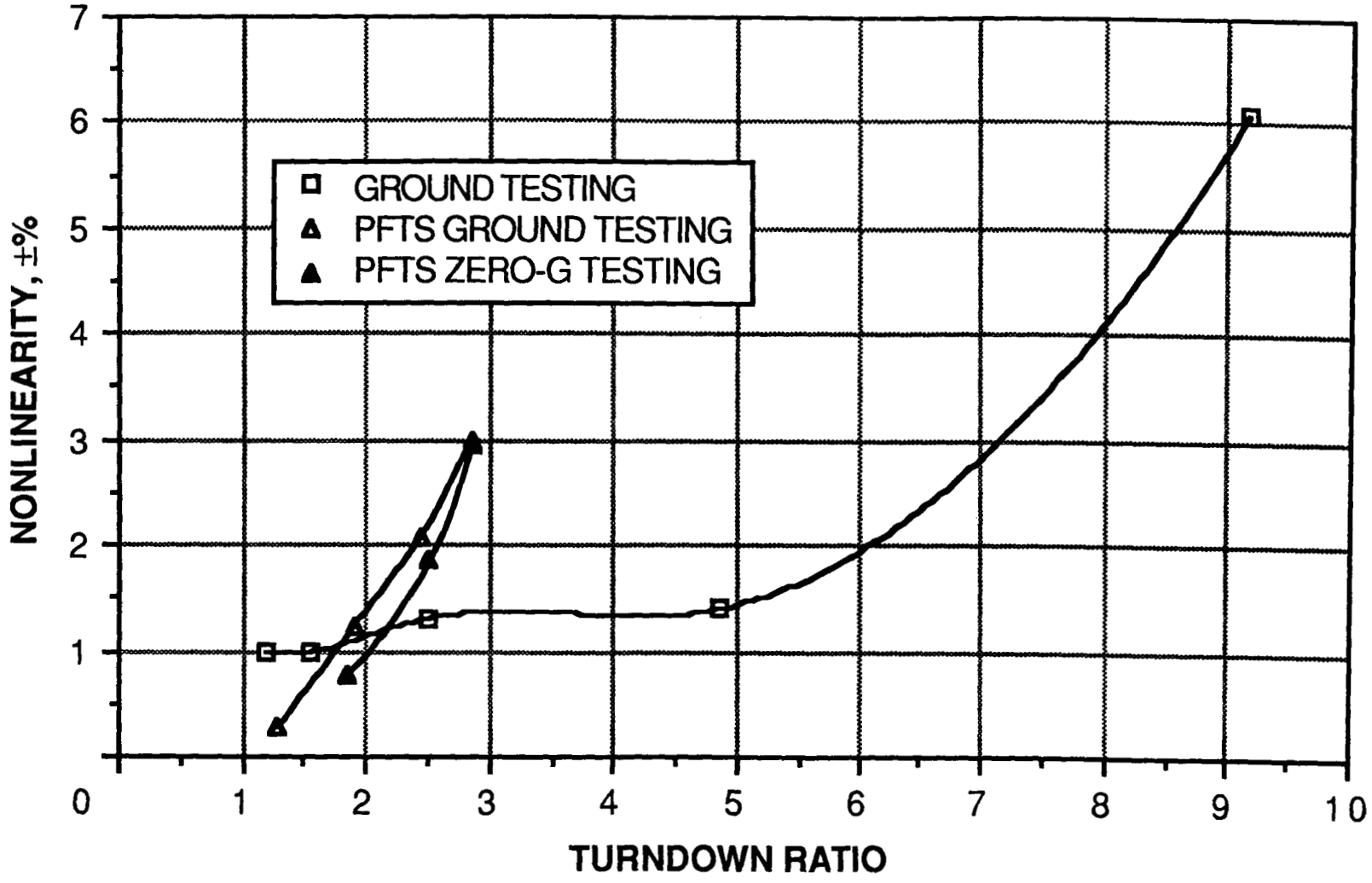

Figure 4.9-2.- Turbine/turbine delta p flowmeter steady-state nonlinearity versus turndown ratio.

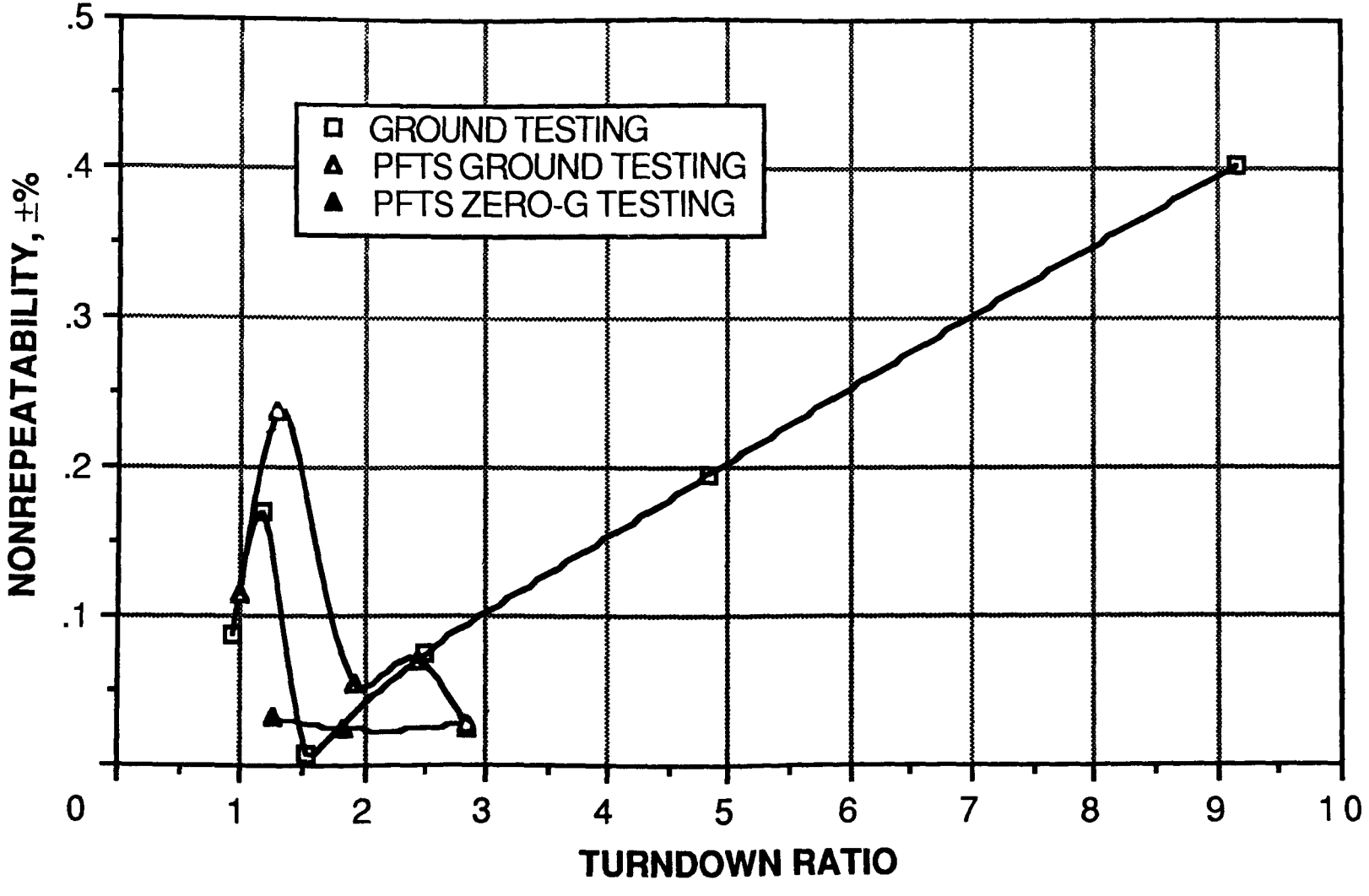

Figure 4.9-3.- Turbine/turbine delta p flowmeter steady-state nonrepeatability versus turndown ratio.

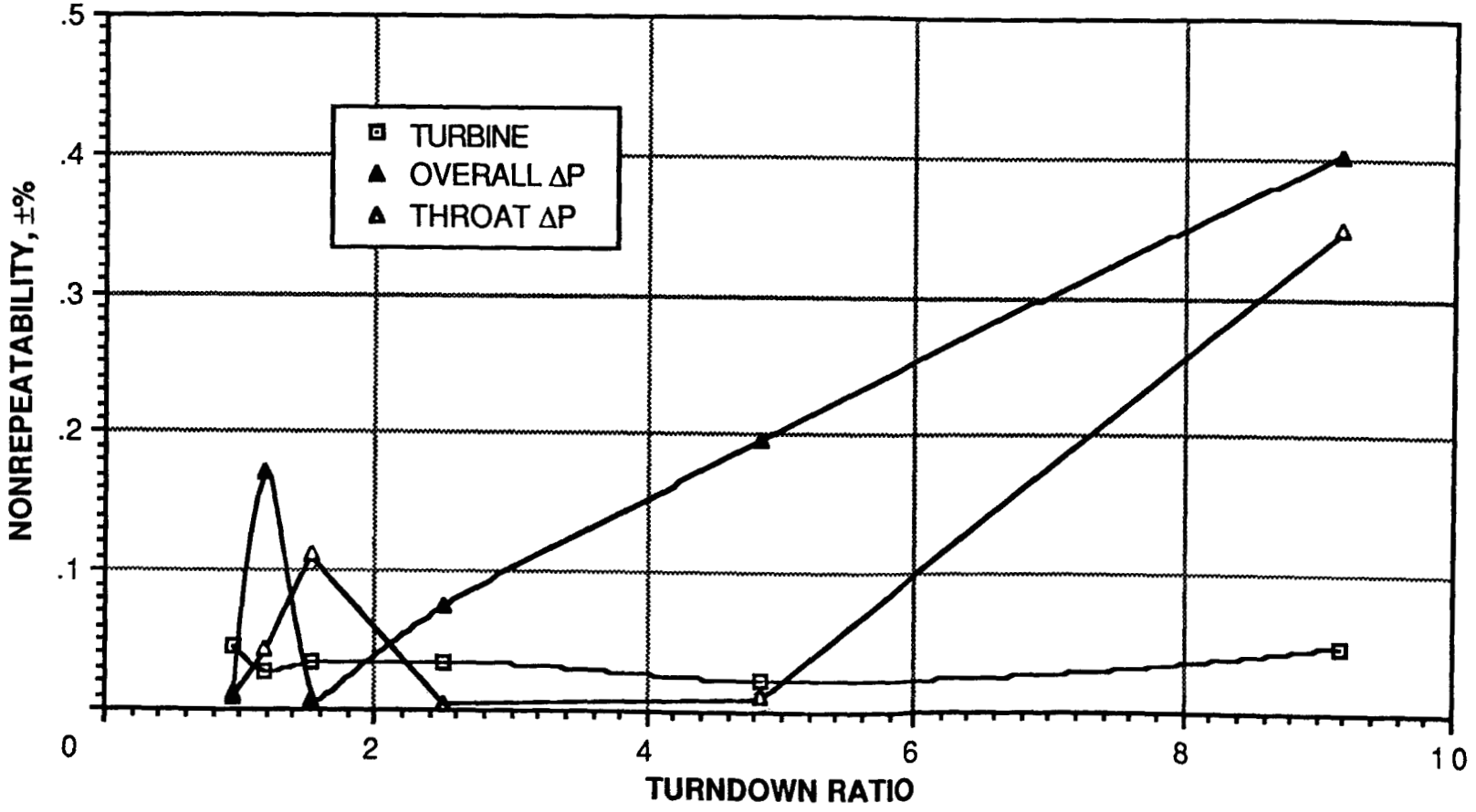

Figure 4.9-4.- Turbine/turbine delta p flowmeter subelement steady-state nonrepeatability versus turndown ratio.

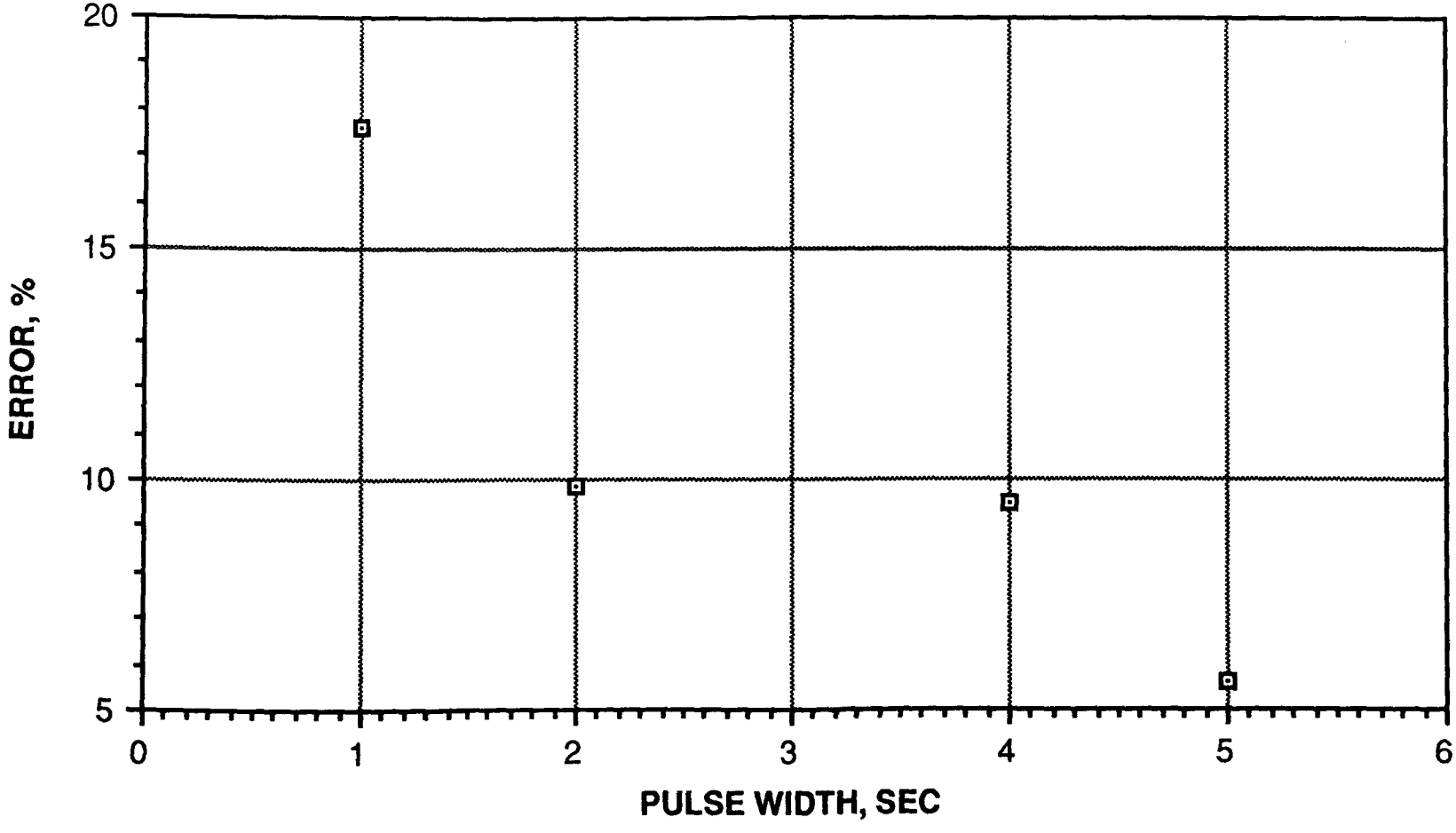

Figure 4.9-5.- Turbine/turbine delta p flowmeter pulse flow error versus pulse width.

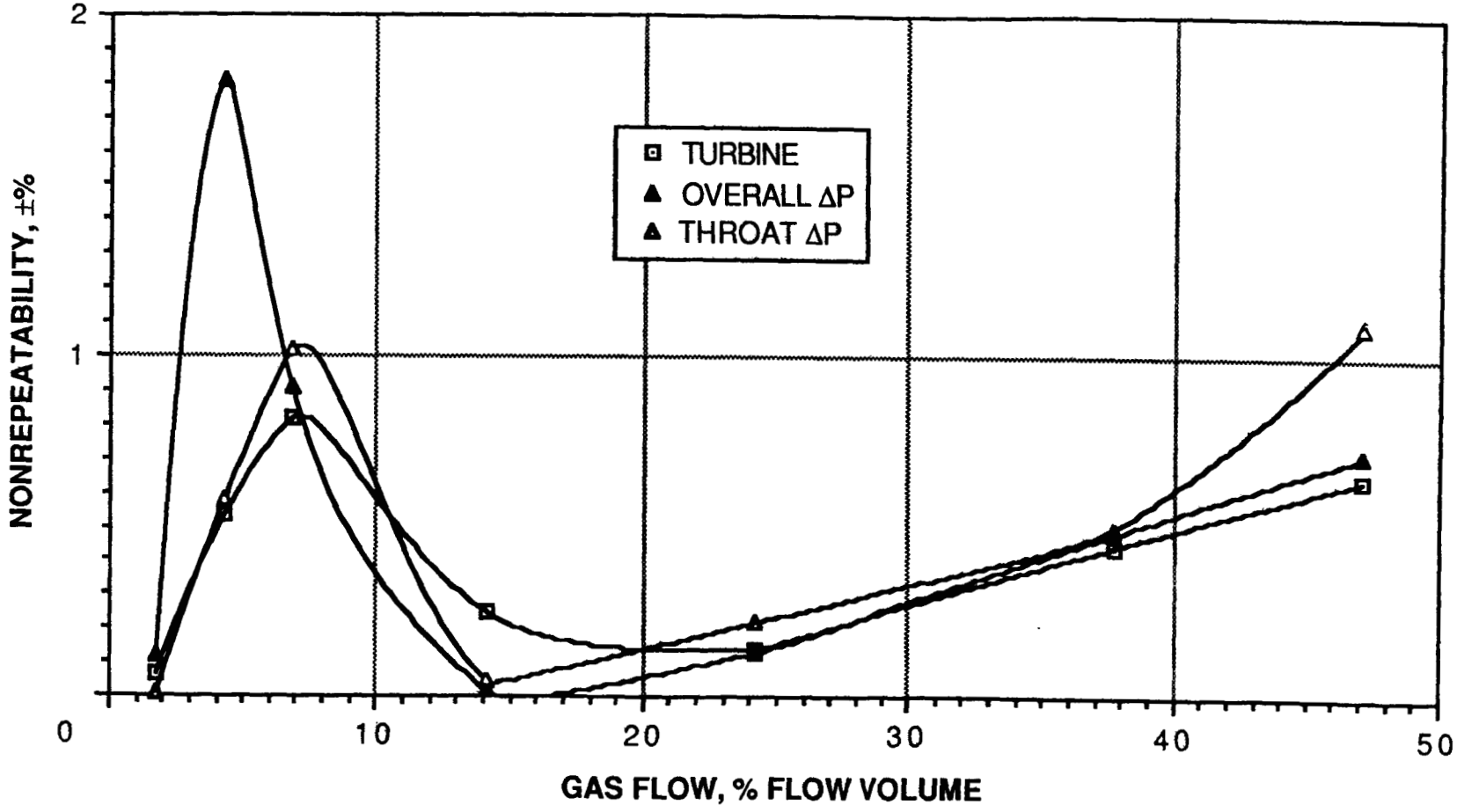

Figure 4.9-6.- Turbine/turbine delta p flowmeter subelement two-phase flow nonrepeatability versus gas flow at 0.33 MPa (47.7 psia).

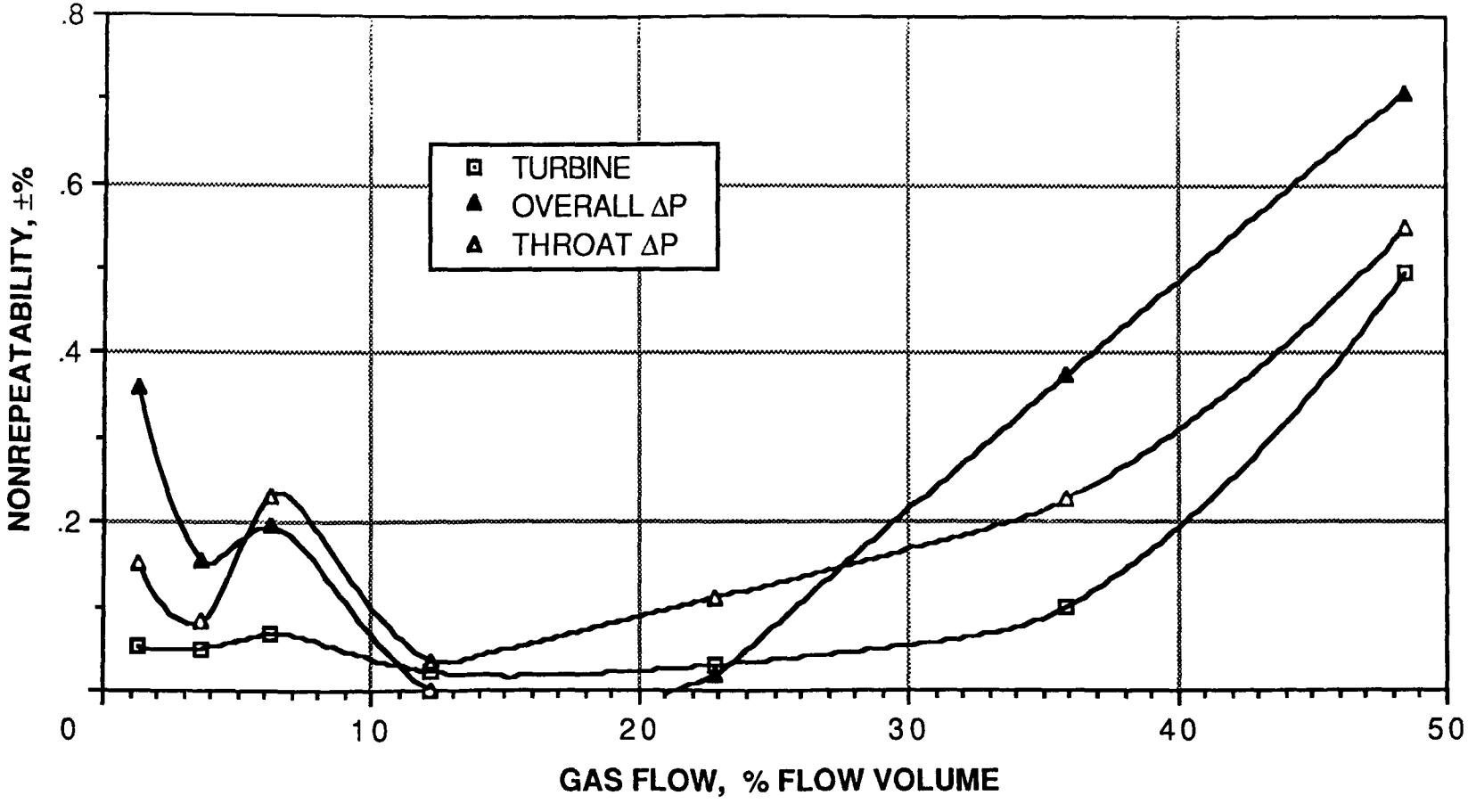

Figure 4.9-7.- Turbine/turbine delta p flowmeter subelement two-phase flow nonrepeatability versus gas flow at 0.65 MPa (93.7 psia).

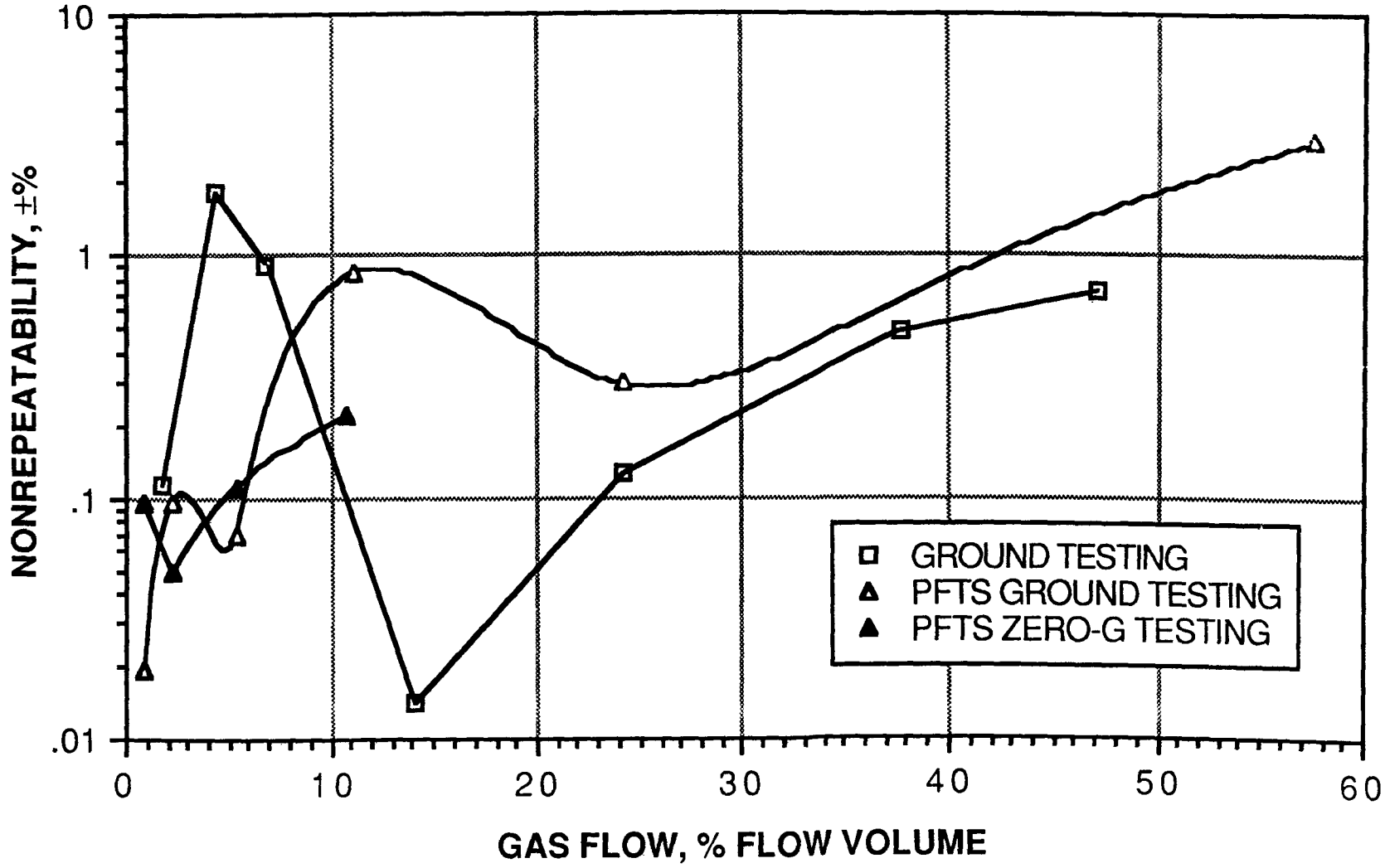

Figure 4.9-8.- Turbine/turbine delta p flowmeter two-phase nonrepeatability versus gas flow.

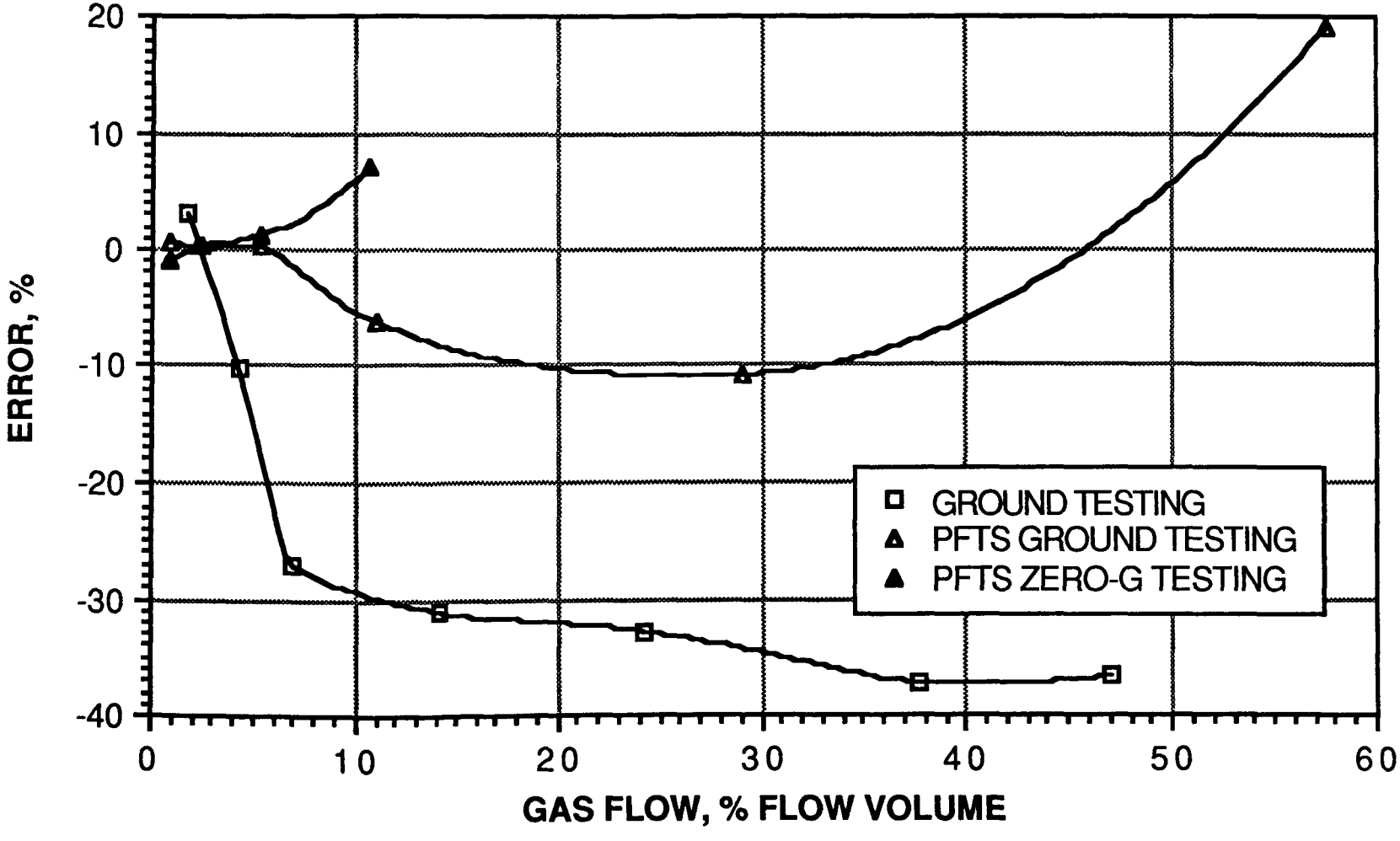

Figure 4.9-9.- Turbine/turbine delta p flowmeter two-phase flow error versus gas flow.

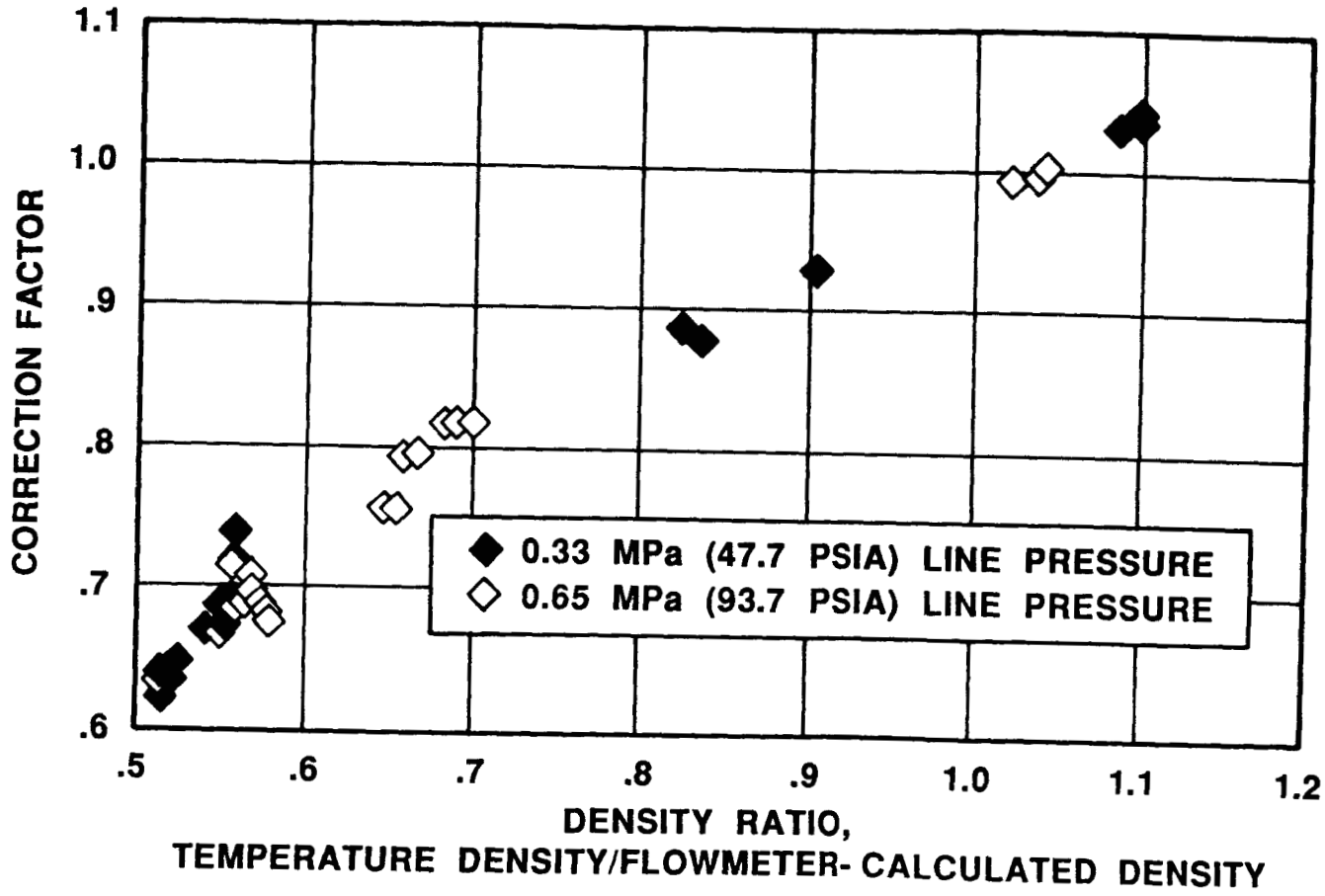

Figure 4.9-10.- Turbine/turbine delta p flowmeter overall delta-pressure component correction factor.

4.10 DRAGBODY FLOWMETER

FLOWMETER DESCRIPTION

Dragbody flowmetering takes advantage of the relationship between fluid flow and fluid momentum transfer to calculate flow velocity (figs. 4.10-1(a) and 4.10-1(b)). Fluid flow past a flow target suspended (by cantilever beam) in the flow field exerts a force on that flow target, bending the suspending cantilever beam. This beam deflection is proportional to the flow velocity and is measured by a strain gauge.

The dragbody flowmeter performance data presented in this document were generated as part of the dragbody/turbine hybrid flowmeter test series. The dragbody flowmeter tested was a 0.02-meter (0.75 inch) Ramapo model V-3/4-SSQ. For more information on this flowmeter and test series, see section 4.11.

FLOWMETER PERFORMANCE

The following conclusions with respect to flowmeter performance can be stated.

1. Steady-state nonlinearity and nonrepeatability increase with increasing turndown ratio (figs. 4.10-2 and 4.10-3).

2. Pulse flow performance is best at the smaller pulse widths (fig. 4.10-4). This flowmeter also demonstrates short response times to pulse flow transients.

3. Two-phase flow errors increase with increasing gas flow volumes (fig. 4.10-5).

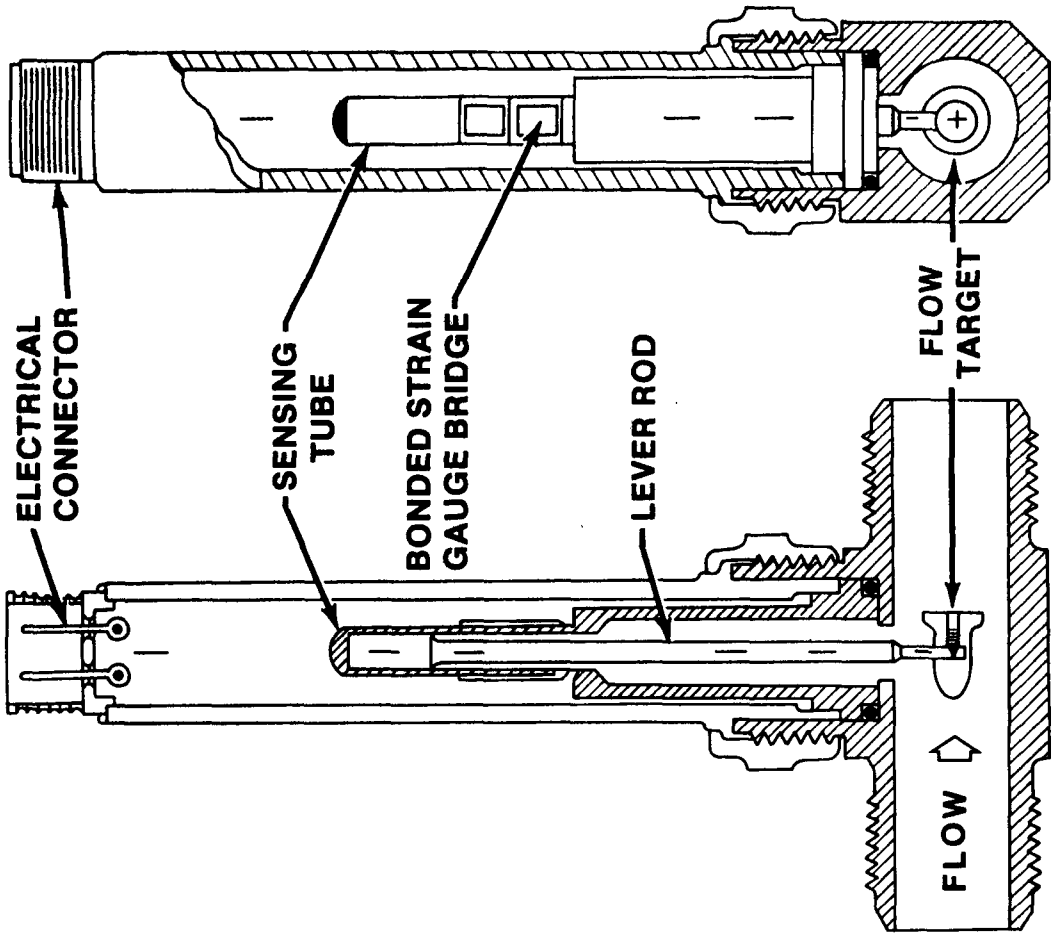

(a) Schematic diagram

Figure 4.10-1.- Dragbody flowmeter.

$$E = K_1 F_s$$

If: $Re < 2000$

$$F_T = C_d A_T \rho(V^2/2g)$$

$$F_T = F_s$$

$$E/K_1 = C_d A_T \rho(V^2/2g)$$

$$(VA_F)^2 = (E/\rho)\ (2g/K_1 C_d)\ (A_F^2/A_T)$$

$$VA_F = \mathbf{KD}\ (E/\rho)^{\frac{1}{2}}$$

$$\mathbf{KD} = (2gA_F^2/K_1 C_d A_T)^{\frac{1}{2}}$$

$$Q = VA_F$$

$$Q = \mathbf{KD}\ (E/\rho)^{\frac{1}{2}}$$

Where:

F_T	Force on target body
F_s	Force on strain gauge
E	Instantaneous voltage ratio output
K_1	Strain gauge coefficient
C_d	Drag coefficient
ρ	Fluid density
V	Fluid velocity
g	Gravitational constant
A_T	Cross-sectional area of target
A_F	Flow area
Q	Volumetric flow rate

(b) Equations and symbol definitions.

Figure 4.10-1.- Concluded.

C-2

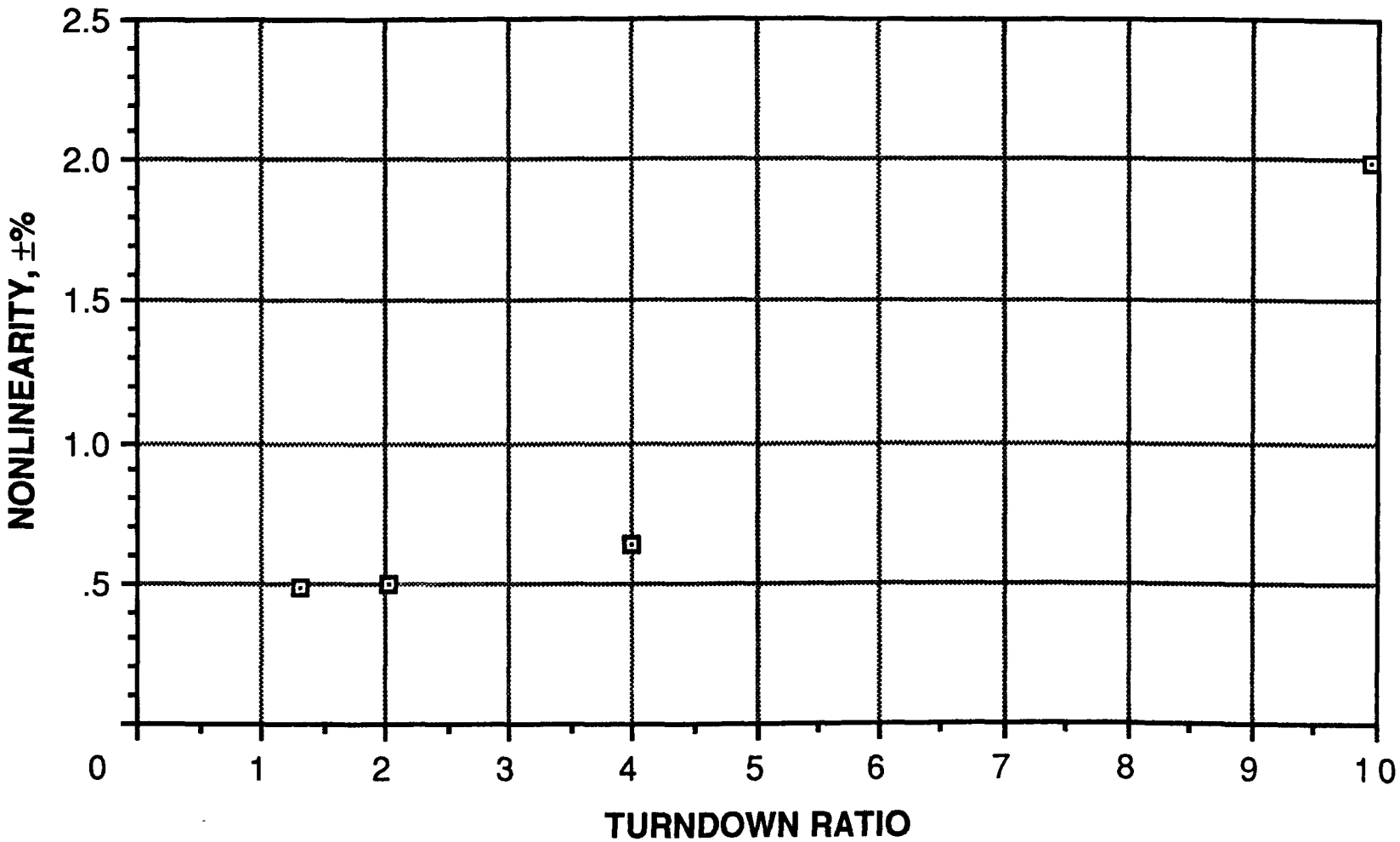

Figure 4.10-2.- Dragbody flowmeter steady-state nonlinearity versus turndown ratio.

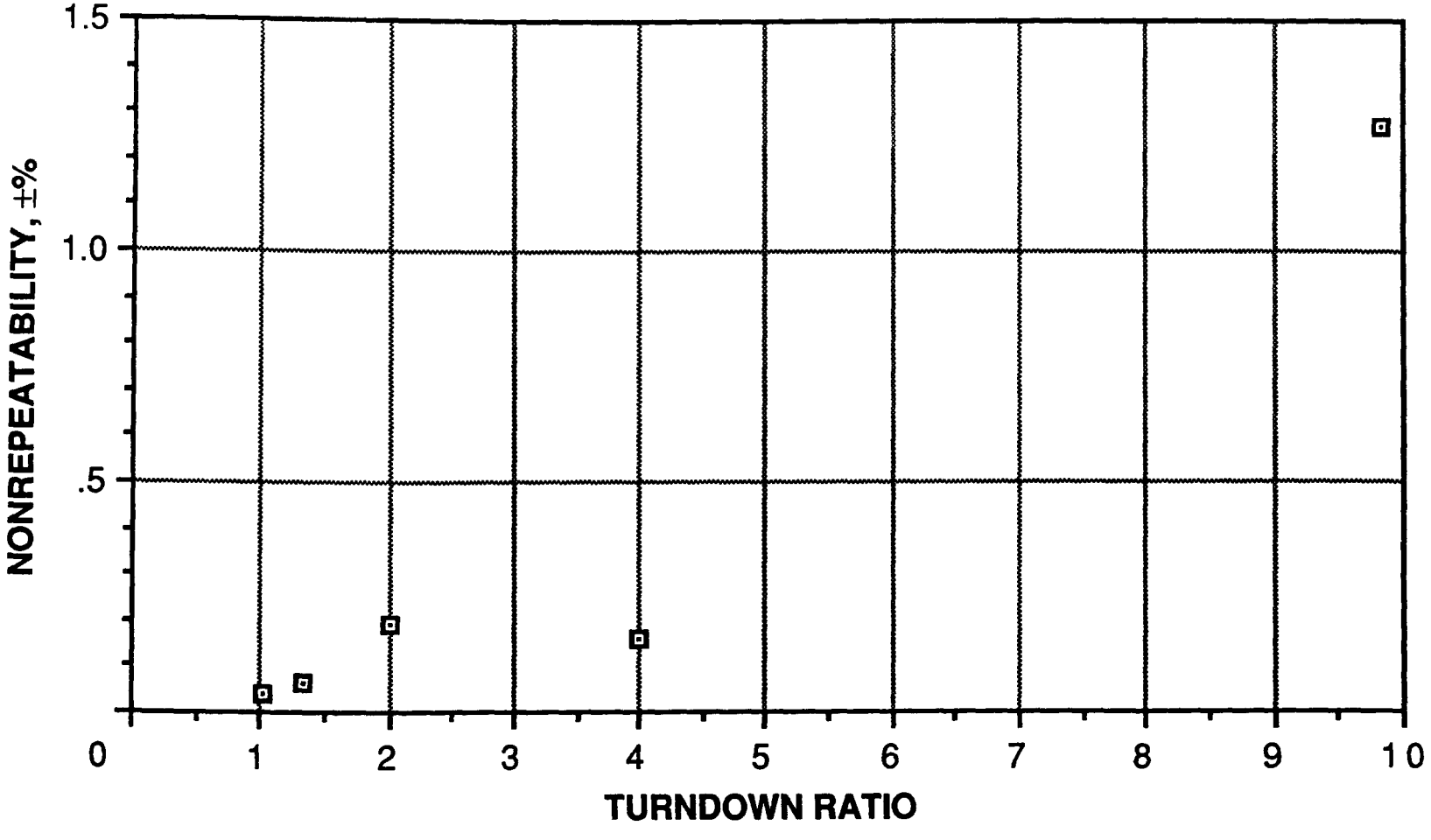

Figure 4.10-3.- Dragbody flowmeter steady-state nonrepeatability versus turndown ratio.

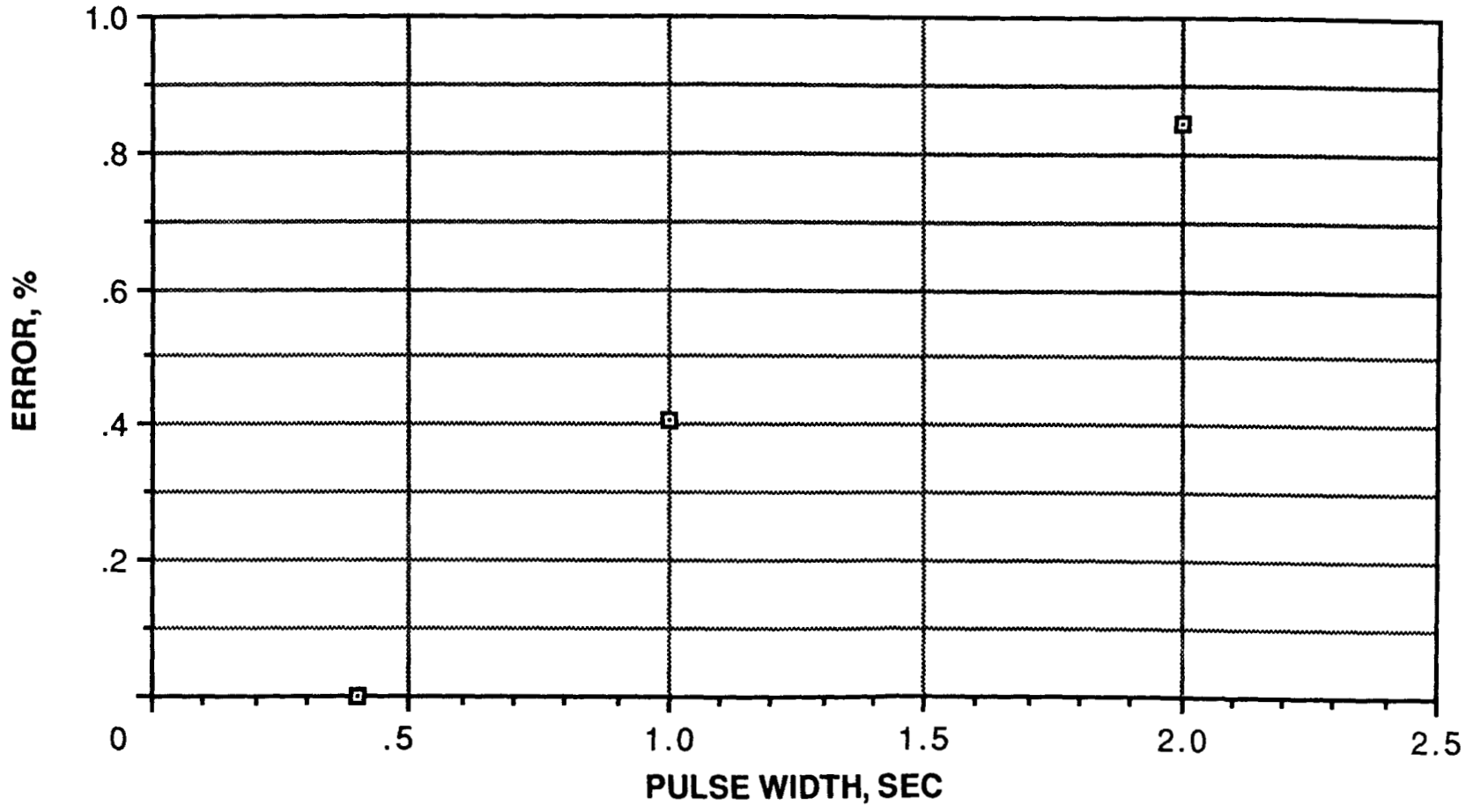

Figure 4.10-4.- Dragbody flowmeter pulse flow error versus pulse width.

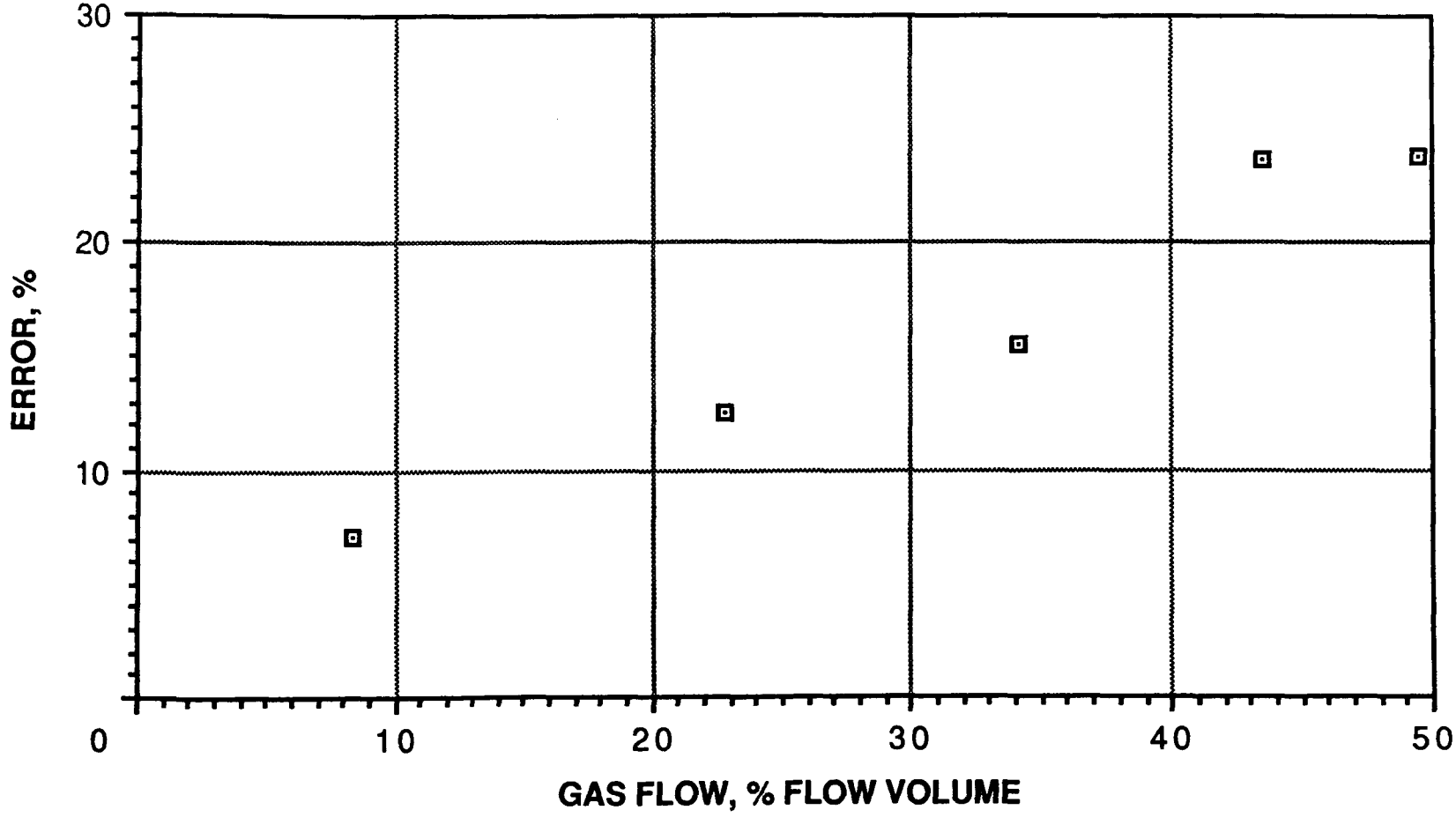

Figure 4.10-5.- Dragbody flowmeter two-phase flow error versus gas flow.

4.11 DRAGBODY/TURBINE HYBRID FLOWMETER

FLOWMETER DESCRIPTION

The dragbody/turbine flowmeter is a hybrid flowmeter. Hybrid flowmeters are flowmetering systems composed of two or more independent flowmeters plumbed in series and operated in tandem such that the output of each flowmeter supplies a portion of the information required to measure mass flow rate. In this case, a typical turbine flowmeter was used to measure volumetric flow rate and a dragbody flowmeter was used to measure fluid density as a function of volumetric flow rate (fig. 4.11-1(a)). The outputs of each flowmeter were combined to calculate mass flow rate, as described in figure 4.11-1(b), for all flow conditions.

The turbine flowmeter used in this test series was a Flow Technology flowmeter, model FT-12M20-LB, with a 30106 magnetic pickup. The dragbody flowmeter used in this test series was a Ramapo, model V-3/4-SSQ. The manufacturer's specifications are presented in tables 4.11-1 and 4.11-2, respectively.

The integration of different flowmeter types as subcomponents of a hybrid flowmeter is relatively unexplored technology. Because of this inexperience, physical integration constraint testing was performed on this hybrid flowmeter in addition to the standard multiple-flow condition testing. This additional testing included evaluation of flowmeter subcomponent separation distances, evaluation of flow mixer effects, and evaluation of preliminary integration calculation techniques. The results of this additional testing are presented in the flowmeter performance section that follows.

FLOWMETER PERFORMANCE

Following are flowmeter performance results and recommendations.

1. Steady-state nonlinearity increases with increasing turndown ratios (fig. 4.11-2).

2. The 10-flow-diameter component flowmeter separation was selected over the close-coupled and 20-flow-diameter separation configurations tested based on steady-state calibration constant and nonrepeatability (figs. 4.11-3 and 4.11-4) comparisons as well as on optimizing for compactness.

3. The tested pulse flow performance for the dragbody subcomponent was comparable to the turbine subcomponent performance. The dragbody calibration constant was relatively constant compared to that of the turbine for the pulse widths tested, although the turbine nonrepeatabilities were better. The nonrepeatability for the turbine meter remained below ± 0.4 percent for the full range of pulse flow testing (fig. 4.11-5). The nonrepeatability for the dragbody meter remained below ± 3.0 percent at the higher flow-rate conditions (≤ 2 turndown ratio) but increased sharply with

increasing pulse frequency (decreasing pulse width) at the lower (turndown ratio of 4) flow rate tested (fig. 4.11-6).

4. This flowmetering technique is suitable for calculating the liquid mass flow for two-phase flow conditions using flow correction factors. Based on gas bubble testing, liquid mass flows can be calculated to within ± 0.5 to ± 5 percent over a range of 4 to 50 percent gas volume injection (fig. 4.11-7).

5. Higher output noise resulted from the use of a three-segment flow mixer during gas bubble ingestion testing. This result suggests that flow mixers should not be used with this combination of hybrid flowmeter subcomponents.

6. The test article was not adversely affected by gas slug injection. The largest recovery time was 6.0 seconds for a 0.14-cubic-meter gas slug.

7. This hybrid flowmeter combination is feasible but would require enhanced parallel microprocessing to become practical for two-phase flow operations. Microprocessing research and further testing are therefore recommended.

8. This hybrid flowmeter should be applicable for on-orbit operations; however, its response to the flow mixer (item 5) suggests that this flowmeter combination is susceptible to gas/liquid positioning during two-phase flow. Zero-g testing is recommended to determine space applicability.

TABLE 4.11-1.- TURBINE FLOWMETER (HYBRID COMPONENT) MANUFACTURER'S SPECIFICATIONS[a]

Manufacturer	Flow Technology
Range, m^3/sec (gal/min)	0.126×10^{-3} to 1.26×10^{-3} (2 to 20)
Inaccuracy, percent	
Liquid	±0.55
Gas	±0.5
Repeatability, percent	±0.05
Operating temperature, K (°F) . .	16.5 to 672 (-430 to 750)
Dynamic response time for step change of flow, msec . . .	≈3

[a]Not investigated in this test program.

TABLE 4.11-2.- DRAGBODY FLOWMETER (HYBRID COMPONENT) MANUFACTURER'S SPECIFICATIONS[a]

Manufacturer	Ramapo
Range, m^3/sec (gal/min)	0.126×10^{-3} to 1.26×10^{-3} (2 to 20)
Inaccuracy, percent full scale	±0.5
Repeatability, percent of reading	±0.15
Operating temperature, K (°F) . .	219.3 to 422 (-65 to 300)

[a]Not investigated in this test program.

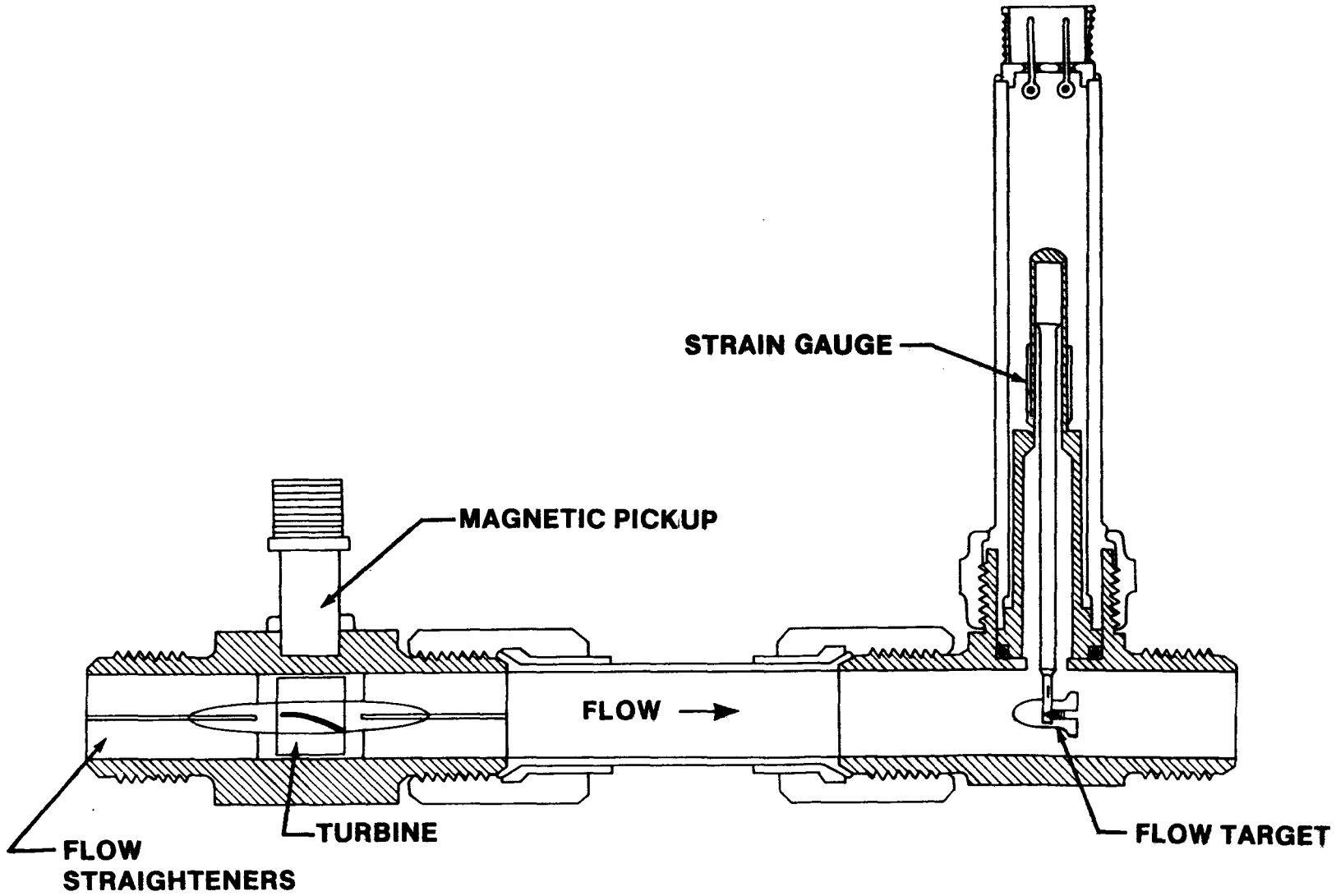

(a) Schematic diagram.

Figure 4.11-1.- Dragbody/turbine hybrid flowmeter.

Dragbody Flowmeter:

$Q_d = KD(E/\rho)^{\frac{1}{2}}$

$KD = (2gA_F^2/K_1C_dA_T)^{\frac{1}{2}}$

$\rho = KD^2E/Q_d^2$

Turbine flowmeter:

$Q_T = KTF$

Combined:

$Q_T = Q_d$

$\rho = KD^2E/(KTF)^2$

$M = Q_T\rho$

$M = ((KTF)KD^2E)/(KTF)^2$

$M = KD^2E/KTF$

Where:

E	Dragbody strain gauge output
ρ	Fluid density
A_F	Dragbody flow area
A_T	Dragbody target body cross-sectional area
C_d	Flow coefficient
g	Gravitational constant
K_1	Dragbody flowmeter strain gauge calibration constant
KT	Turbine calibration constant
F	Turbine output frequency
Q_d	Volumetric flow rate (dragbody)
Q_T	Volumetric flow rate (turbine)
M	Mass flow rate

(b) Equations and symbol definitions.

Figure 4.11-1.- Concluded.

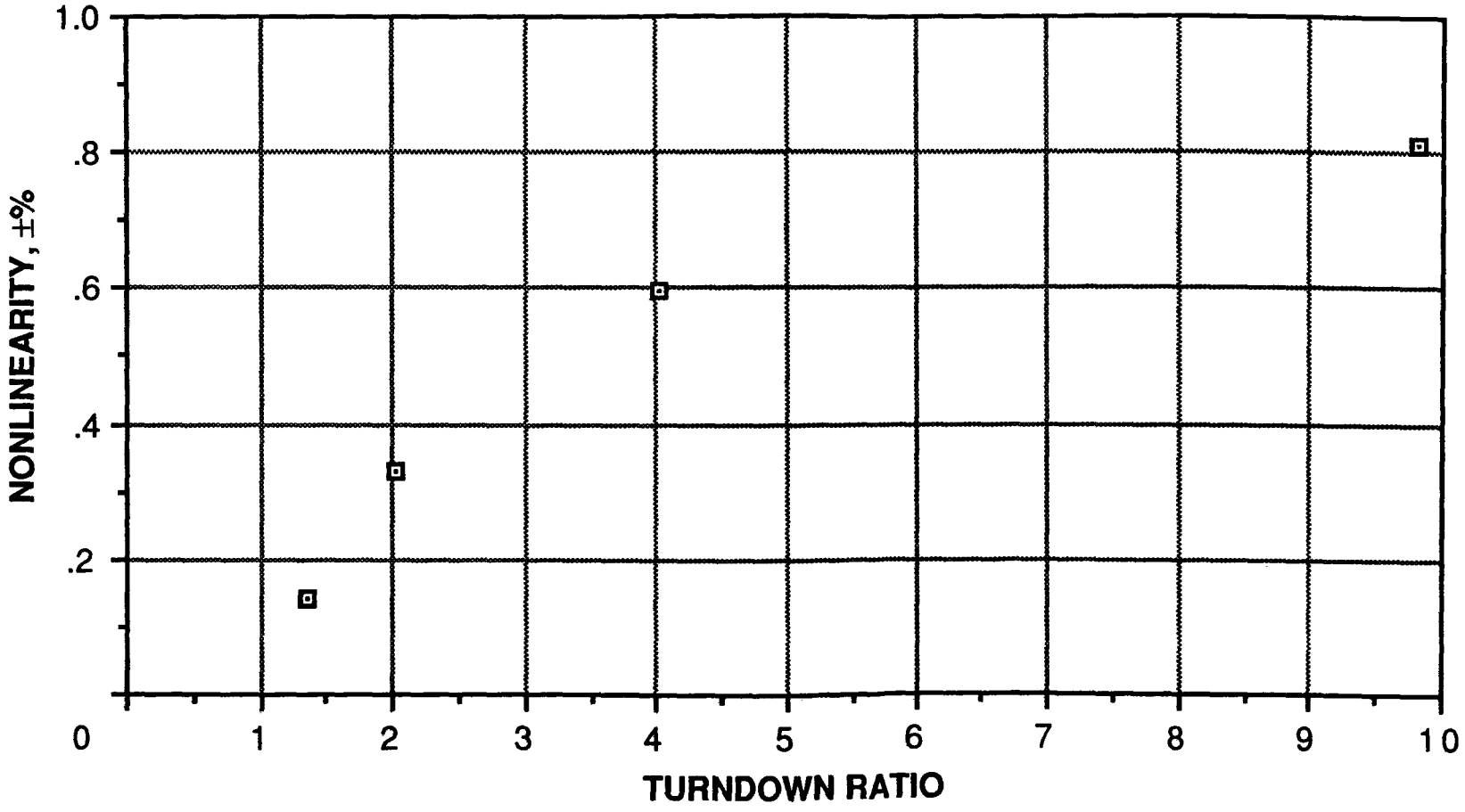

Figure 4.11-2.- Dragbody/turbine flowmeter combined steady-state nonlinearity versus turndown ratio.

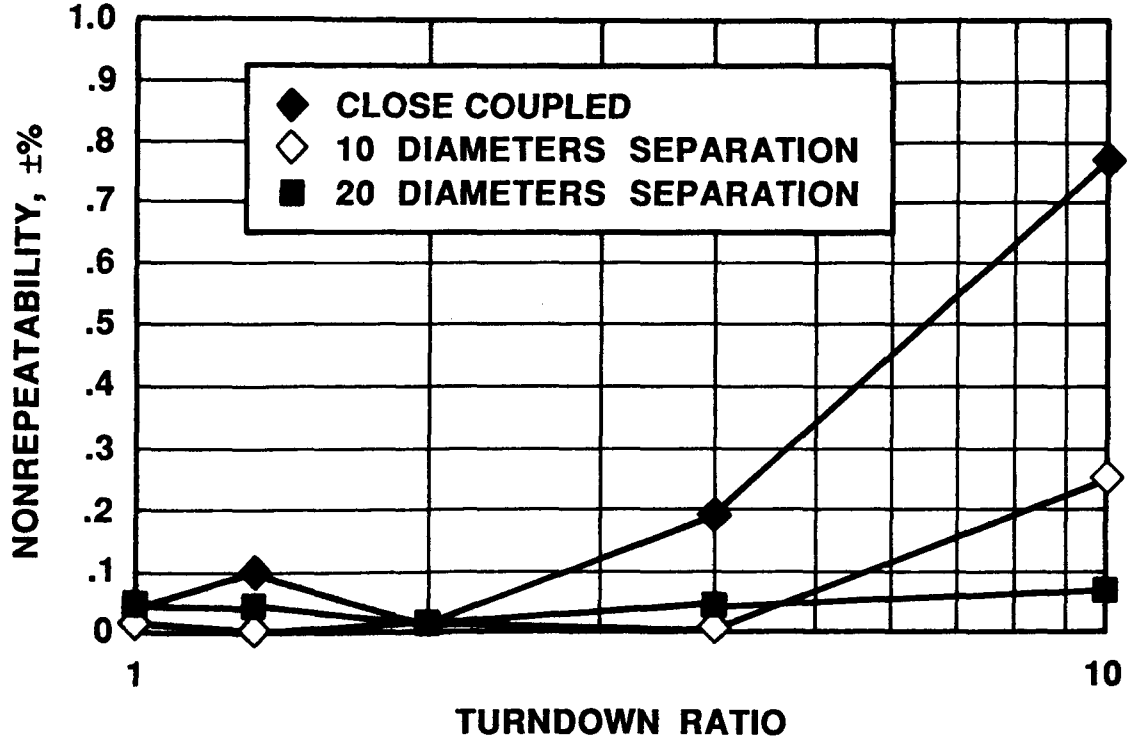

Figure 4.11-3.- Dragbody/turbine flowmeter component steady-state nonrepeatability versus turndown ratio.

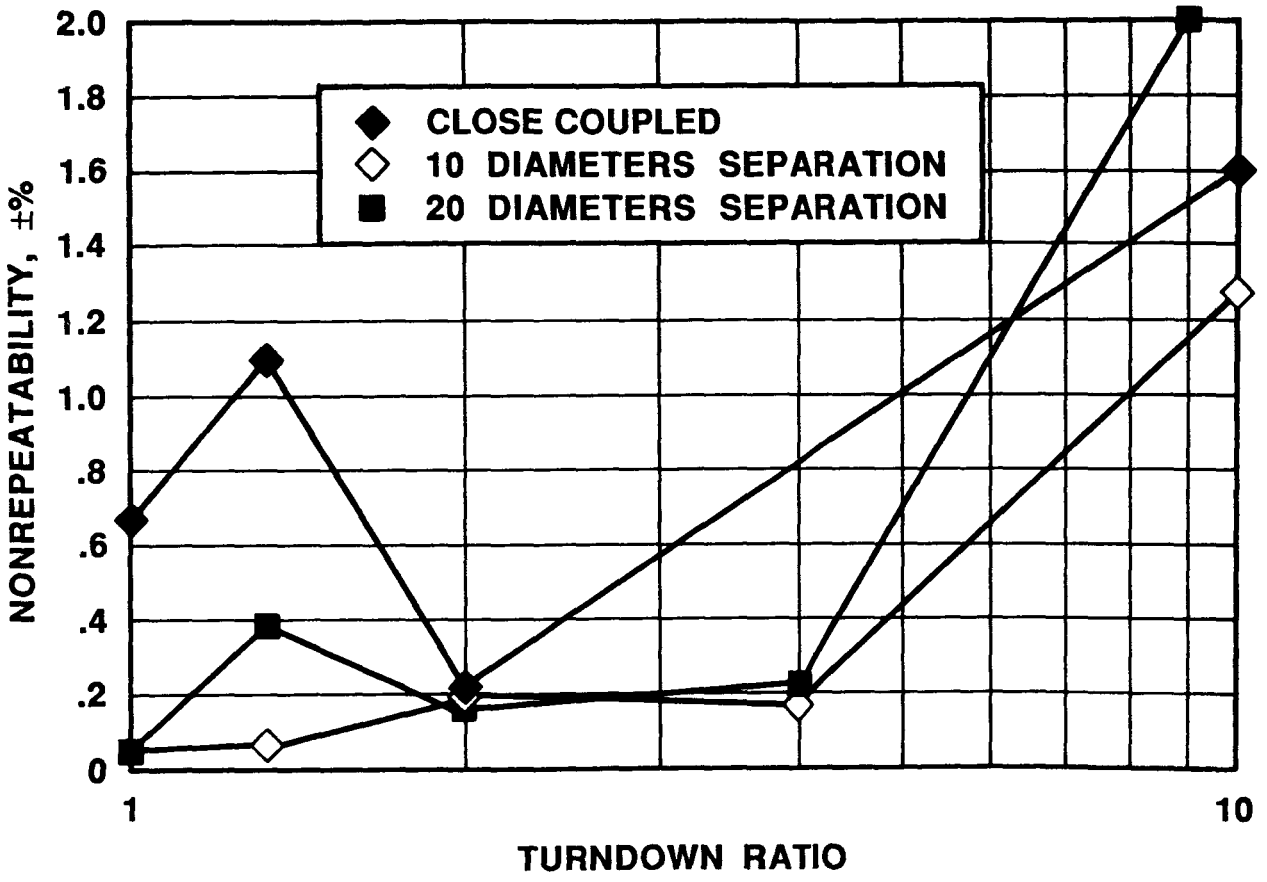

Figure 4.11-4.- Dragbody/turbine flowmeter dragbody component steady-state nonrepeatability versus turndown ratio.

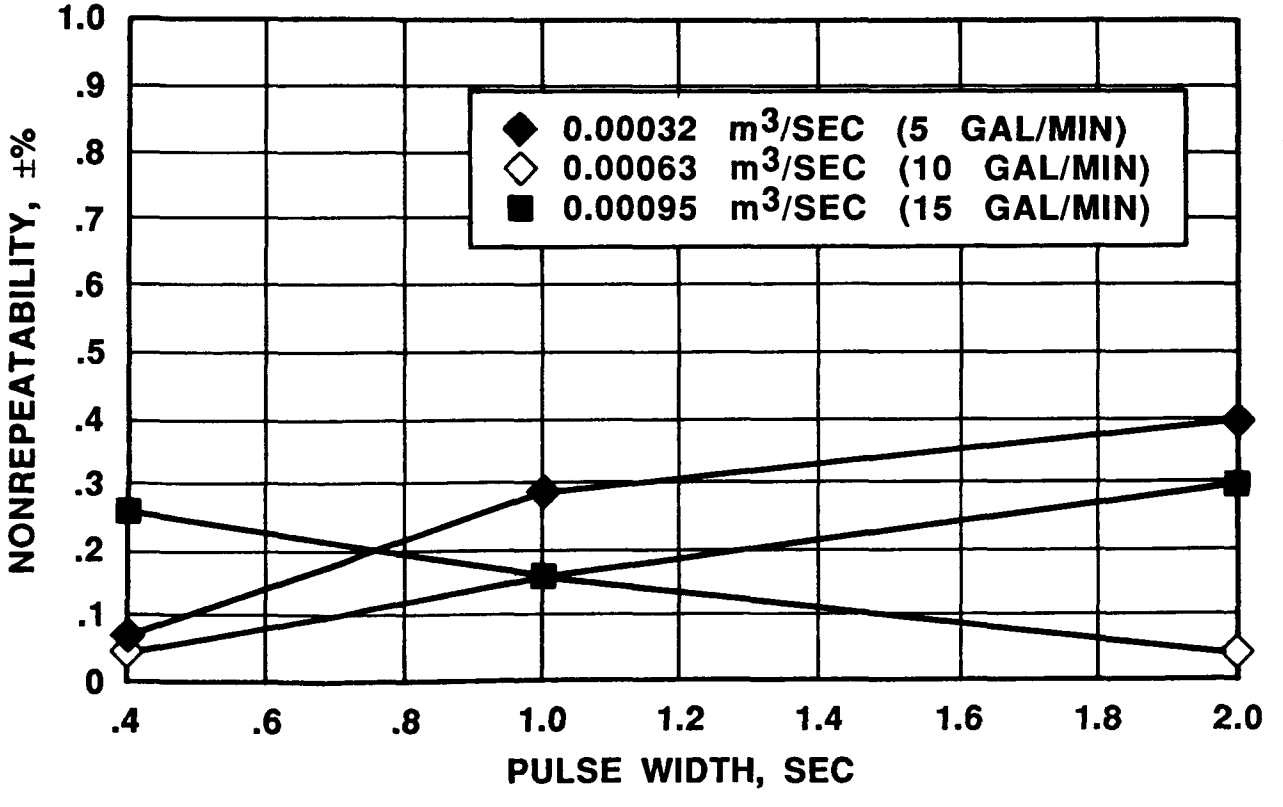

Figure 4.11-5.- Dragbody/turbine flowmeter turbine component nonrepeatability versus pulse width.

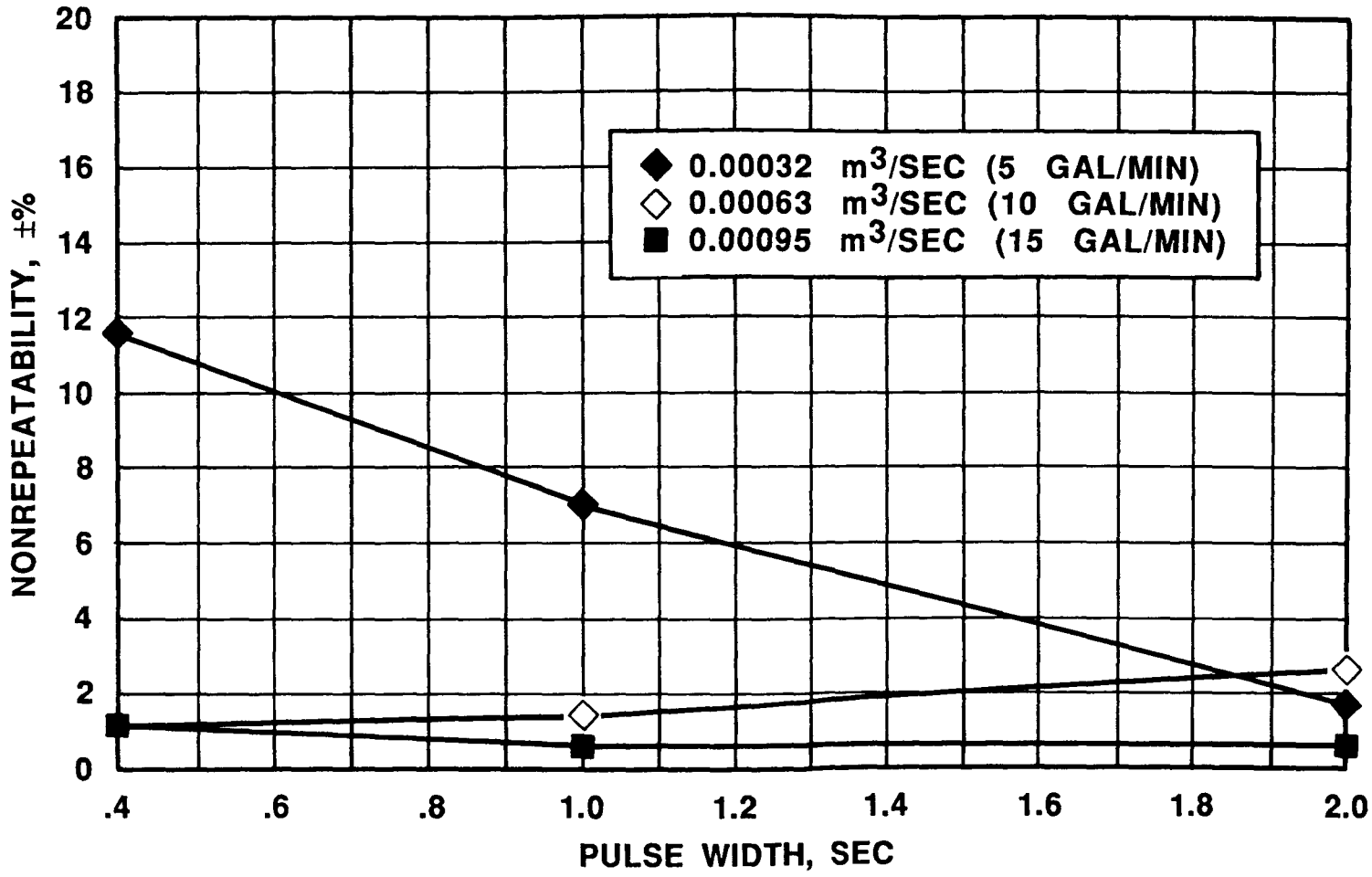

Figure 4.11-6.- Dragbody/turbine flowmeter dragbody component nonrepeatability versus pulse width.

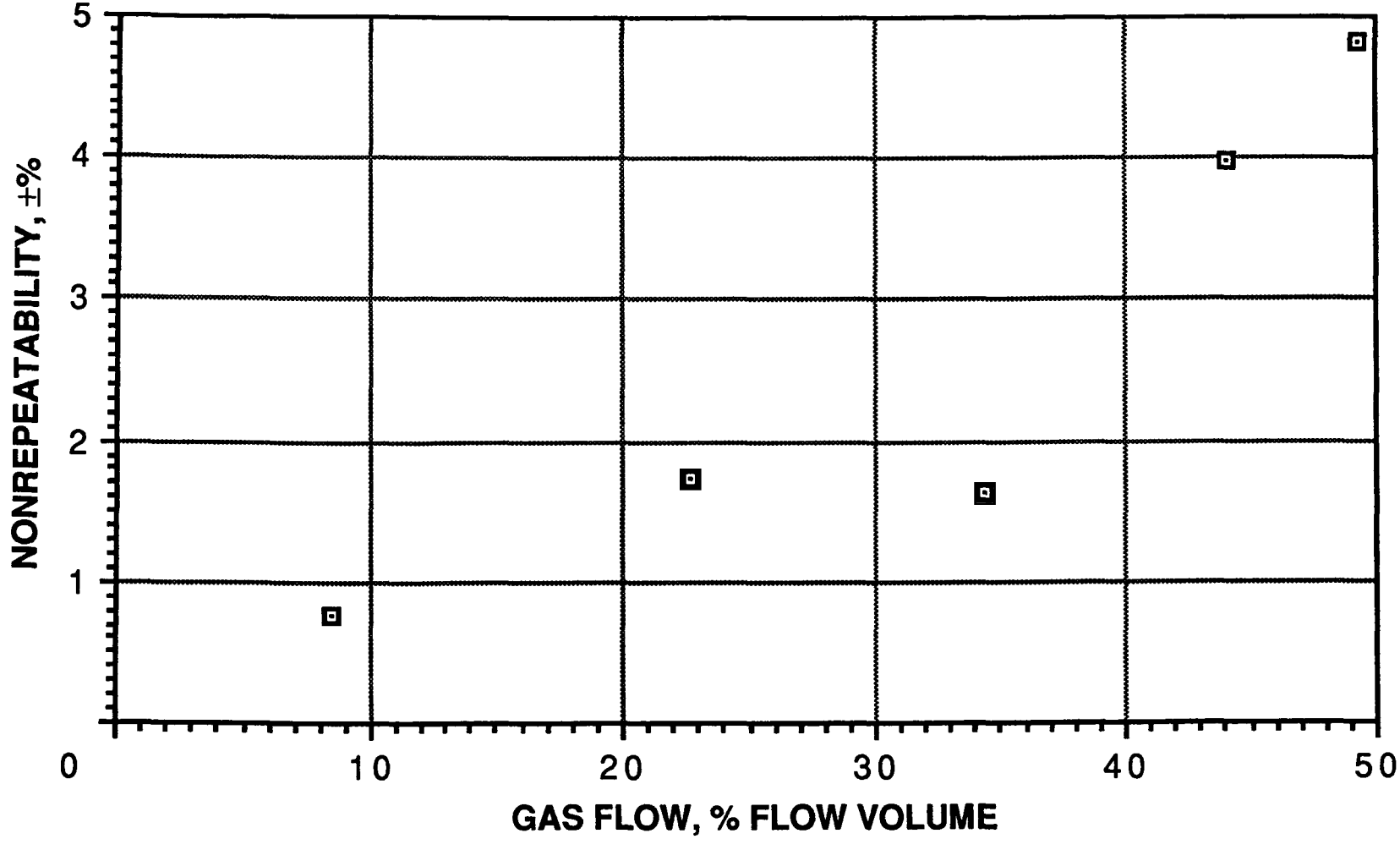

Figure 4.11-7.- Dragbody/turbine flowmeter combined two-phase flow nonrepeatability versus gas flow.

5.0 FLOWMETER COMPARISON SUMMARY

Many flowmetering techniques were investigated in this test program for their applicability to potential on-orbit operating conditions. The capabilities and limitations of each flowmetering technique are discussed and compared in this section relative to several major areas of consideration. All of these areas of consideration must be addressed before the best flowmeter(s) for any particular on-orbit application can be selected.

The information and the discussions of this comparison summary section are aimed at helping flowmeter users distinguish between broad families of flowmetering types potentially applicable to on-orbit operations, but are not intended to recommend specific flowmeter models or manufacturers. The flowmeter performance data and physical specifications presented in this section are derived from ground test data unless specifically labeled as manufacturer's information and represent only those flowmeters tested in this program. Performance of flowmeters of other models and sizes, and from other manufacturers, of each flowmetering type may vary substantially.

5.1 PERFORMANCE

Performance of a flowmeter in an application is a major selection consideration. The fluid system designer must know the approximate flow conditions (steady-state flow, two-phase flow, flow-rate range, etc.) to which the flowmeter would likely be exposed for a particular application.

The predominant flow condition likely to occur during fluid-transfer operations, and the flow condition that flowmeters are generally designed to measure, is single-phase, steady-state flow. Not surprisingly, performance of all the flowmeters tested, except the area averaging ultrasonic and offset ultrasonic flowmeters, was relatively good under steady-state flow conditions (figs. 5.1-1 to 5.1-4). The area averaging and offset ultrasonic flowmeters tested were early versions of these configurations which might be improved with further development. All of the flowmeters tested performed best at the lower (5 to 10 typical operating range) turndown ratios during steady-state flow. Of particular note, nonlinearity and nonrepeatability performance of the turbine and coriolis flowmeters was good to excellent. Several other flowmeters demonstrated equal or superior nonlinearity or nonrepeatability performance, but not both.

Pulse flow conditions are relatively rare but do occur in fluid systems requiring fast response and/or short flow time operations such as those found in reaction control propulsion systems. The fact that performance of all the flowmeters tested was better at increasing pulse widths (decreasing pulse frequencies) is understandable because all of the flowmeter designs are optimized for steady-state operations. Of the flowmeters tested, the turbine demonstrated good to excellent pulse flow nonrepeatability (less than ±1 percent) and error (less than ±5 percent) performance (figs. 5.1-5 to 5.1-7). A few other flowmeters demonstrated comparable nonlinearity or nonrepeatability performance, but not both. The dragbody flowmeter demonstrated relatively good pulse flow performance and

a remarkably swift response to flow changes which might be useful in particularly dynamic fluid systems.

The third type of flow experienced in fluid-transfer operations is two-phase flow. The two forms of two-phase flow are relatively steady-state gas bubble flow and periodic gas slug flow. Gas bubble flow is the more common of the two forms and can be generated in cryogenic fluids through system heat transfer or in Earth-storable fluids through the release of gas from solution caused by fluid system or local pressure changes. Of the flowmeters tested, the bearingless turbine, the universal venturi tube, and the vortex shedding flowmeters demonstrated relatively good gas bubble flow nonrepeatability and error performance (figs. 5.1-8 to 5.1-11). Gas slug flow is not common but can occur if ullage gas becomes mixed with the liquid being transferred during the transfer process (cryogens and Earth-storable fluids) or if relatively large quantities of gas are generated during first flow (most likely with cryogens). All of the flowmeters tested survived this flow condition, but few of them demonstrated anything close to repeatable or accurate performance. Generally, the flowmetering techniques with the minimum of moving components, such as the universal venturi tube and the vortex shedding flowmeters, performed the best, although the clamp-on ultrasonic flowmeter, with no moving parts, did not perform particularly well.

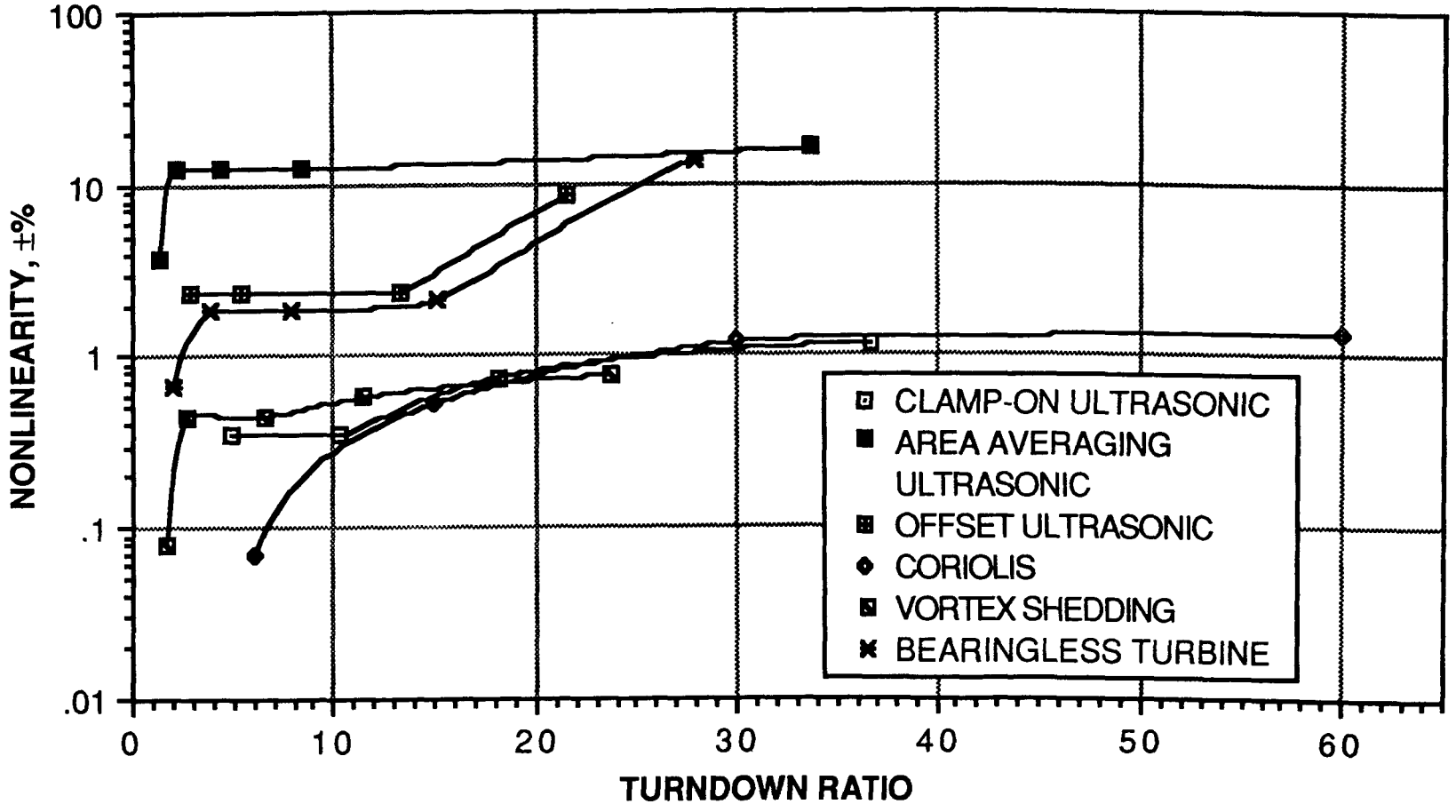

Figure 5.1-1.- Flowmeter concept steady-state nonlinearity versus turndown ratio comparison A.

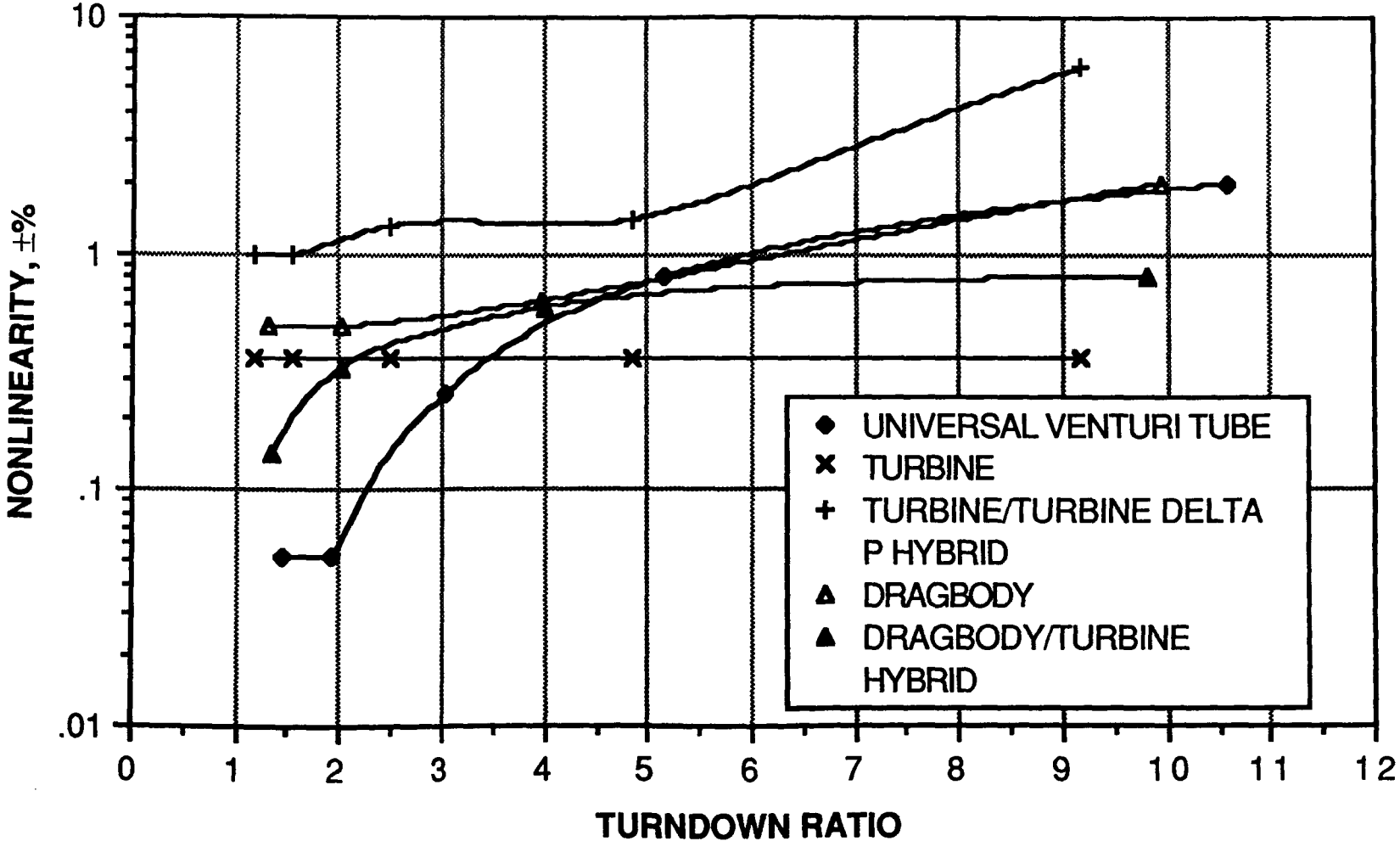

Figure 5.1-2.- Flowmeter concept steady-state nonlinearity versus turndown ratio comparison B.

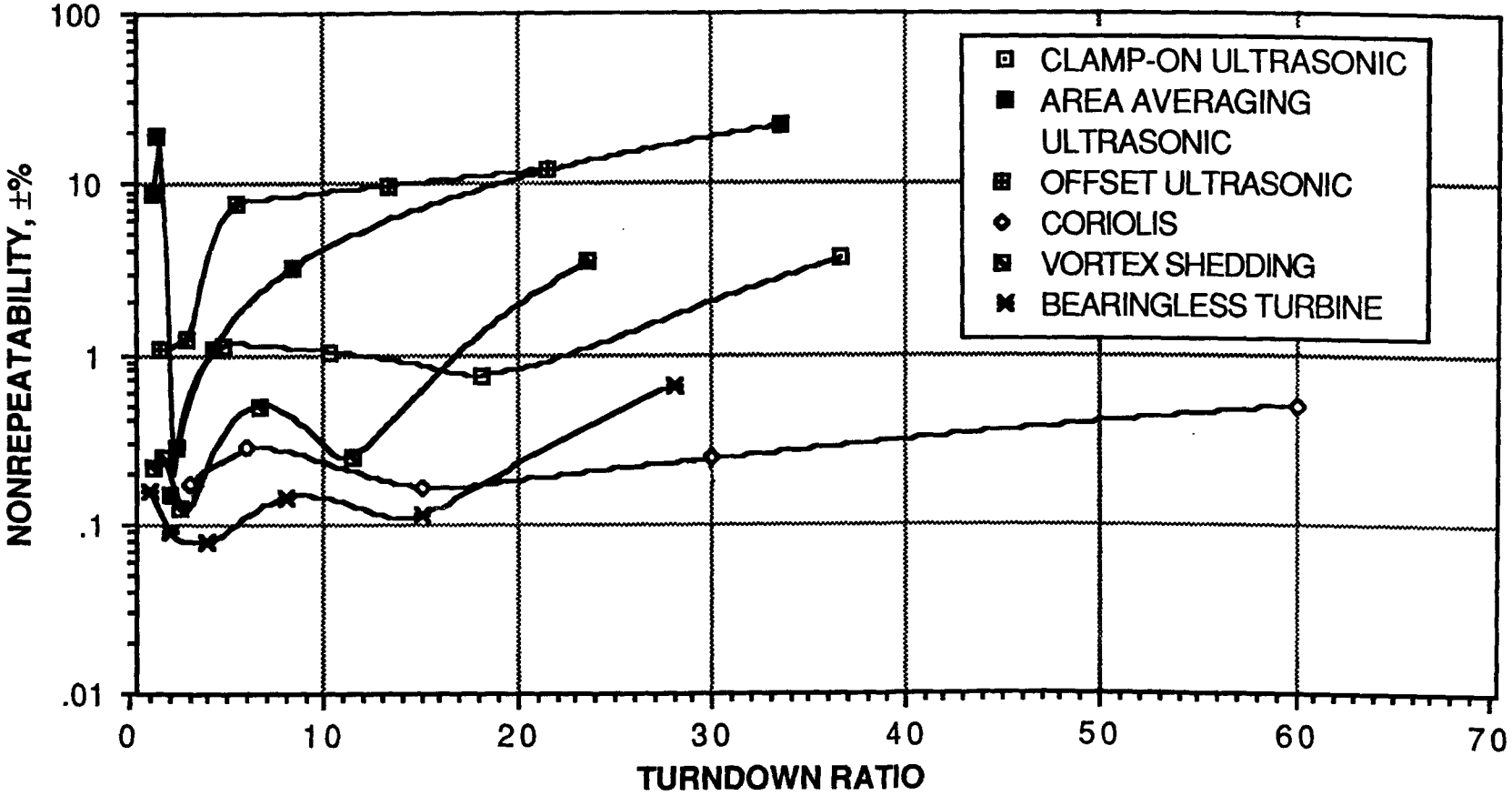

Figure 5.1-3.- Flowmeter concept steady-state nonrepeatability versus turndown ratio comparison A.

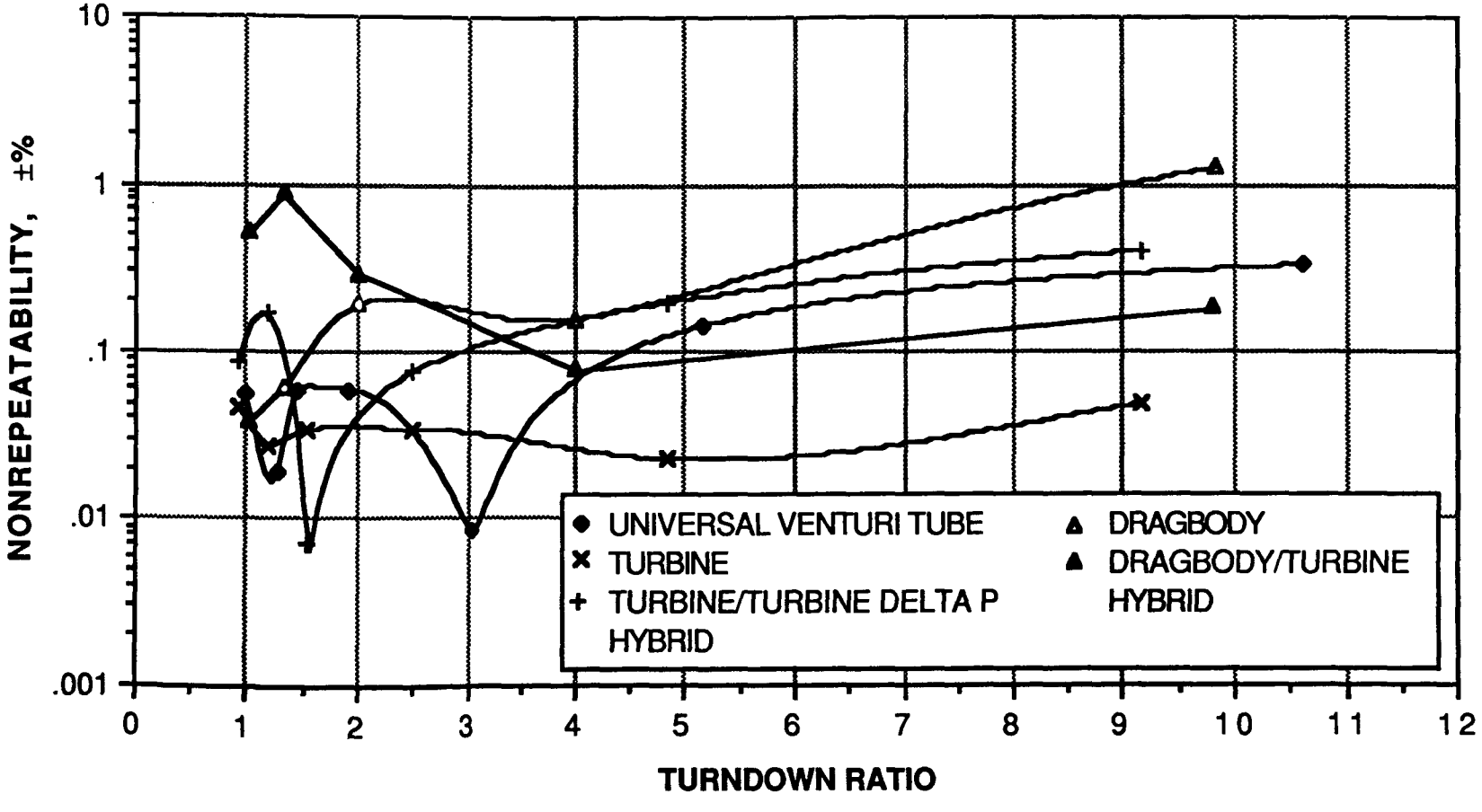

Figure 5.1-4.- Flowmeter concept steady-state nonrepeatability versus turndown ratio comparison B.

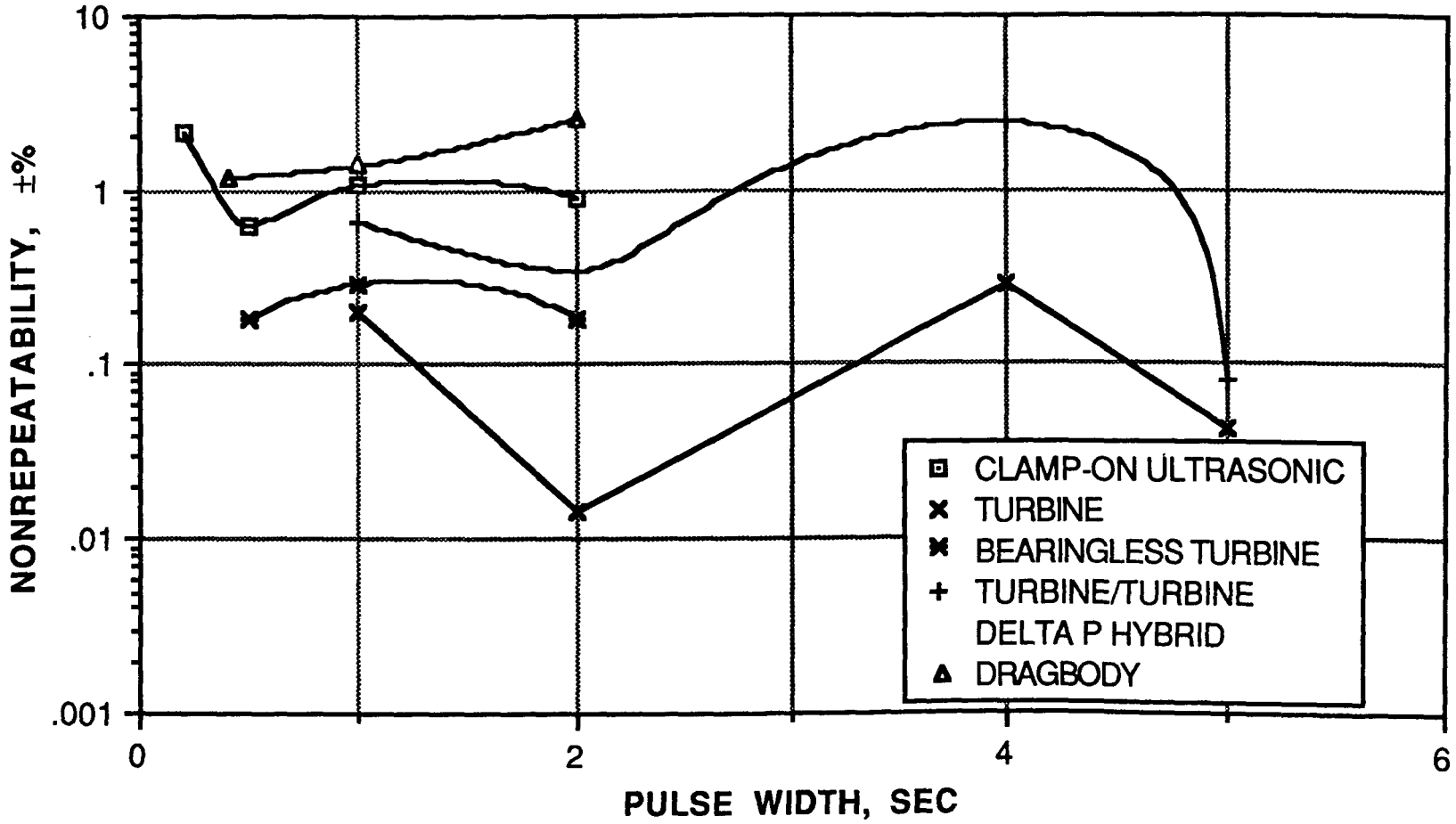

Figure 5.1-5.- Flowmeter concept pulse flow nonrepeatability versus pulse width comparison A.

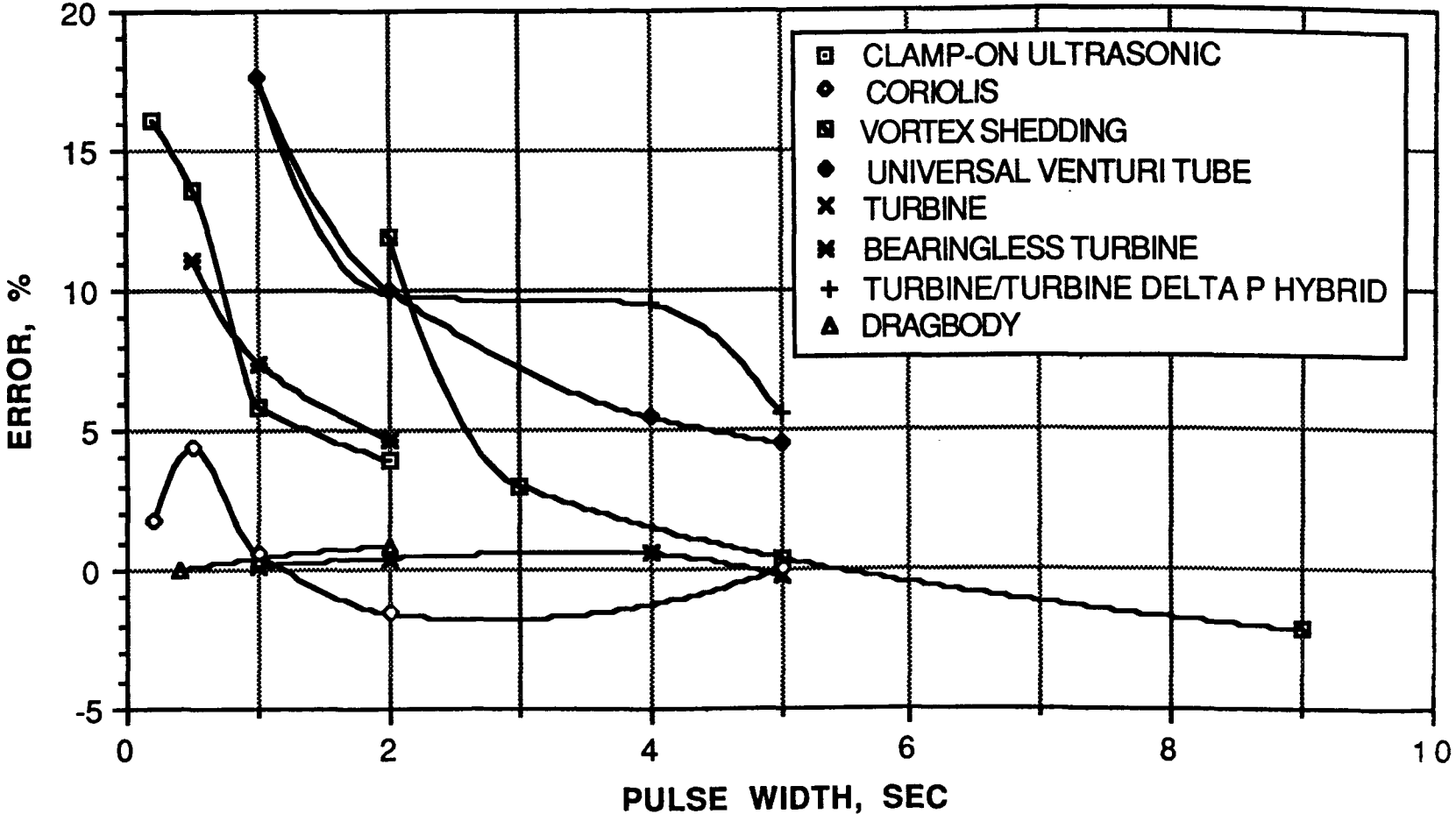

Figure 5.1-7.- Flowmeter concept pulse flow error versus pulse width comparison.

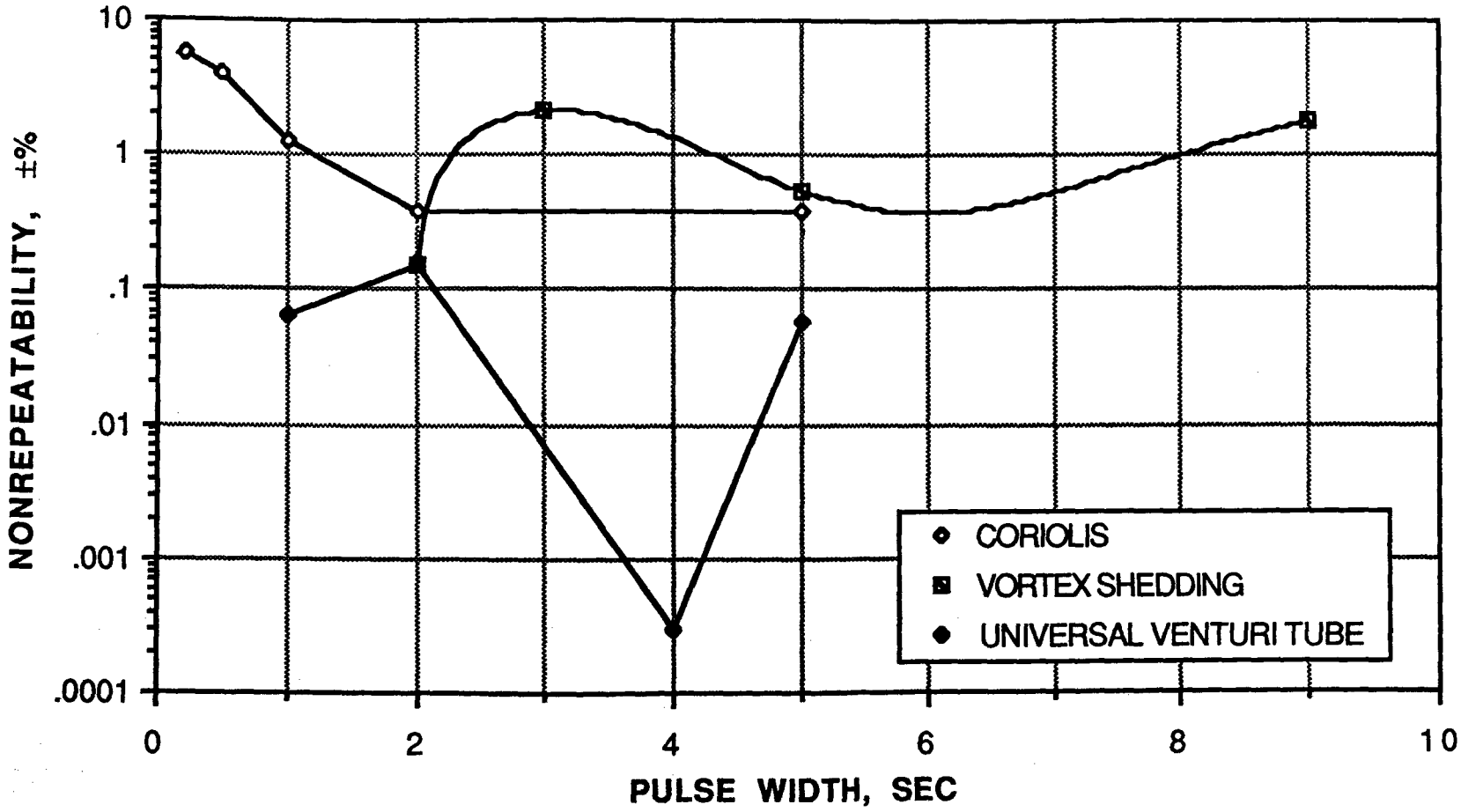

Figure 5.1-6.- Flowmeter concept pulse flow nonrepeatability versus pulse width comparison B.

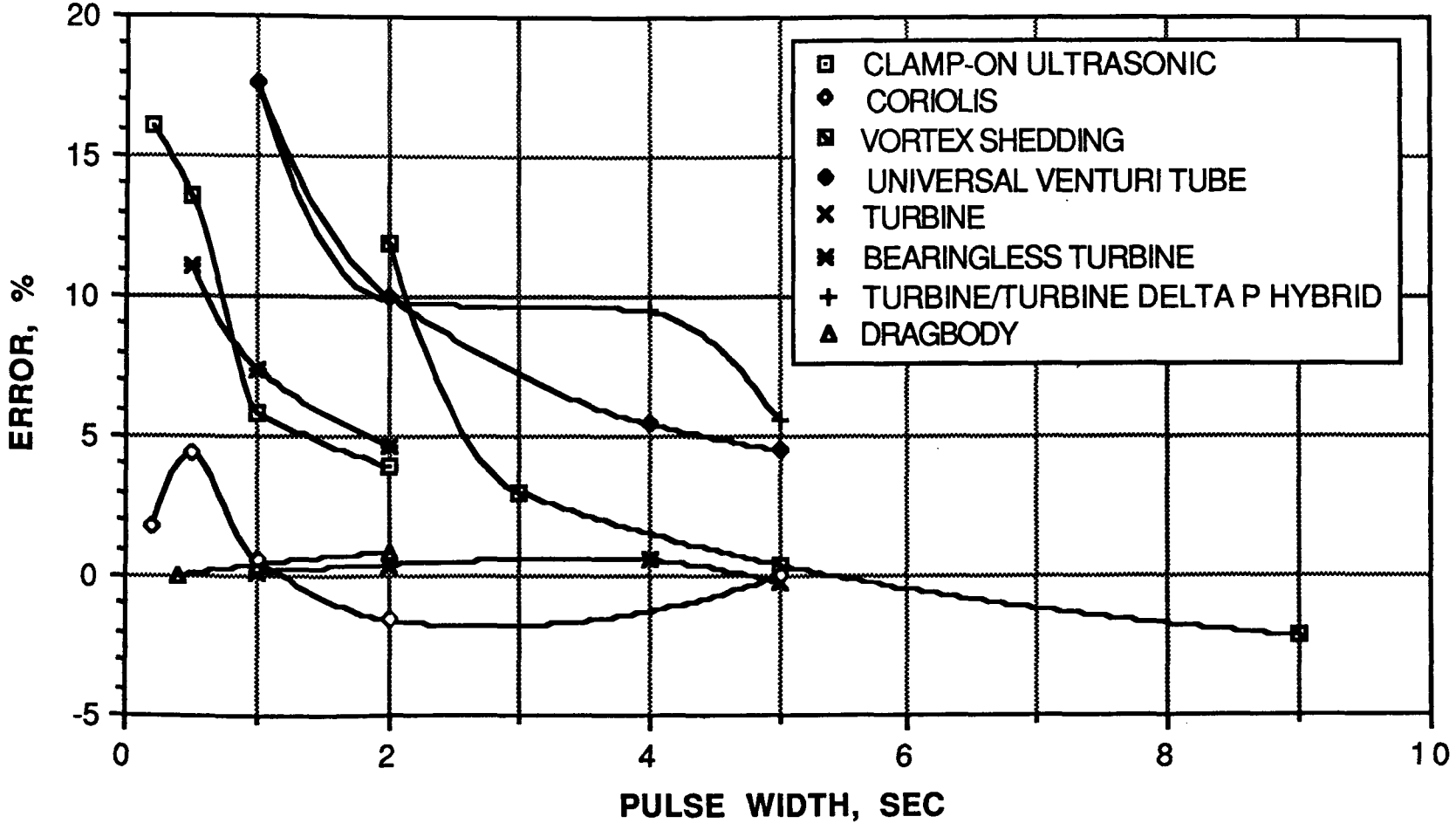

Figure 5.1-7.- Flowmeter concept pulse flow error versus pulse width comparison.

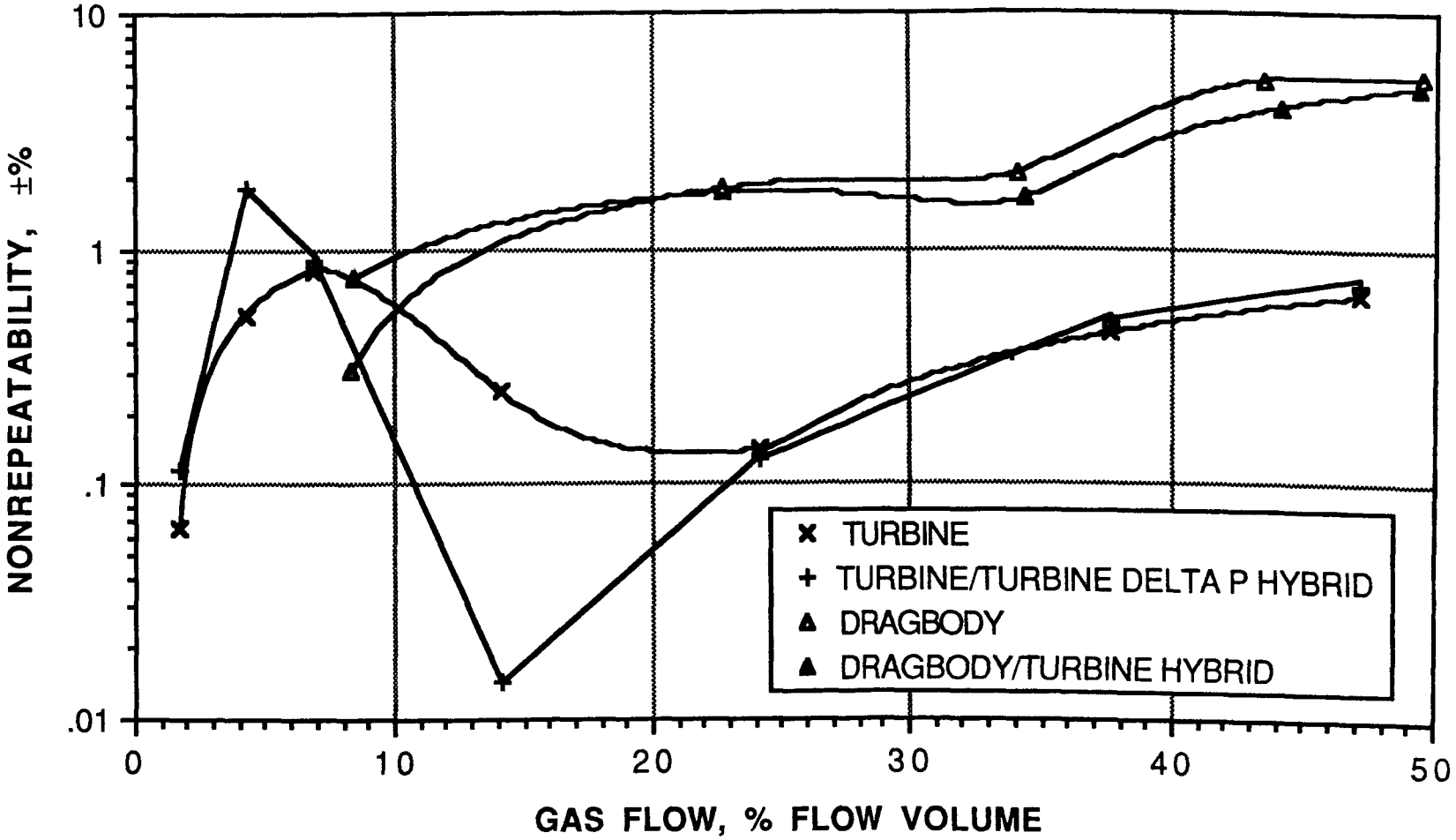

Figure 5.1-8.- Flowmeter concept two-phase flow nonrepeatability versus gas flow comparison A.

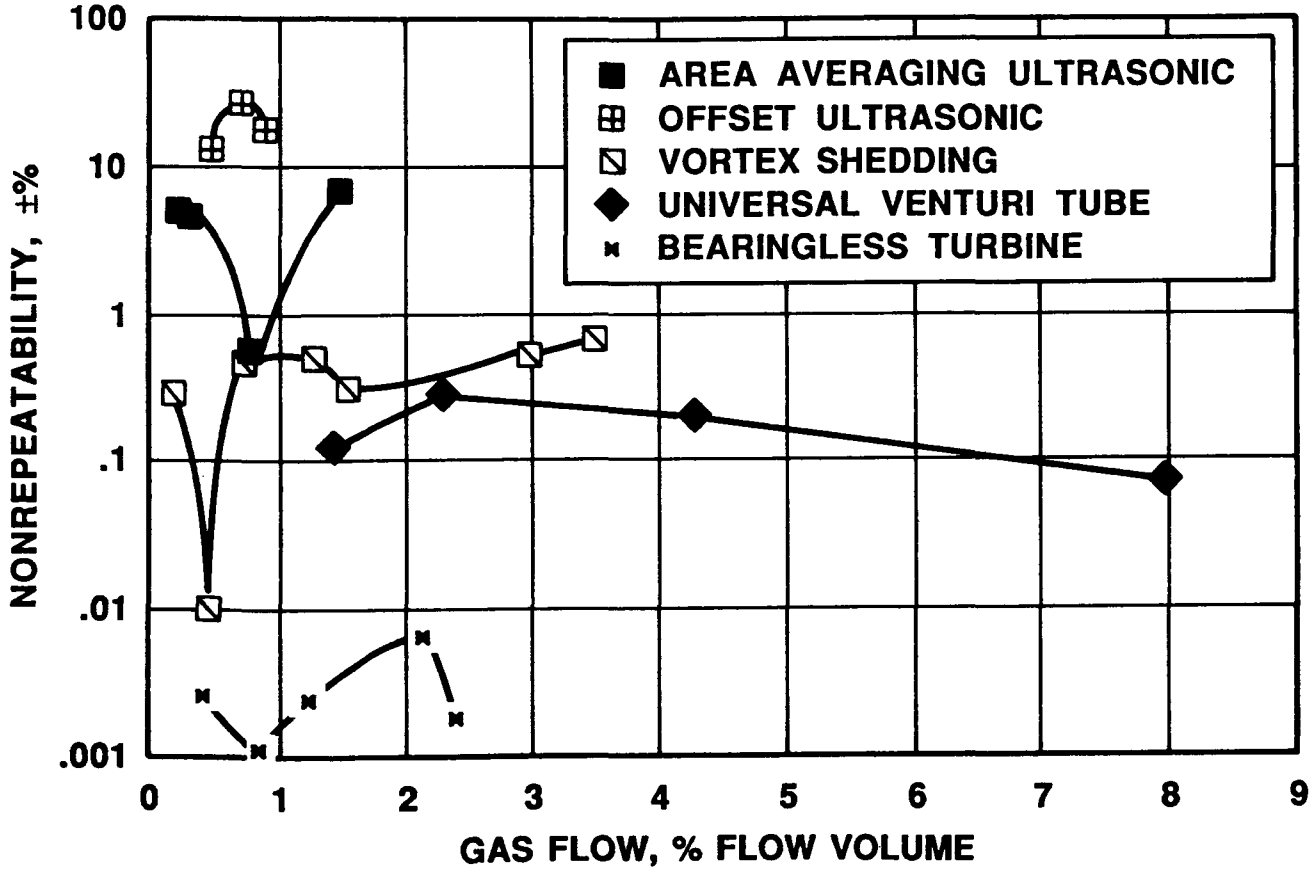

Figure 5.1-9.- Flowmeter concept two-phase flow nonrepeatability versus gas flow comparison B.

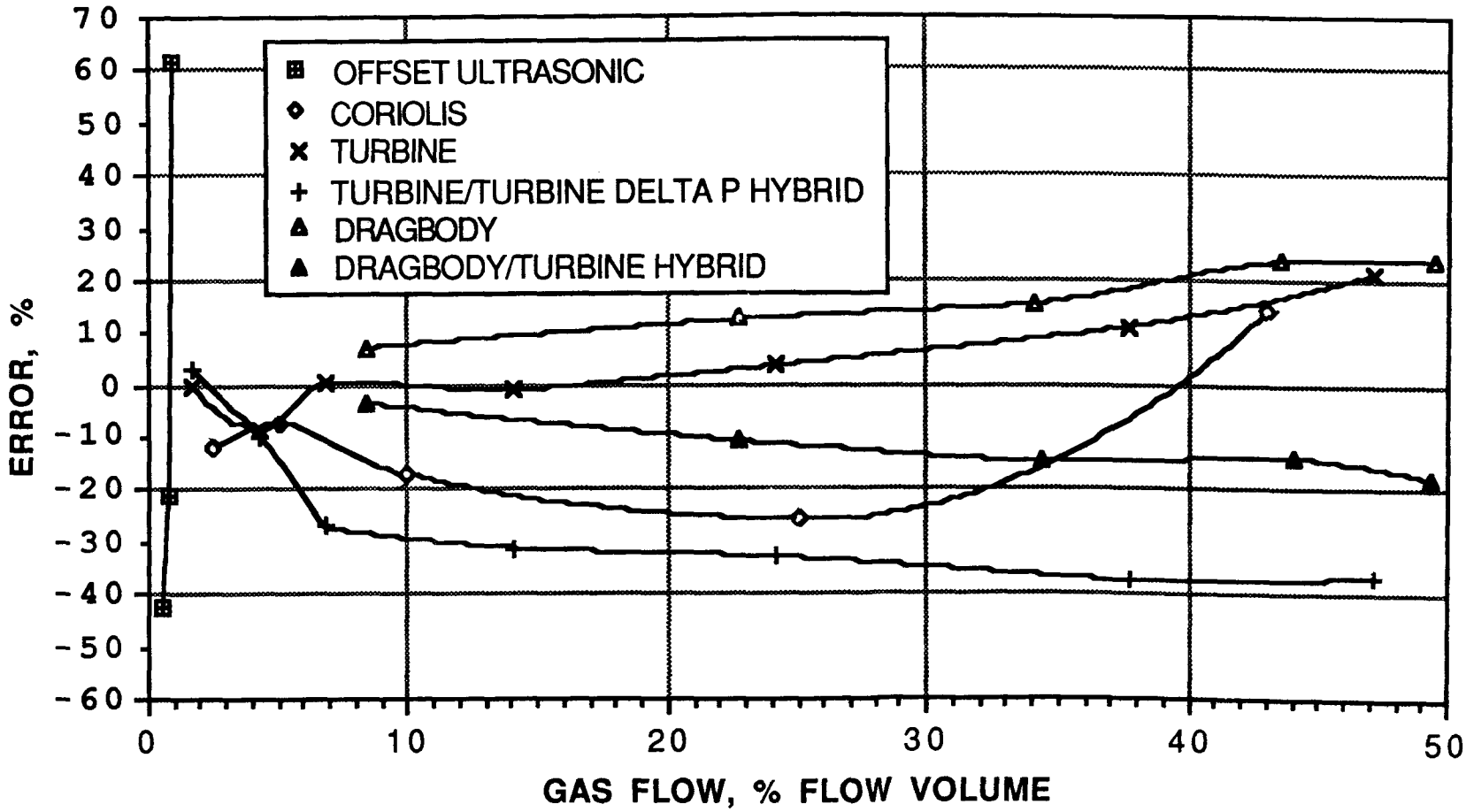

Figure 5.1-10.- Flowmeter concept two-phase flow error versus gas flow comparison A.

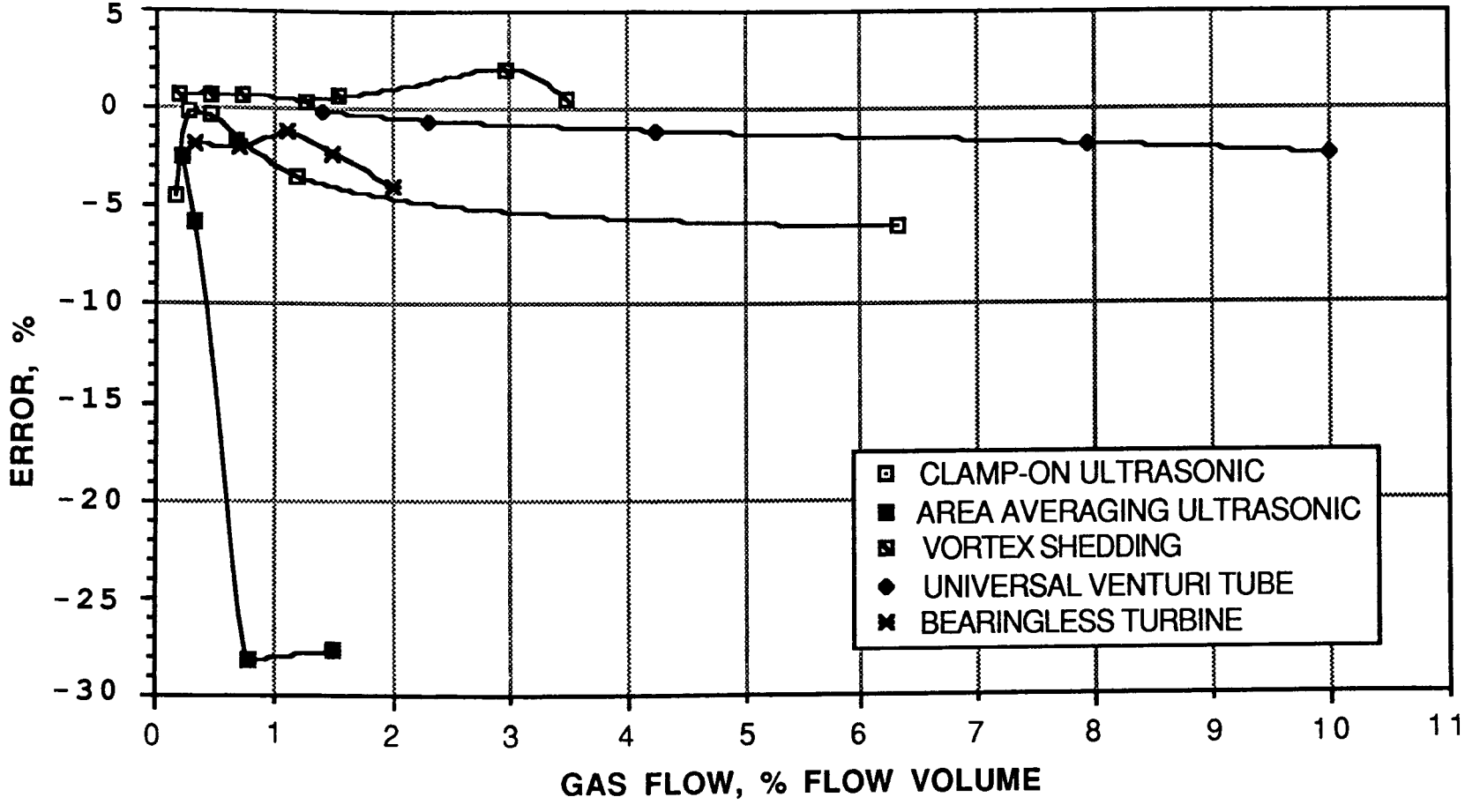

Figure 5.1-11.- Flowmeter concept two-phase flow error versus gas flow comparison B.

5.2 OPERATING CONDITIONS

The fluid operating conditions must be considered when selecting flowmeters for a specific application. In particular, the fluid system designer must know the fluid(s) being metered and the system operating temperatures and pressures before a flowmeter can be selected.

The type of fluid being metered can limit flowmeter selections if it is a potentially hazardous fluid and/or if it is being used under marginally acceptable conditions. Flowmeters with few flow obstructions and with simple flow paths (clamp-on ultrasonic, universal venturi tube, etc.) are recommended for chemically reactive fluids to minimize the potential for reaction ignition within the flowmeter. Similarly, flowmeters with a minimum of flow obstructions or flow modifiers are recommended for fluids flowing at marginally equilibrium conditions such as gas in solution to minimize the possibility of equilibrium collapse. The criticality of this consideration is dependent on the sensitivity of the flow system to these fluid changes.

Fluid operating pressures and temperatures are more of a flowmetering technology availability/desirability limiting factor than is type of fluid. The pressure and temperature limitations (per the manufacturer's specifications) for the flowmeters tested in this program (table 5.2-1) imply that pressure is probably not a limiting concern for any of the flowmetering techniques except for potential mass and volume packaging impacts. (See sec. 5.4.) However, operating temperature may be a technology availability constraint. In particular, the ultrasonic flowmetering techniques are currently limited to liquid nitrogen/oxygen temperatures or higher because of transducer crystal limitations. The other flowmetering techniques have similar transducer temperature constraints; however, a wider range of suitable transducer types is generally available giving an effectively larger operable temperature range capability. The flow system designer should investigate the transducer technology available for each candidate flowmeter before selecting a flowmeter.

Fluid operating conditions such as flow-rate range and fluid contamination should be considered; however, they are more flowmeter detail design issues than flowmetering concept selection criteria and should be addressed and solved accordingly.

TABLE 5.2-1.- FLOWMETER CONCEPT MANUFACTURER PRESSURE AND TEMPERATURE LIMITATIONS[a]

Flowmeter type	Maximum pressure (b)		Temperature (b)			
			Minimum		Maximum	
	MPa	psi	K	°F	K	°F
Clamp-on ultrasonic	(c)	(c)	210.9	-80	533.2	500
Area averaging ultrasonic	20.68	3 000	73.2	-328	473.2	392
Offset ultrasonic	20.68	3 000	73.2	-328	473.2	392
Coriolis	38.54	[d]5 590	33.2	-400	477.6	400
Vortex shedding	10.34	1 500	77.6	-320	477.6	400
Universal venturi tube	(e)	(e)	(e)	(e)	(e)	(e)
Bearingless turbine	20.68	3 000	199.8	-100	422.0	300
Turbine/turbine delta p						
Turbine component[f]	68.94	10 000	16.5	-430	672.0	750
Turbine component[g]	17.2	2 500	3.7	-453	672.0	750
Delta-p component	(e)	(e)	(e)	(e)	(e)	(e)
Dragbody/turbine hybrid						
Dragbody component	68.94	10 000	77.6	-320	672.0	750
Turbine component	68.94	10 000	16.5	-430	672.0	750

[a]Not verified in this test program.
[b]Pressure and temperatures listed represent manufacturer limits for the type of flowmeter tested, not necessarily the flowmeter tested.
[c]Pressure limits constrained by pipe pressure limits.
[d]Smaller coriolis unit tested max. pressure 19.3 MPa (2800 psi).
[e]Constrained by differential pressure instrumentation limitations.
[f]Ground testing turbine flowmeter.
[g]Zero-g (PFTS) testing turbine flowmeter.

5.3 OPERATING ENVIRONMENT

Externally imposed operating environments must be considered in the selection of flowmeter candidates, particularly where these conditions would exist during flowmeter operations.

Acceleration and vibration effects should be addressed for those flow systems that require flow operations during propulsive (acceleration generating) or other dynamic, vibration-producing activities (compressor operations, crew activities, turbine operations, etc.) that could result in energy being transmitted to the flowmeter. All of the zero-g tested flowmeters exhibited some sensitivity to changes in gravity (acceleration) environments and/or orientation differences exposed to the one-g (ground) environment. In most cases, the effects were minor and would probably require at most some special calibration attention; however, in the case of the coriolis flowmeter, the orientation and the acceleration change effects were significant and would require more than special calibration attention. Vibration environment effects were not generally significant in any flowmetering concept tested, although, again, the coriolis flowmeter was more susceptible to vibration relative to other flowmetering concepts. In all cases, acceleration and vibration effects should be compensated for at the flowmeter component level (software or hardware) of the fluid system.

Imposed environments such as magnetic flux, electromagnetic radiation, and ionizing radiation can generally be controlled at the system design level. However, if they are not controlled at the system level, then some component-level protection must be provided to the flowmeter electronics (controller/computer, transducers, etc.). This protection could take the form of hardening the electronic component designs and/or removing the bulk of the electronics (controller/computer) to more protected locations, if any.

5.4 PACKAGING

The physical packaging of flowmetering systems (flowmeter device, attached electronics, cabling, etc.) should be considered in the selection process.

Mass is always a concern for launch packaging and should be minimized in all fluid system designs. Most of the flowmeters tested (table 5.4-1) were designed for ground operations and therefore tended to be heavy. Optimization of the flowmeter designs to flight configurations could, in most cases, reduce their masses. In particular, the coriolis and various ultrasonic flowmeters should be improved to reduce casing, body, and electronics package masses.

Volume is not always a flow system design or launch package constraint but can give the flow system designer an idea of the flowmeter configuration constraints (table 5.4-2). The configuration constraints should be considered by the fluid system designer as part of the selection process.

TABLE 5.4-1.- TESTED FLOWMETER CONCEPT MASSES

Flowmeter type	Size		Mass (a)					
	m	in.	Device		Electronics		Delta p	
			kg	lbm	kg	lbm	kg	lbm
Clamp-on ultrasonic	0.04	1.5	0.7	1.5	10.2	22.5	0	0
Area averaging ultrasonic	.04	1.5	8.4	18.6	11.8	26.1	0	0
Offset ultrasonic	.013	.5	1.1	2.5	11.8	26.1	0	0
Coriolis	.04	1.5	17.5	38.5	4.5	9.9	0	0
	.013	.5	1.6	3.6	4.5	9.9	0	0
Vortex shedding[b]	.05	2.0	2.9	6.5	2.9	6.5	0	0
Universal venturi tube	.025	1.0	1.5	3.4	(c)	(c)	(d)	(d)
Turbine[e]	.05	2.0	3.2	7	(f)	(f)	0	0
Turbine[g]	.019	.75	.4	.9	(f)	(f)	0	0
Bearingless turbine	.025	1.0	1.8	4	.9	1.9	0	0
Turbine/turbine delta p	.05	2.0	3.2	7	(f)	(f)	1.1	2.5
	.019	.75	.4	.9	(f)	(f)	1.1	2.5
Dragbody[h]	.019	.75	.8	1.8	1.4	3.1	0	0
Dragbody/turbine hybrid	.019	.75	1.4	3.0	(c)	(c)	0	0

[a]Masses estimated without flanges or connectors.
[b]Only total masses known; component mass is estimated.
[c]Nonmanufacturer's electronics used: general facility instrumentation.
[d]Four sets of Δp transducers used.
[e]Ground testing turbine flowmeter.
[f]Nonmanufacturer's electronics used: Fluke 1752 data acquisition system.
[g]Zero-g (PFTS) testing turbine flowmeter.
[h]Includes Ramapo model 320-R Wheatstone bridge signal conditioner.

TABLE 5.4-2.- TESTED FLOWMETER CONCEPT VOLUMES

Flowmeter type	Size		Volume (a)					
			Device		Electronics		Delta p	
	m	in.	m^3	in^3	m^3	in^3	m^3	in^3
Clamp-on ultrasonic	0.04	1.5	9.3×10^{-4}	57	297.5×10^{-4}	1815	0	0
Area averaging ultrasonic	.04	1.5	18.8	115	108.2	660	0	0
Offset ultrasonic	.013	.5	11.8	72	108.2	660	0	0
Coriolis	.04	1.5	192.7	1176	68.7	419	0	0
	.013	.5	20.5	125	68.7	419	0	0
Vortex shedding	.05	2.0	4.6	28	28.4	173	0	0
Universal venturi tube	.025	1.0	7.4	45	(b)	(b)	(c)	(c)
Turbine[d]	.05	2.0	6.6	40	(e)	(e)	0	0
Turbine[f]	.019	.75	1.8	11	(e)	(e)	0	0
Bearingless turbine	.025	1.0	4.9	30	6.9	42	0	0
Turbine/turbine delta p	.05	2.0	6.6	40	(e)	(e)	6.7×10^{-4}	41
	.019	.75	2.6	16	(e)	(e)	6.7	41
Dragbody[g]	.019	.75	2.0	12	29.5	180	0	0
Dragbody/turbine hybrid	.019	.75	4.3	26	(b)	(b)	0	0

[a]Volumes estimated without flanges or connectors.
[b]Nonmanufacturer's electronics used: general facilities instrumentation.
[c]Four sets of Δp transducers used.
[d]Ground testing turbine flowmeter.
[e]Nonmanufacturer's electronics used: Fluke 1752 data acquisition system.
[f]Zero-g (PFTS) testing turbine flowmeter.
[g]Includes Ramapo model 320-R Wheatstone bridge signal conditioner.

5.5 MAINTENANCE

Flow system life and maintenance requirements should be considered as one of the factors for selection. All of the flowmetering concepts support short-service-life (<2 or 3 years) fluid system design requirements. Longer fluid system service life requirements significantly increase the importance of flowmeter life and maintenance issues.

Selection of flowmeter designs that minimize the requirement for repair and/or calibration maintenance should be stressed for all long-service-life applications, particularly for those fluid system applications in which maintenance is impractical or impossible (some free-flyers, most satellites, etc.). There are two types of flowmeter design strategies for minimizing maintenance. The first strategy is simply to use flowmeters that incorporate few parts that are likely to fail or deteriorate such as the clamp-on ultrasonic, the universal venturi tube, or some of the vortex shedding variations that have few if any moving or deformable parts exposed to the fluid flow. Flowmeters such as the bearingless turbine or a typical turbine flowmeter incorporating hydrodynamic bearings that have little or no rotating element bearing deterioration can also be used. The second strategy would be to use redundant flowmeters. If there are no packaging issues (sec. 5.4), then any of the flowmetering concepts could be used. If there are packaging constraints, one of the hybrid flowmeter designs could satisfy the redundancy requirements more efficiently. The specific redundancy requirements needed for any particular application are left to the discretion of the fluid system designer but are likely to be functions of service life requirement, operating conditions/environments, and the criticality of flowmetering to the success of the mission.

Where maintenance is feasible and planned, the flowmetering design maintainability should be considered. In particular, two interrelated aspects of maintenance should be addressed: flowmeter replacement/removal fluid system impacts and replacement/removal techniques. Flowmeter maintenance should have a minimum impact on the fluid system. Flowmeters such as the clamp-on ultrasonic, some vortex shedding variants, and the bearingless turbine (with some transducer development) minimize fluid system impacts by allowing the sensing element electronics most likely to fail to be removed and replaced without breaching the fluid system lines. Fluid system impacts for maintenance of the other flowmetering concepts would depend heavily on the installation/removal technique used (couplings, cut and weld, etc.) but would still require breaching the fluid system, exposing the fluid system to contamination, or producing other conditions having the potential for damage or danger.

Another long-service-life issue is calibration. All flowmeters are susceptible to calibration deterioration over time whether it is caused by radiation disruption of electronic sensing and computer components or caused by cumulative deformation of relatively delicate flow-exposed sensing components. The need for recalibration may be minimized by selecting flowmeters with as few flow-exposed degradable components as possible, in accordance with the first strategy discussed previously, but even these flowmeters will require recalibration eventually (electronic

component replacement, etc.). Ground calibration may not be sufficient for many of the zero-g service flowmeters because of the differences between their ground and zero-g performance characteristics. (See sec. 4.0.) Currently available flowmeter zero-g calibration information is insufficient to base any on-orbit calibration recommendations on. Further study is required.

5.6 TECHNOLOGY DEVELOPMENT

All of the flowmetering techniques will require some development for flight use. In particular, electronics packaging, electronics software, and some hardware packaging must be optimized for long-term on-orbit flight operations for all of the flowmetering concepts. The extent of these modifications will depend on the particular flowmetering concept selected and the fluid system requirements.

Some of the flowmetering concepts could be significantly improved with further technology development research in a few areas such as hardware redesign to allow bidirectional flow measurement and transducer development to expand flowmeter operating temperature ranges and to improve on-orbit maintainability. It is left to the fluid system designer to decide whether this additional research would be worthwhile for a particular application.

APPENDIX A: GLOSSARY OF TERMS AND CALCULATIONS

Gas bubble (two phase) ingestion flow

Steady-state liquid flow through the test article in which various controlled volumes of gas bubbles are continuously injected. During gas bubble ingestion flow, the test article is subjected to startup flow transients, steady-state liquid flow, entrained gas bubble flow, and, finally, flow termination transients.

Gas slug injection flow

Steady-state liquid flow through the test article in which gas slugs (single, relatively large gas bubbles) of various volumes are injected. During gas slug injection flow, the test article is subjected to startup transient flow, steady-state flow, passage of a single large gas bubble, and, finally, flow termination transients.

K-factor

Flowmeter calculation calibration constant derived through testing and/or by the flowmeter manufacturer.

Nonlinearity

Relative magnitude of K-factor variances expressed as the comparison of the difference between maximum and minimum values divided by the sum of the maximum and minimum values observed during testing. Nonlinearities presented in this document are based on K-factors as a function of turndown ratio and calculated over turndown ratio ranges referenced to 1.0. For example, nonlinearity at a turndown ratio of X is the nonlinearity calculated over the turndown ratio range from 1.0 to X.

$$NL = \pm((\text{max. value} - \text{min. value})/(\text{max. value} + \text{min. value}))(100)$$

Nonrepeatability

Statistical comparison of any three test runs at similar flow conditions describing consistency of flow-rate measurement at those flow conditions.

$$NR = \pm 0.5 * [|\text{run 1 error} - \text{run 2 error}| + |\text{run 1 error} - \text{run 3 error}| + |\text{run 2 error} - \text{run 3 error}|]/3$$

Overall error

Error which describes flowmeter performance including initial startup and final run termination transients. This error can be calculated for any type of flow. In all cases, data are considered from the point of initial startup to the point at which the flowmeter indicates zero flow after flow through the test facility has been terminated.

$$OE = ((\text{initial mass} - \text{net wt transferred})(100))/(\text{net wt transferred})$$

Pulse flow

Intermittent flow through the test article in which flow is controlled by a rapid-acting valve following an open/closed duty cycle. During pulse flow test runs, the test article is subjected to startup flow transients followed by short-term (or no) steady-state flow and then termination of flow transients.

Slewing rate

The rate of a displayed measurement to increase from 0 to 90 percent of the true value. (This term describes the delay time between instrumentation receiving a signal and displaying a true measurement of that signal.)

Steady-state error

Error which describes test article performance with the startup transient and flow termination transients discarded. This error can be calculated for a wide range of flow conditions:

* Steady-state flow = data taken after startup and before run termination.

* Pulse flow = data taken over a multiple-pulse range at the midpoint of each run.

* Gas bubble ingestion flow = data taken after start of gas ingestion and before run termination.

* Gas slug injection flow = data taken after slug passage from test article and before run termination.

Steady-state flow

Flow through the test article in which flow rate is kept as constant as the test facility will allow. During steady-state test runs, the test article is subjected to startup flow transients, steady flow, and, finally, flow termination transients.

Turndown ratio

The full-scale flow-rate capability of the test article divided by the average flow rate seen during a test run or a set of common test runs (i.e., increasing turndown ratios imply decreasing flow rates).

TD = full-scale flow/average flow

APPENDIX B: REFERENCE DOCUMENTS

Seriale-Grush, J. M.: 1-1/2-Inch Controlotron Flowmeter Performance Evaluation. NASA Lyndon B. Johnson Space Center Internal Note JSC-20412, July 1985.

Burge, S.: Panametrics Area Averaging Flowmeter Test. NASA Lyndon B. Johnson Space Center Internal Note JSC-22023, Apr. 1986.

Burge, S.: Panametrics Offset Flowmeter. NASA Lyndon B. Johnson Space Center Internal Note JSC-22071, May 1986.

Graham, E.: 1.5-Inch Micro Motion Mass Flowmeter Performance Evaluation. NASA Lyndon B. Johnson Space Center Internal Note JSC-20648, Aug. 1985.

Stafford, D. G.: Eastech 2-Inch Vortex Shedding Flowmeter Performance Evaluation. NASA Lyndon B. Johnson Space Center Internal Note JSC-20857, Aug. 1986.

Stafford, D. G.: BIF 1-Inch Universal Venturi Tube Flowmeter Performance Evaluation. NASA Lyndon B. Johnson Space Center Internal Note JSC-22077, May 1986.

Seriale-Grush, J. M.: Bearingless Turbine Flowmeter Performance Evaluation. NASA Lyndon B. Johnson Space Center Internal Note JSC-20682, Sept. 1985.

Seriale-Grush, J. M.: Bearingless Turbine Flowmeter Performance Evaluation - Vibration Screening Test. NASA Lyndon B. Johnson Space Center Internal Note JSC-20984, Mar. 1985.

Seriale-Grush, J. M.: Bearingless Turbine Flowmeter Performance Evaluation - Zero-g Screening Phase. NASA Lyndon B. Johnson Space Center Internal Note JSC-22025, Feb. 1986.

Burge, S.: Turbine/Turbine Delta p Flowmeter Test. NASA Lyndon B. Johnson Space Center Internal Note JSC-22233, Oct. 1986.

Burge, S.: Turbine/Delta p Two-Phase Zero-g Flowmeter Test. NASA Lyndon B. Johnson Space Center Internal Note JSC-22546, June 1987.

Kowalski, R. R.: Ramapo/Turbine Hybrid Mass Meter Test. NASA Lyndon B. Johnson Space Center Internal Note JSC-22269, Mar. 1987.

U.S. GOVERNMENT PRINTING OFFICE:1988-561-009/80549

1. Report No.	2. Government Accession No.	3. Recipient's Catalog No.
NASA TM-100465		

4. Title and Subtitle	5. Report Date
FLOWMETER EVALUATION FOR ON-ORBIT OPERATIONS	August 1988
	6. Performing Organization Code: 992-15-00-00-72
7. Author(s): R. S. Baird	8. Performing Organization Report No.: S-578
	10. Work Unit No.
9. Performing Organization Name and Address: Lyndon B. Johnson Space Center, Houston, Texas 77058	11. Contract or Grant No.
	13. Type of Report and Period Covered: Technical Memorandum
12. Sponsoring Agency Name and Address: National Aeronautics and Space Administration, Washington, D.C. 20546	14. Sponsoring Agency Code

15. Supplementary Notes

16. Abstract

Various flowmetering concepts were flow tested to characterize relative capabilities and limitations for on-orbit fluid-transfer operations. Performance results and basic operating principles of each flowmetering concept tested are summarized, and basic considerations required to select the best flowmeter(s) for fluid system applications are discussed. Concepts tested were clamp-on ultrasonic, area averaging ultrasonic, offset ultrasonic, coriolis mass, vortex shedding, universal venturi tube, turbine, bearingless turbine, turbine/turbine differential-pressure hybrid, dragbody, and dragbody/turbine hybrid flowmeters. Fluid system flowmeter selection considerations discussed are flowmeter performance, fluid operating conditions, system operating environments, flowmeter packaging, flowmeter maintenance, and flowmeter technology. No one flowmetering concept tested was shown to be best for all on-orbit fluid systems.

17. Key Words (Suggested by Author(s))		18. Distribution Statement
Fluid dynamics Flow measurement Ultrasonic flowmeter Reduced-gravity testing	Vibration testing Coriolis force flowmeter	Unclassified - Unlimited Subject Category 34

19. Security Classif. (of this report)	20. Security Classif. (of this page)	21. No. of pages	22. Price*
Unclassified	Unclassified	140	

*For sale by the National Technical Information Service, Springfield, Virginia 22161